Species richness and diversity along an altitudinal gradient in moist temperate forest of Garhwal Himalaya.

C. M. Sharma*, Sarvesh Suyal, Sumeet Gairola, S.K. Ghildiyal

Department of Botany, HNB Garhwal University, Post Box # 51, Srinagar Garhwal 2461 74, Uttarakhand, India.
sharmacmin@gmail.com, sarveshsuyal@gmail.com, sumeetgairola@gmail.com, skghildiyal@gmail.com

Abstract: In the present study we have described the impact of altitude on the species richness, species diversity and dispersion behaviour of different tree species in Himalayan temperate forest. We have observed that the values of all the growth indices i.e., Margalef's index (0.17 to 1.14), Menheink's index (0.27 to 0.80), Species diversity (0.99 to 2.34) and Simpson's diversity index (1.49 to 8.73) were maximum at the lower altitudes (2250-1850m asl), medium at mid-altitudes (2600-2400m asl) and lowest at the higher altitudes (2800-2700m asl). Significantly negative correlation of density and species richness with altitude and slope was recorded. The study suggests that the distribution and species richness pattern of different tree species are largely regulated by the altitude and climatic factors. [Journal of American Science 2009;5(5):119-128]. (ISSN: 1545-1003).

Key words: altitude; slope; diversity; species richness; dispersion

1. Introduction

Species richness is a simple and easily interpretable indicator of biological diversity (Peet, 1974). Many types of environmental changes influence the processes that can both augment or erode diversity (Sagar et al. 2003). Ellu & Obua (2005) have suggested that different altitudes and slopes influence the species richness and dispersion behaviour of tree species. Moreover, Kharakwal et al. (2005) have pointed out that altitude and climatic variables like temperature and rainfall are the determinants of species richness. Difference in insolation period may occur according to altitude, thereby forming a range of microclimates in multifaceted landscapes. Diversity of life-forms usually decreases with increasing altitude and one or two life-forms remain at extreme altitudes (Pavón et al. 2000). Altitude itself represents a complex combination of related climatic variables closely correlated with numerous other environmental properties (soil texture, nutrients, substrate stability, etc.; Ramsay and Oxley, 1997). Within one altitude the cofactors like topography, aspect, inclination of slope and soil type further effect the forest composition (Holland and Steyn 1975).

Austin et al., (1996) have analyzed association between species richness, climate, slope position and soil nutrient status. Earlier in a critical literature review on species richness patterns in relation to altitude, Rahbek (1997) viewed that approximately half of the studies detected a mid-altitude peak in species richness and Grytnes and Vetaas (2002) have also reviewed these aspects in Nepalese Himalaya. Along the altitude, the geographic and climatic conditions change sharply (Kharkwal et al., 2005). Bongers et al., (1999) stated that drought indicating factors (length of dry period and cumulative water deficit) were more important for determining species distribution. Veenendaal et al. (1996) showed that elevation above 2000m asl may accumulate snow and have persistent cold temperature in winter. Along the altitudinal gradient, the upper limit of species richness remains high up to a considerable altitudinal level (2500m asl) and tree richness increases with increasing moisture in the Indian Himalayan region (Rikhari et al., 1989). Singh et al. (1994) found that productivity does not change upto and approximately 2500m asl in the Himalayan region. However, several others explanations have been given for a linear relationship between species richness and altitude (Givnish, 1999).

The present investigation was carried out in a moist temperate forest of the Garhwal Himalaya, which comes under district Uttarkashi of Uttarakhand to reveal (i) the impact of altitude on species richness in various temperate forest types and (ii) Assessment and analysis of change in dispersion behaviour of various tree species along altitudinal gradient for proper management, sustainable utilization and conservation of the forest resources in temperate region of Garhwal Himalaya.

2. Materials and Methods

2.1. Study Area

The study was conducted in Chaurangikhal moist temperate forest (30° 39.125' N latitude and 78° 31.156' E longitude) encompassing an area of about 750ha in district Uttarkashi (8016 km^2) of Garhwal Himalaya situated 29 km away from Uttarkashi town, during the years 2006-2007 (Figure 1). The district lies in the upper catchment of two great rivers of India viz, Ganges (called Bhagirathi upto Devprayag) and the Yamuna. Some of the tributaries of these rivers are Jodhganga, Jalandhari, Bhilangana, Duggada and Assiganga. Seven forest types; (i) pure *Abies pindrow*, (ii) pure conifer (iii) mixed *Abies pindrow* (iv) conifer mixed broad-leaved (v) mixed *Quercus floribunda* (vi) mixed broad-leaved and (vii) mixed *Pinus roxburghii,* were selected between 1850 to 2800m asl at various altitudes and slope gradients (Table 1). Broad land use categories of the area include permanent settlements (villages), irrigated and rainfed agricultural fields, scrub land, mixed broad-leaved forests, sub-alpine Oak-Fir forest, summer camping sites and alpine meadows locally known as "Kharaks" and "Bugyals", respectively.

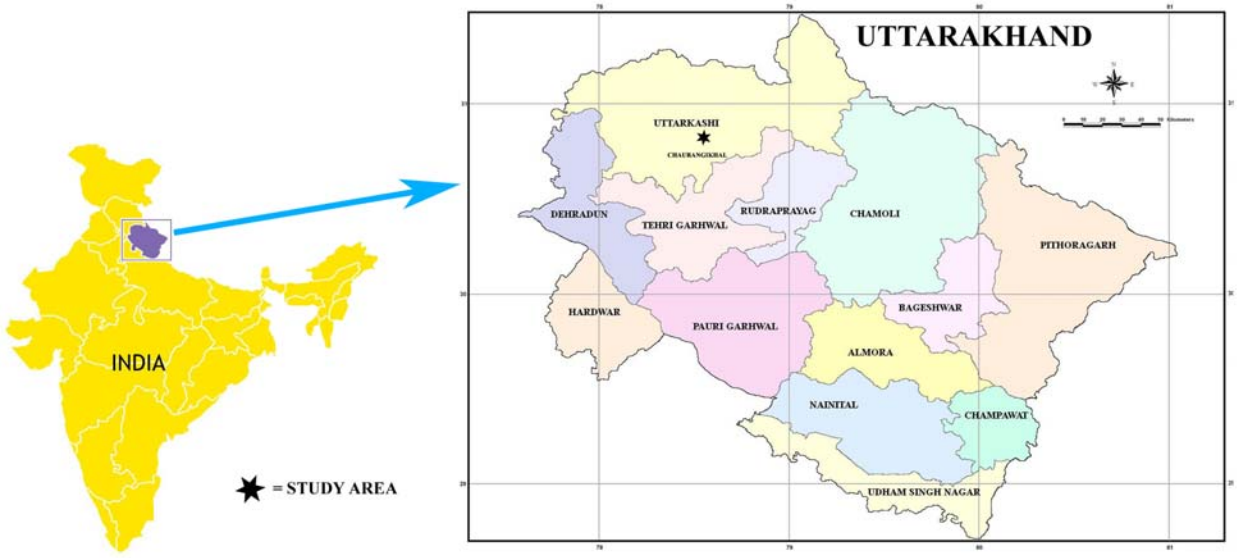

Figure 1. Map of the study area.

Table 1. The environmental variables across different altitudes

FT	Forest Type	Altitude (m asl)	Slope Aspect	Slope (Degree)	Nature of slope	Position
1	Pure *Abies pindrow* forest.	2800-2700	South-East facing.	38	Very steep	Upper
2	Mixed *Abies pindrow* forest.	2800-2650	North-East facing.	30	Very steep	Upper
3	Conifer mixed broad-leaved forest.	2700-2600	South-East facing.	25	Steep	Upper
4	Mixed broad-leaved forest.	2700-2600	South-West facing.	25	Steep	Upper
5	Pure *Abies pindrow* forest.	2600-2500	South facing.	28	Very steep	Middle
6	Pure *Quercus semecarpifolia* forest.	2600-2500	West facing.	18	Moderate	Middle
7	Conifer mixed broad-leaved forest.	2600-2450	North facing.	14	Moderate	Middle
8	Mixed *Quercus floribunda* forest.	2600-2400	South facing.	16	Moderate	Middle
9	Mixed broad-leaved forest	2400-2250	South-West facing.	15	Moderate	Lower
10	Pure *Pinus roxburghii* forest	2250-1850	South-West facing.	15	Moderate	Lower

The climate of the study area is moist temperate type, which receives moderate to high snowfall from December to February. Meterological details (1998-2007) of the study area are given in Figure 2. Mean annual maximum temperature was 18.51 ± 3.70 °C, whereas mean annual minimum temperature was 5.71

± 1.81 °C. Mean annual rainfall was 1825.39 ± 417.54 mm. Mean Relative humidity round the year in the study area ranged from 15 % to 86 %. The rainy season accounts for about three-quarters of the annual rainfall. In the study area the year is represented by three main seasons; the cool and relatively dry winter (December to March); the warm and dry summer (mid-April to June); and a warm and wet period (July to mid-September) called as the monsoon or rainy season. Apart from these main seasons, the transitional periods interconnecting rainy and winter, and winter and summer seasons are referred to as autumn (October to November) and spring (February to March). Geologically, the rocks were complex mixture of mainly sedimentary, low grade metamorphosed with sequence capped by crystalline nappe (Valdiya, 1980).

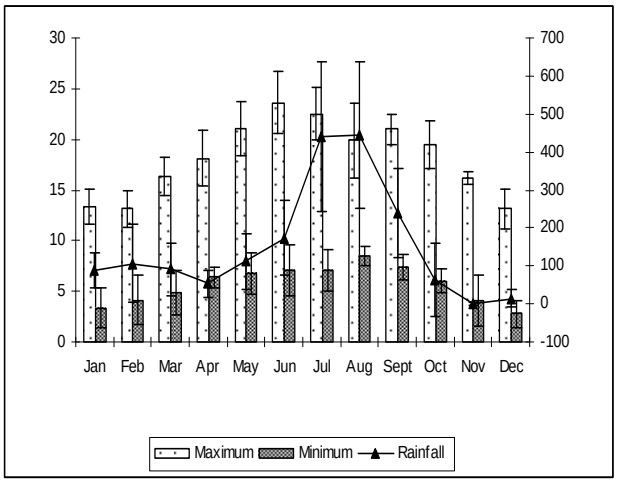

Figure 2. Climatic details of the study area (1998-2007).

2.2. Data Analysis

The study was conducted during the years 2006-2007. After the reconnaissance survey, ten forest cover types having different species compositions, altitudes, slopes and aspects were identified (table 1). Each forest type was named according to the composition of dominant tree species as per Ram Prakash (1986), viz., ≥ 75% as pure; 50-75% as mainly; 25-50% as mixed and < 25% miscellaneous. Physiographic factors i.e., altitude (m asl), slope steepness (Degree), direction of the slope, slope position (Upper, Middle, and Lower) across different cover types were measured by GPS (Garmin, Rino-130). A total of 120 plots (twenty plots in each forest type) measuring 10m X 10m each, were sampled at the study area. Plots were laid out by stratified random approach; stratification allowed equal repetition. The trees were identified with the help of Flora of the District Garhwal North West Himalaya (Gaur, 1999) and others. Trees were considered to be individuals ≥ 10 cm dbh (diameter at breast height i.e., 1.37m) (Knight, 1963). Trees were analyzed by 10m X 10m sized quadrats respectively. Total Species Richness was simply taken as a count of number of species present in that forest type. Species richness (number of species per unit area) was calculated as: SR = S-1/ln (N); where, SR = Margalef (1958) index of species richness, S = Number of species and N = total number of individuals. Menhinik's index of richness (Whittaker, 1977) was calculated as: Richness=S/√N, where, S= number of species, and N= total number of individuals of all species. The ratio of abundance to frequency (A/F) for different species was determined for eliciting the distribution pattern. This ratio has indicated regular (<0.025), random (0.025-0.05) and contagious (>0.05) distribution patterns (Whitford, 1949). The diversity (H') was determined by using Shannon-Wiener information index (Shannon and Weaver, 1963) as: $H' = - \sum n_i /n \log_2 n_i /n$; where, n_i was the IVI value of a species and n was the sum of total IVI values of all species in that forest type. Simpson's diversity index (Simpson, 1949) was calculated as: D = 1-Cd, where, D = Simpson's diversity and Cd = Simpson's concentration of dominance = $(\sum n_i /n)^2$.

3. Results

3.1. Species richness and diversity parameters

In the present study, the total species richness and Margalef's index were recorded from 2 to 9 and 0.17 to 1.14, across 1850-2800m asl altitudinal gradient. At the highest elevation (2800-2700m asl), the minimum species richness (2 species) and Margalef's index (0.17) were recorded, while maximum values (9 species and 1.14) of these parameters were encountered at lower elevation (2250-1850 m asl). A peak level of species richness (7 to 9 species) was recorded at a range between 2600-1850 m asl; However, species richness (constant 6 species) and Margalef's index (0.88 to 0.98) did not vary sharply between 2700-2500m asl elevation. Above 2600m asl, the both respective parameters (species richness & Margalef's index) decreased from 5 to 2 species and 0.68 to 0.17 exponentially with increase in elevation and subsequently dropped to a minimum at the highest (2800m asl) elevation (Table 2 and Figure 3). Menheink's index was recorded between 0.272 to 1.039, the minimum value was observed at the highest elevation 2800-2700m asl, whereas the maximum

value was recorded at mid-elevation 2600-2500m asl. Interestingly, second highest value (0.849) was also recorded at upper elevation 2700-2600m asl which declined (0.272) at middle elevation (Table 2 and Figure 3).

Table 2. Total species richness and diversity parameters of tree species along altitudinal gradient.

Altitude (m asl)	SR	MI	MeI	H'	D
2800-2700	2	0.174	0.272	0.992	1.494
2800-2650	3	0.358	0.433	1.003	2.426
2700-2600	5	0.683	0.657	1.923	4.709
2700-2600	6	0.886	0.849	2.094	5.715
2600-2500	6	0.988	1.039	2.137	5.732
2600-2500	5	0.748	0.784	1.852	4.674
2600-2450	6	0.798	0.684	2.089	5.708
2600-2400	7	0.955	0.793	2.379	6.775
2400-2250	7	0.881	0.661	2.313	6.766
2250-1850	9	1.148	0.805	2.349	8.736

Abbreviations: SR= Species Richness; MI= Marglef's Index; MeI= Menheink's Index; H= Shannon Wiener Diversity Index; D= Simpson's Diversity Index.

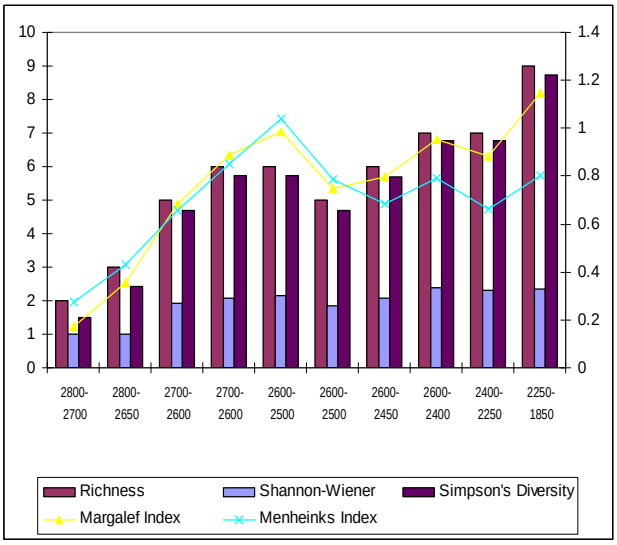

Figure 3. Species richness and diversity parameters along altitudinal gradient.

The low elevation appeared likely to be drier although precipitation varied inconsistently with elevation (Singh et al., 1994). At the highest elevation (2800-2700m asl) the maximum species diversity (0.52) and Simpson's diversity (0.80) was recorded for *Quercus semecarpifolia*, while minimum species diversity (0.47) and Simpson's diversity (0.69) for *Abies pindrow*. Just beneath this, at 2800-2650m asl elevation the highest species diversity (0.51) and Simpson's diversity (0.99) was recorded for *Q. semecarpifolia* and *Symplocos paniculata* whereas, the lowest values (0.15 and 0.49) of these parameters were observed for *A. pindrow*. At the 2700-2600m asl elevation the maximum species diversity (0.53) and Simpson's diversity (1.00) was recorded for *A. pindrow* and *Buxus wallichiana*. At middle elevation (2700-2600m asl), the highest species diversity (0.52) and Simpson's diversity (1.00) were recorded for *Q. semecarpifolia* and *Lyonia ovalifolia*, while the lowest values (0.10 and 0.80) were recorded for *L. ovalifolia* and *Q. semecarpifolia*. Between 2600-2500m asl, the maximum species diversity (0.53) and Simpson's diversity (0.99) were recorded for *A. pindrow* and *Acer acuminatum* while, minimum values of both the respective parameters (0.15 and 0.84) were recorded for *A. acuminatum* and *A. pindrow*. At 2600-2500m asl, maximum species diversity (0.52) was recorded for *Q. semecarpifolia* and minimum(0.15) for *Persea duthiei*. Between2600-2450m asl the highest species diversity (0.52) and Simpson's diversity (0.99) were recorded for *A. pindrow* and *L. ovalifolia*, while the lowest values (0.21 and 0.79) were recorded for *L. ovalifolia* and *A. pindrow*. Between 2600-2400m asl, the maximum species diversity (0.53) was recorded for *Q. floribunda* and minimum (0.09) for *A. spectabilis*. At 2400-2250m asl the highest species diversity (0.52) and Simpson's diversity (1.00) were recorded for *Q. floribunda* and *A. pindrow*, while the lowest values (0.09 and 0.90) were recorded for *A. pindrow* and *Q. floribunda*. At lowest elevation (2250-1850m asl) the maximum values of species diversity (0.53) was recorded for *Pinus roxburghii* and minimum (0.08) for *Myrica esculenta*. The overall maximum species diversity (Shannon-Wiener index) (2.37) was recorded at comparatively lower elevation (2600-2400m asl). However, second maximum species diversity (2.34) and the maximum Simpson's diversity (8.73) were recorded at the lowest elevation (2250-1850m asl), whereas, minimum species diversity (Shannon-Wiener index) (0.99) and Simpson's diversity (1.49) were observed at the highest elevation (2800-2700m asl) respectively (Table 2, 3 and Figure 3).

Table 3. Species diversity and Simpson's diversity of tree species along altitudinal gradient.

Tree Species	Altitude (m asl)																			
	2800-2700		2800-2650		2700-2600		2700-2600		2600-2500		2600-2500		2600-2450		2600-2400		2400-2250		2250-1850	
	H'	D	H'	D	H'	D	H'	D	H'	D	H'	D	H'	D	H'	D	H'	D	H'	D
Abies pindrow	0.47	0.695	0.35	0.495	0.53	0.866	0.29	0.993	0.53	0.847	0.41	0.978	0.52	0.794	0.27	0.995	0.09	1.000	-	-
A. spectabilis	-	-	-	-	-	-	-	-	-	-	-	-	-	-	0.09	1.000	-	-	-	-
Acer acuminatum	-	-	-	-	-	-	-	-	0.15	0.999	-	-	-	-	-	-	-	-	-	-
Alnus nepalensis	-	-	-	-	-	-	-	-	-	-	-	-	-	-	-	-	-	0.000	0.19	0.998
Betula alnoides	-	-	-	-	-	-	-	-	-	-	-	-	-	-	-	-	-	-	0.14	0.999
Buxus wallichiana	-	-	-	-	0.12	1.000	-	-	-	-	-	-	-	-	-	-	-	-	-	-
Carpinus vominea	-	-	-	-	-	-	-	-	-	-	-	-	-	-	0.19	0.998	-	-	-	-
Lyonia ovalifolia	-	-	-	-	0.26	0.995	0.10	1.000	0.27	0.995	0.26	0.996	0.21	0.998	0.40	0.980	0.27	0.995	0.50	0.935
Myrica esculenta	-	-	-	-	-	-	-	-	-	-	-	-	-	-	-	-	-	-	0.08	1.000
Persea dutheii	-	-	-	-	-	-	0.48	0.949	0.47	0.958	0.15	0.999	0.45	0.966	0.41	0.978	0.16	0.999	-	-
Pinus roxburghii	-	-	-	-	-	-	-	-	-	-	-	-	-	-	-	-	-	-	0.53	0.825
Pyrus pashia	-	-	-	-	-	-	-	-	-	-	-	-	-	-	-	-	0.28	0.995	0.13	0.999
Quercus floribunda	-	-	-	-	-	-	-	-	-	-	-	-	0.47	0.955	0.53	0.882	0.52	0.909	0.12	0.999
Q. leucotrichophora	-	-	-	-	-	-	-	-	-	-	-	-	-	-	-	-	0.52	0.914	0.30	0.993
Q. semecarpifolia	0.52	0.800	0.51	0.932	0.52	0.903	0.52	0.806	0.50	0.935	0.52	0.790	0.22	0.997	-	-	-	-	-	-
Rhododendron arboreum	-	-	-	-	0.49	0.945	0.43	0.973	-	-	0.52	0.912	0.22	0.997	0.49	0.942	0.48	0.954	0.35	0.987
Symplocos paniculata	-	-	0.15	0.999	-	-	0.27	0.995	-	-	-	-	-	-	-	-	-	-	-	-
Taxus baccata	-	-	-	-	-	-	-	-	0.21	0.998	-	-	-	-	-	-	-	-	-	-

Abbreviations: H'= Shannon-Wiener index; D = Simpson's Diversity index

The overall pattern of species richness, Margalef's index, Menheink's index, Shannon-Wiener index (species diversity) and Simpson's diversity index showed a sharp decline at the highest altitude (2800-2700m asl). A similar pattern of tree species richness in timberline area was reported by Rawal et al. (1991). Tree species richness increases with increasing moisture in the Indian Central Himalaya (Rikhari et al.1989). In this study, a negative relationship was found between species richness, Margalef's index, Menheink's index, species diversity and Simpson's diversity index vs elevation (Table 2, 3 and Figure 3, 4). Sagar et al. (2008) have suggested that species richness decreases with an increase in species dominance.

3.2. Distribution pattern (A/F) ratio

Hubbell et al. (1999) reported that the dispersal limitation is an important ecological factor for controlling species distribution pattern and a connection between biotic and abiotic ecological factors. A number of tree species found in the Himalaya showed varying patterns of distribution. The extension of climate gradient enabled several species to realize their fullest range of elevational adaptability. An analysis of dispersion pattern (Table 4) indicated that maximum species had random distribution at the altitude between 2800-1850m asl. At the higher altitude (2800-2600m asl) maximum tree species were distributed in random pattern, interestingly same tendency was observed for the species at lower altitude (2600-1850m asl), while at middle altitudinal range (2600-2450m asl) most of the species were distributed in contiguous pattern and rarely in regular pattern also. The *Abies pindrow* and *Rhododendron arboreum* changed their dispersion pattern from contiguous (2400-2250m asl) to random (2600-2450m asl) followed by again contiguous (2700-2600m asl) to finally random at the higher altitude (2800-2650m asl). *Quercus* species was found distributed in random pattern from lower (2250-1850m asl) to the higher (2800-2700m asl) altitudes. *Persea duthiei* showed contiguous to random distribution patterns while *Lyonia ovalifolia* showed regular and random and finally contiguous patterns along lower, middle and higher altitudinal ranges. The species-aggregation relationship predicts that spatial aggregation of individuals within species results in lower species richness Sagar et al. (2008).

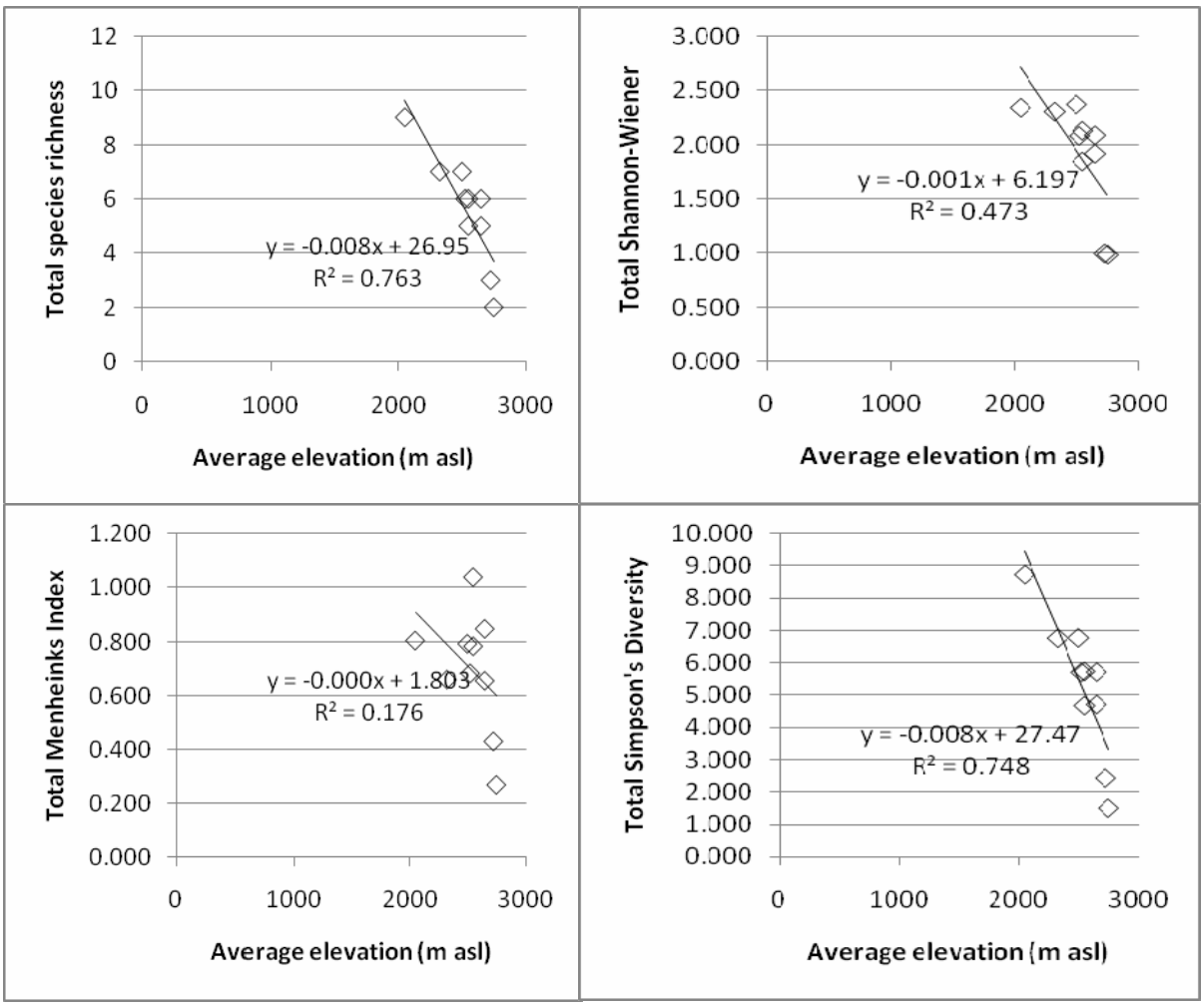

Figure 4. Species richness and diversity parameters of tree species along increasing elevation.

According to Odum (1971), the clumped distribution is common in nature, while random distribution is found only in uniform environments. The clumping of individuals of a species may be due to insufficient mode of seed dispersal (Richards, 1996) or when death of trees creates a large gap encouraging recruitment and growth of numerous saplings (Armesto et al., 1986). Connell (1978) suggested that the uniform dispersion pattern of species in tropical forests largely enable the maintenance of high levels of diversity. The changes in the dispersion patterns may reflect the reactions of species to disturbance as well as to changes in the habitat conditions (Sagar et al., 2003).

4. Discussion

A number of tree species found in the Himalaya exhibit varying patterns of distribution. The extension of climatic gradient enabled several species to realize their fullest range of elevational adaptability. Distributional ranges of several species were segregated along the widened altitudinal ranges (Kharakwal et al., 2005). He & Legendre (2002) reported species-area relation, which predicts that species richness increases with increasing area. Pausas & Austin (2001) also suggested that over any large region the distribution of species richness is likely to be governed by two or more environmental factors and not by a single factor. Pangtey et al. (1991) argued that the effect of monsoon is not substantially weakened at higher altitudes and also the amount of rainfall is not much different from that of the lower altitudinal range of Central Himalaya. This has also been used to explain the patterns of decrease in species richness with altitude (Rahbek, 1997). In the temperate

Table 4. Dispersion behaviour of tree species along altitudinal gradient.

Tree Species	Family	Altitude (m asl)									
		2800-2700	2800-2650	2700-2600	2700-2600	2600-2500	2600-2500	2600-2450	2600-2400	2400-2250	2250-1850
Abies pindrow	Pinaceae	0.04(R)	0.05(R)	0.02(Re)	0.07(C)	0.02(Re)	0.04(R)	0.03(R)	0.06(C)	0.10(C)	-
A. spectabilis	Pinaceae	-	-	-	-	-	-	-	0.10(C)	-	-
Acer acuminatum	Aceraceae	-	-	-	-	0.30(C)	-	-	-	-	-
Alnus nepalensis	Betulaceae	-	-	-	-	-	-	-	-	-	0.10(C)
Betula alnoides	Betulaceae	-	-	-	-	-	-	-	-	-	0.08(C)
Buxus wallichiana	Buxaceae	-	-	0.10(C)	-	-	-	-	-	-	-
Carpinus vaminea	Corylaceae	-	-	-	-	-	-	-	0.08(C)	-	-
Lyonia ovalifolia	Eriaceae	-	-	0.04(R)	0.15(C)	0.07(C)	0.19(C)	0.03(R)	0.03(R)	0.02(Re)	0.04(R)
Myrica esculenta	Myricaceae	-	-	-	-	-	-	-	-	-	0.10(C)
Persea dutheii	Lauraceae	-	-	-	0.10(C)	0.04(R)	0.30(C)	0.04(R)	0.03(R)	0.08(C)	-
Pinus roxburghii	Pinaceae	-	-	-	-	-	-	-	-	-	0.05(R)
Pyrus pashia	Rosaceae	-	-	-	-	-	-	-	-	0.05(R)	0.05(R)
Quercus floribunda	Fagaceae	-	-	-	-	-	-	0.04(R)	0.04(R)	0.04(R)	0.05(R)
Q. leucotrichophora	Fagaceae	-	-	-	-	-	-	-	-	0.04(R)	0.03(R)
Q. semecarpifolia	Fagaceae	0.03(R)	0.02(Re)	0.03(R)	0.06(R)	0.03(R)	0.03(R)	0.05(R)	-	-	-
Rhododendron arboreum	Ericaceae	-	-	0.05(C)	0.04(R)	-	0.08(C)	0.04(R)	0.02(Re)	0.03(R)	0.07(C)
Symplocos paniculata	Symlocaceae	-	0.10(C)	-	0.04(R)	-	-	-	-	-	-
Taxus baccata	Taxaceae	-	-	-	-	0.08(C)	-	-	-	-	-

Abbreviations: R = Random; Re = Regular; C = Contiguous

Table 5: Carl Pearson correlation coefficient between different parameters:

	Altitude	Slope	Density	TBC	SR	MI	MEI	H'	Cd	D
Altitude	1.000									
Slope	0.719*	1.000								
Density	-0.848**	-0.635*	1.000							
TBC	-0.207	0.196	0.461	1.000						
SR	-0.874**	-0.817**	0.684*	-0.175	1.000					
MI	-0.750*	-0.750*	0.457	-0.392	0.960**	1.000				
MEI	-0.420	-0.499	0.001	-0.669*	0.723*	0.887**	1.000			
H	-0.688*	-0.804**	0.501	-0.464	0.932**	0.952**	0.807**	1.000		
Cd	0.590	0.732*	-0.413	0.559	-0.851**	-0.889**	-0.784*	-0.978**	1.000	
D	-0.865**	-0.819**	0.674*	-0.198	1.000**	0.964**	0.732*	0.942**	-0.866**	1.000

**. Correlation is significant at the 0.01 level; *. Correlation is significant at the 0.05 level.

forests mean tree species richness was maximum in mixed broad-leaved forest which decreased from highly to least disturbed forests (Kumar & Ram, 2005). Consequently, our study revealed the maximum species richness of tree species at lower elevation, compared to higher elevational forests as suggested by Kumar & Ram (2005). Rathore (1993) has noticed high species richness and diversity in the *Pinus roxburghii*-mixed broad-leaved forests. In another study Singh et al. (1994) reported that *P. roxburghii*-mixed broad-leaved forests had the highest species richness, while high elevation forests had the lowest. Burns (1995) and Austin et al. (1996) have found that the total species richness was greatest at lower elevation and warmer sites. The overall pattern of species richness showed a sharp decline as the altitude increased beyond 3000m asl. A similar pattern of tree species richness (deciduous) in timberline area was reported by Rawal et al. (1991).

Between 2450-2600 and 2600-2500 m asl, species richness fluctuated due to change in the climatic conditions (Table 2 and Figure 3). More than 60%

(Maximum) plant species were either present at 1850m asl, where the temperature cover a range from 10°C to 24°C (Champion & Seth, 1968). The low elevational sites were relatively densely populated probably because human interference in these areas facilitates the introduction and establishment of non-native species (Rawal & Pangtey, 1994). The human impact at lower altitudes was evident in the form of open spaces left after selective tree felling. These spaces may exacerbate the establishment of shade–intolerant species and enhance the regeneration of mixed pine-broadleaved forest (Wangda & Ohsawa, 2006). As a result of which the maximum tree species were encountered at lower elevation (Pine-mixed broad-leaved forest) compared to higher elevational sites. In this study the richness of non-native species like *Pinus roxburghii, Pyrus pashia, Lyonia ovalifolia, Betula alnoides* and *Alnus nepalensis* was more prevalent in early successional/ pioneer communities, because the species richness is believed to be more in pioneer communities (Rajmanek, 1989). Occurrence of *Abies pindrow, Quercus semecarpifolia, Q. leucotrichophora* and *Rhododendron arboretum* community (Table 4) almost on all the sites along the altitudinal gradient suggests their tolerance to biotic pressures and wider ecological amplitude. *Pinus roxburghii* is an early successional species and Oak a climatic climax, while the successional stage of *Abies pindrow* forest is considered to be climax for west-Himalaya (Champion & Seth, 1968). The expected compositional changes in *Q. leucotrichophora* forests are associated with biomass destruction. All *Quercus spp*. are repeatedly lopped for their fuel wood and fodder values. This activity reduces vigour and seed production (Saxena & Singh, 1984) in this species. Large scale extraction of selected species also causes structural change in plant communities (Spurr & Barnes 1980). Heavy browsing by animals at seedling and sapling stages is also responsible for poor representation in recruitment classes of *Q. leucotrichophora, Q. floribunda and Q. semecarpifolia* (Dhar et al. 1997). Accompanying frequent reproduction and expanding populations of two co-dominant native species, *Rhododendron arboreum* and *Lyonia ovalifolia*, result in structural/compositional changes, because they are unpalatable and less preferred for fuel wood. Poor recruitment of dominant *A. pindrow* and *Q. semecarpifolia* and other species in high elevation forests indicates possible decline in their populations. The prevention of recruitment of dominant natives is considered to be a causal process resulting in changes in structural and functional aspects of reserve's ecosystem (Macdonald et al., 1989). For analysis of variability in dispersion, about half of the analyzed species in this study showed no effect of disturbance on dispersal behaviour and were characterized by clumped distribution. Clumping in these species may be due to patchy distribution of microhabitats suitable for plant growth in forest soils. The correlation between various parameters is shown in Table 4.

5. Conclusions

The present study highlights a very poor status of total species richness in the entire forest area along with regulation of tree species at various altitudes. Our findings revealed that lower elevational cover-types had comparatively higher number of species than lower number of species at higher elevational cover-types which implies that higher elevational forest types should be conserved with necessary implementations. Lower altitudinal forest types preferred optimum species richness, diversity and related parameters including soil status. At the higher altitudinal forest types species richness and diversity were found lesser prevalent because of high dependency of the people on fuel wood, extraction of NTFPs from the forest for generation of income. Significantly negative correlation of density and species richness with altitude and slope was recorded. The study suggests that the distribution and species richness pattern of different tree species are largely regulated by the altitude and climatic factors.

Acknowledgements:

We thankfully acknowledge the financial support provided by the Department of Science and Technology, Government of India, New Delhi, vide its Project No. SP/SO/PS-52/2004.

Correspondence to:
Dr. C.M. Sharma
Professor
Department of Botany, HNB Garhwal University,
Post Box # 51, Srinagar Garhwal 2461 74,
Uttarakhand, India.
Telephone: 91-1346-250806
Cellular phone: 91-9412079937
Email: sharmacmin@gmail.com

References

[1] Peet RK. The measurement of species diversity. Annual Review of Ecology and Systematics 1974;5:285–307.

[2] Sagar R, Raghubanshi AS, Singh JS. Tree species composition, dispersion and diversity along a disturbance gradient in a dry tropical forest region of India. Forest Ecology and Management 2003;186:61-71.

[3] Ellu G, Obua J. Tree condition and natural regeneration in disturbed sites of Bwindi Impenetrable forest national park, southwestern Uganda. Tropical Ecology 2005;46(1):99-111.

[4] Kharkwal G, Mehrotra P, Rawat YS, Pangtey YPS. Phytodiversity and growth form in relation to altitudinal gradient in the Central Himalayan (Kumaun) region of India. Current Science 2005;89(5):873-878.

[5] Pavón NP, Hernandez-Trejo H, Rico-Gray V. Distribution of plant life forms along an altitudinal gradient in the semi-arid valley of Zapotitlan, Mexico. Journal of Vegetation Science 2000;11:39–42.

[6] Ramsay PM, Oxley ERB. The growth form composition of plant communities in the Ecuadorian paramos. Plant Ecology 1997;131:173–192.

[7] Holland PG, Steyn DG. Vegetational responses to latitudinal variations in slope angle and aspect. Journal of Biogeography 1975;2:179-183.

[8] Austin MP, Pausas JG, Nicholls AO. Patterns of species richness in relation to environment in southeastern New South Wales, Australia. Australian Journal of Ecology 1996;21:154-164.

[9] Rahbek C. The relationship among area, elevation and regional species richness in Neotropical birds. American Naturalist 1997;149:875-902.

[10] Grytnes JA, Vetaas OR. Species richness and altitude: A comparison between null models and interpolated plant species richness along the Himalayan altitudinal gradient, Nepal. American Naturalist, 2002;159:294-304.

[11] Bongers F, Poorter L, Van Rompaey RS, Parren MPE. Distribution of moist forest canopy tree species in Liberia and Côte d'Ivoire: response curves to a climatic gradient. Journal of Vegetation Science 1999;10:371–382.

[12] Veenandaal EM, Swaine MO, Agyeman VK, Blay D, Abebrese IK, Mullins CE. Differences in plant and soil water relations in and around a forest gap in West Africa during the dry season may influence seedling establishment and survival. Journal of Ecology 1996;83:83-90.

[13] Rikhari HC, Chandra R, Singh SP. Pattern of species distribution and community characters along a moisture gradient within an oak zone of Kumaun Himalaya. Proceedings of Indian National Science Academy 1989;55(B):431-438.

[14] Singh SP, Adhikari BS, Zobel DB. Biomass productivity, leaf longevity and forest structure in central Himalaya. Ecological Monograph 1994;64:401-421.

[15] Givnish TJ. On the causes of gradients in tropical tree diversity. Journal of Ecology 1999;87:193–210.

[16] Valdiya KS. Stratigraphic scheme of the sedimentary units of the Kumaon lesser Himalaya. In: Valdiya, K.S. and Bhatiya, S.B.(eds.) Stratigraphy and correlations of the lesser Himalayan formations, Hindustan Publication Corporation, Delhi, India. 1980:7-48.

[17] Ram Prakash. Forest Management. International Book Distributors, Dehradun, India. 1986:214.

[18] Gaur RD. 1999. Flora of the District Garhwal North West Himalaya (with ethanobotanical notes). Transmedia Publication, Srinagar (Garhwal) India.

[19] Knight DH. A distance method for constructing forest profile diagrams and obtaining structural data. Tropical Ecology 1963;4:89-94.

[20] Margalef DR. Information theory in ecology. Genetics and Systematics 1958;3:36-71.

[21] Whittaker RH. Evolution of species diversity in land plant communities. Evolutionary Biology 1977;10:1–67.

[22] Whitford PB. Distribution of woodland plants in relation to succession and clonal growth. Ecology 1949;30: 199-288.

[23] Shannon CE, Weaver W. The mathematical theory of communication. University of Illinois Press, Urbana, USA. 1963.

[24] Simpson EH. Measurement of diversity. Nature 1949;163:688.

[25] Rawal RS, Bankoti NS, Samant SS, Pangtey YPS. Phenology of tree layer species from the timberline around Kumaun in central Himalaya, India. Vegetatio 1991;93:109–118.
[26] Sagar R, Raghubanshi AS, Singh JS. Comparasion of community composition and species diversity of understorey and overstorey tree species in a dry tropical forest of northern India. Journal of Environmental Management 2008;88**:**1037-1046.
[27] Hubbell SP, Foster RB, O'Brien S, Wechsler B, Condit R, Harms K, Wright SJ, Loo de Lau S. Light-gap disturbances, recruitment limitation and tree diversity in a Neotropical forest. Science 1999;283:554-557.
[28] Odum EP. Fundamentals of Ecology. Saunders Company, Philadelphia, USA. 1971.
[29] Richards PW. The tropical rainforest 2nd ed. Cambridge University Press, Cambridge. 1996.
[30] Armesto IJ, Mitzel JD, Villagram C. A comparison of spatial patterns of trees in some tropical and temperate forests. Biotropica 1986;18:1-11.
[31] Connell JH. Diversity in tropical rainforest and coral reefs. Science 1978;199:1302-1309.
[32] He F, Legendre P. Species diversity patterns derived from species-area models. Ecology 2002;83:1185-1198.
[33] Pausas JG, Austin MP. Patterns of plant species richness in relation to different environments: An appraisal. Journal of Vegetation Science 2001;12:153-166.
[34] Pangtey YPS, Rawal RS, Bankoti NS, Samant SS. Phenology of high altitude plants of Kumaun in central Himalaya. International Journal of Biometeorology 1991;34:122-127.
[35] Kumar A, Ram J. Anthropogenic disturbances and plant biodiversity in forests of Uttaranchal, Central Himalaya. Biodiversity Conservation 2005;14:309-331.
[36] Rathore SKS. Resorce utilization patterns in a central Himalayan Catchment. Ph.D. Thesis, Kumaun University, Nainital, India. 1993.
[37] Burns BR. Envoronment correlates of species richness at Waipoua Forest sanctuary. New Zealand. New Zealand Journal of Ecology 1995;19:153-162.
[38] Champion HG, Seth SK. A Revised survey of the forest types of India. Manager of Publication, Government of India, New Delhi, India, 1968:404.
[39] Rawal RS, Pangtey YPS. High altitude forests in a part of Kumaun, Central Himalaya. Proceedings of Indian National Science Academy 1994;60(B):557-564.
[40] Wangda P, Ohsawa M. Structure and regeneration dynamics of dominant tree species along altitudinal gradient in dry valley slopes of the Bhutan Himalaya. Forest Ecology and Management 2006;230(1-3):136-150.
[41] Rajmanek M. Invasibility of plant communities. In: Drake JA, Mooney HA, di Castri F, Groves RH, Kruger FJ, Rajmanek M, Williamson M, eds. Biological invasions: a global prospective. SCOPE 37: John Wiley and Sons.1989:281-300.
[42] Saxena AK, Singh JS. Tree population structure of certain Himalayan forest associations and implications concerning the future composition. Vegetatio 1984;58:9-61.
[43] Spurr SH, Barnes BV. Forest Ecology. New York: John Wiley. 1980.
[44] Dhar U, Rawal RS, Samant SS. Structural diversity and representativeness of forest vegetation in protected area of Kumaun Himalaya, India: implications for conservation. Biodiversity Conservation, 1997;6:1045-1062.
[45] Macdonald IAW, Loope LL, Usher MB, Hamann O. Wildlife conservation and the invasion of nature reserves by introduced species: a global prospective. In: Drake JA, Mooney HA, di Castri F, Groves RH, Kruger FJ, Rajmanek M, Williamson M, eds. Biological invasions: a global prospective. SCOPE 37: John Wiley and Sons. 1989:281-300.

Dengue Virus Infections in Patients Suspected of Malaria/Typhoid in Nigeria

Baba M M [1], Marie-Francois Saron,[2] Vorndam A V [3], Adeniji J A [4], Diop O [5] and Olaleye D[6]
1 Mrs. Marycelin M Baba, B.Sc, M. Sc, PhD MHPM, ACMLS (marycelinb@yahoo,com) : Department of Medical Laboratory Science, College of Medical Sciences, University of Maiduguri, Nigeria
2 Dr. Marie-Francois Saron B.Sc, M. Sc, PhD: Department of Virology, Institut Pasteur De Dakar, Senegal (mfsaron@pasteur.fr)
3 Dr Vorndam Vance: B.Sc, M. Sc, PhD**:** Dengue Laboratory,CDC, Puerto Rico (avv1@cdc.org)
4 Dr J. A. Adeniji, B.Sc, M. Sc, PhD: Department of Virology, College of Basic Medical Sciences, University of Ibadan, Nigeria (adek1808@yahoo.com)
5 Dr Ousmane Diop, Institut Pasteur de Dakar, Sengal (diop@pasteur.sn)
6 Prof D Olaleye, Department of Virology, College of Basic Medical Sciences, University of Ibadan, Nigeria (ibvirology@yahoo.com)

ABSTRACT
Dengue fever is clinically difficult to diagnose especially in the developing countries with no established diagnostic facility and could easily be mistaken for malaria, typhoid etc. This study was designed to determine the significance of these viruses in febrile illnesses. About 1948 serum samples from suspected cases of malaria and typhoid were collected from June 2001 to July 2002 in six ecological zones in Nigeria. 59 pools of *Aedes Spp* from Rain forest were tested by RT-PCR and for virus isolation. MAC-ELISA was used to test all the sera for IgM and IgG antibodies. All IgM positive sera were further analyzed by RT-PCR and Plaque reduction neutralization test (PRNT). Thirteen (0.67%) of the1948 sera were positive for DEN 1and 2 IgM from 4 zones. Mixed infections of DEN-2 and WN virus observed in two samples, eventually had neutralizing antibody for WNV. Overall, PRNT and ELISA results for DEN were in concordance. Dengue IgG antibodies in Sahel savanna (81.7%), Rain forest (69.0%), and Wooded savanna (69.0%) were significantly different from Grass (38.15%) and Sudan (32.6%) savanna. One IgM positive serum had detectable RNA to DEN. Fourteen of 59 pools of Aedes spp showed viral RNA to DEN 1-4. The prevalence of the antibodies to these viruses and the ages as well as the gender of the patients was not significantly different. Misdiagnosis of DEN infection for malaria/typhoid has been detected. [Journal of American Science 2009;5(5):129-134]. (ISSN: 1545-1003).

Keywords: Dengue, virus, febrile illness, malaria, typhoid and Nigeria.

1. Introduction

The clinical outcomes of DEN virus infection could vary from asymptomatic infection to mild febrile dengue fever (DF) to severe and life threatening dengue hemorrhagic fever (DHF)/dengue shock syndrome (DSS) (Gunther et. al. 2007). The four closely related, but antigenically distinct, serotypes of DENs (DEN-1, DEN-2, DEN-3, and DEN-4) do not cross-protect but cross react. Infection with one of these serotypes provides lifelong immunity to the infecting serotype only. Therefore, persons can acquire a second dengue infection from a different serotype, and second infections place them at greater risk for dengue hemorrhagic fever (DHF), the more severe form of the disease (Morb. Morta.Wkly Rep. 2007). These viruses are transmitted between human and monkey hosts by the mosquitoes of the genus *Aedes*, and principally *Aedes aegypti* (Holmes et al. 1999) and A. albopictus popularly known as the 'Asian tiger mosquito'. The early symptoms of arbovirus infections (High grade fever, headache, fatigue, malaise, nausea, vomiting) mimic malaria, typhoid, measles and influenza which are hyper endemic in the environment, thereby rendering the diagnosis of this viral infections very confusing. In such situations, these infections are quite often misdiagnosed and so, inappropriately treated. Consequently these cases often result in high rate of morbidity, complications and mortality. Yet health Institutions in Nigeria lack appropriate diagnostic facilities for this group of viruses even with the existence of factors (human populations, increased urbanization, incursion of human activity into the new ecosystems, increased global travel, climatic changes, and collapse of vector control and public health programs (Gubler 1988), which favor the emergence of arboviruses globally. This study was designed to survey the epidemiology of arboviral infections, with particular
reference to Dengue viruses (DENs) in febrile patients suspected of malaria/typhoid Nigeria.

2. Materials and Methods

2.1 Study Population:

Patients with febrile illness sent to the laboratory for either malaria or Widal tests were used

for the study. The common clinical manifestations on these patients by the time of sample collection include: fever, headache, and abdominal discomfort, and diarrhea, gastroenteritis while enteric fever, hepatitis, and HIV were less common. The commonest of all was fever either intermittent or recurrent.

2.3 Study Areas:
With more than eight ecological zones in Nigeria, six were randomly selected for the study. The selected zones were Guinea/ Grass savanna (Abuja), Rain forest (Ibadan), Wooded / Guinea savanna (Gombe), Deltaic / Swan savanna (Calabar), Sudan savanna (Kano) and Sudan / Sahel savanna (Maiduguri). A brief closed-ended questionnaire was designed to collect demographic data and clinical history of most of these patients.

2.4 Sample Collection A total of 1948 serum samples were collected in June 2001 and July 2002 from febrile patients. About 5ml of blood was collected by venu puncture from febrile patients. The blood was allowed to clot at room temperature and the serum was carefully collected after centrifugation at 2,000 rpm for 10 minutes and stored at -20^{o}C until tested. Most often scoop nets and occasionally, human beings were used as baits in catching mosquitoes from the field. The mosquitoes were caught alive and stored at -20^{0}C in Nigeria and were eventually transported with cold ice pack to Dakar for analysis.

2.5 Serology
Stock antigens were prepared in mouse brain from viruses supplied by WHO Collaborating Centre for Reference and Research on Arboviruses (CRORA), IPD, Senegal. All reactants were appropriately standardized.

2.5.1 Detection of IgM Antibodies:
An IgM capture ELISA (MAC– ELISA) as previously described by Vorndam and Kuno (5) was used for the detection of IgM antibodies against DENs. The virus with a higher Optical density (OD) was considered the infectious agent as reported by Vorndam and Kuno (1977). IgM positive samples were further subjected to PRNT as described by Mangiafico et al. (1988).

2.5.2 Detection of IgG Antibodies. For the detection of IgG antibodies against DENs, an IgG capture ELISA was used as previously described by Chunge et al. (1989). Binding of the IgG antibodies was detected using goat anti-human IgG antibodies labeled horseradish peroxidase. Unfortunately these samples were not confirmed by Plaque reduction neutralization technique (PRNT) because of the large sample size and the cost of the reagents.

2.5.3 Interpretation of Results: The standard deviation of a battery of negative sera was calculated. A value of three standard deviations from the mean was used as the cut -off value to minimize false results as suggested by Innis et al (Innis et al. 1989)

2.6 Mosquito Processing
The field- caught mosquitoes were identified to the species level when possible. The identified mosquitoes were placed in 12x 75mm tubes in pools of 50. Each pool was tested by RT-PCR assay using a set of primer and with a cell culture technique. The cell culture assay was conducted by inoculating 100µl aliquot of clarified supernatant from the mosquito pool onto sub confluent AP-61 cell and incubated for 8-10 days. The presence of the virus was determined by the use of indirect Immunofluorescence assay as described by Beckwith et al. (2000)

2.7 RT - PCR in Sera and Mosquitoes

2.7.1 The Extraction of RNA from Serum/Mosquito Suspension/Tissue Culture Extract
RNA extraction was carried out according to the specifications of the kit's (Q1 a Amp viral RNA Mini Kit) manufacturer. For each batch of mosquito suspension/serum/ extracted, positive controls (cell culture of the seed virus concerned) and uninoculated cell as negative control were included.

2.7.2 RT- PCR for Detection and Genotyping of DEN Viruses
2.7.2.1 The First Round of Amplification.
[The method previously described for dengue (Lanciotti et al. 1992) was adopted]
A semi-nested RT-PCR was carried out. All relevant aspects of the RT-PCR (Mgcl2, primers, RT, Taq polymerase, number of cycles, and annealing temperatures) were initially optimized by using quantitated purified DEN virus RNA to achieve a maximum level of sensitivity before testing the field samples. The reaction product was electrophoresed on a 1% composite agarose gel in 0.4M Tris- 0.05 M sodium acetate- 0.01 M EDTA buffer. The gel was stained with ethidium bromide. The resulting DNA band was visualized on a UV transilluminator. The target viral RNA was converted to a DNA copy (cDNA) prior to enzymatic DNA amplification by using RT and the dengue virus downstream consensus primer (D2), homologous to the genomic RNA of the four serotypes. Subsequently, Taq polymerase amplification was performed on the resulting cDNA with the upstream dengue virus consensus primer (DS1).

2.7.2.2 Dengue Virus Genotyping by

Second-Round Amplification with Type Specific Primers (nested PCR) as previously described by Lanciotti et al. (1992)

In this method, type-specific primers replaced dengue virus downstream consensus primer, while dengue upstream primer was retained. The Tag DNA dependent DNA polymerase amplified the products of the first amplification to generate a DNA strand of different length, which was identified by gel electrophoresis. Thus the second amplification differentiated dengue species into different serotypes.

3.0 RESULTS

3.1 Pattern of Dengue Virus Infections in Nigeria

3.1.1 IgM Capture ELISA for Dengue Viruses

Figure 1 shows the IgM and its corresponding IgG antibodies to the different serotypes of DEN in the four ecological zones. For example in Figure 1, sample 6 appeared to be a recent infection with DEN-2 having a high OD value (1.151) while sample 4 seemed to be a case of anamnestic response.

. Thirteen (0.6%) of the 1948 sera were positive for DEN1 and 2 IgM antibodies from 4 of the 6 ecological zones in Nigeria studied. The zones with positive cases were Rain forest (DEN-2), Grass savanna (DEN-2), Deltaic savanna (DEN2), and Sahel Savanna (DEN1 and 2). (Table1).

3.2 Plaque Reduction Neutralization Test on DEN IgM Positive Sera:

All the sera that were DEN IgM positive by MAC-ELISA were found positive by PRNT. (Data not included). Two sera which showed mixed infections of WNV and dengue by MAC-ELISA were later confirmed to be positive for WNV by PRNT. Failure to carry out PRNT for all the samples limits this study from giving the precise status of these patients with regards to dengue virus infections in Nigeria. This is because a negative acute-phase specimen is inadequate for ruling out such an infection underscoring confirmation by demonstrating virus-specific serum IgG antibodies in the same or later specimen.

3.3 The Prevalence of DEN IgG Antibodies in Nigeria

The zonal distribution of DEN IgG antibodies is displayed on Table 2. The prevalence of DEN IgG antibodies and the zones were significantly different with the highest in Sahel savanna (81.7%), followed by Rain forest (69.0%) and Wooded (69.0%) and the least in Sudan savanna (32.6%) and Grass savanna (38.1%).

3.4 Age and Gender Distribution of Patients with Dengue Virus IgM Antibodies

The prevalence of these antibodies and the ages as well as the gender of the patients were not significantly different (X^2=P>0.05).

3.5 Virus Isolation from Mosquitoes

No dengue virus could be isolated from *Aedes* mosquitoes (59 pools) tested.

3.6 RT-PCR on Aedes Mosquitoes/ IgM Positive Sera for WNV

The results of RT-PCR on Aedes species are presented on table 2. Fourteen of 59 pools of mosquitoes (*Aedes spp*) tested showed DEN viral RNA and these include one DEN-1, 4 DEN-2, 5 DEN-3 and 4 DEN-4. However, one DEN IgM negative serum was positive by RT-PCR. Samples that showed non-specific bands were not considered. TITAN (Combination of reverse-transcription of viral RNA and subsequent Taq polymerase amplification in a single reaction vessel) seemed to exhibit higher degree of sensitivity and specificity compared with separate reverse-transcription and PCR. Sequencing of RT-PCR results was beyond the scope of this study.

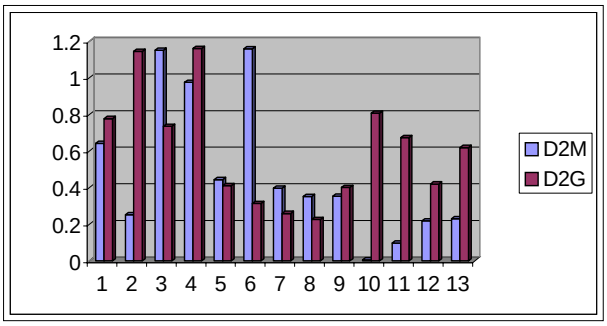

Figure 1: DEN IgM and the Corresponding IgG Antibody

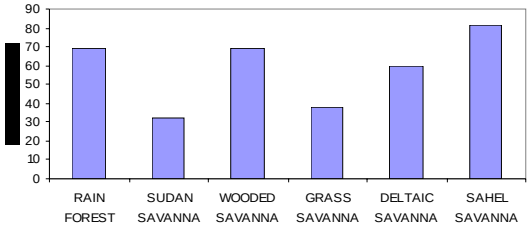

Figure 2: Zonal Distribution of DEN IgG Antibodies

Table 1: Dengue Virus Infections in Different Ecological Zones in Nigeria

	ECOLOGICAL ZONE	TOWN/ CITY	TOTAL NO TESTED	NO POSITIVE (%)	DENGUE SEROTYPE	REACTION WITH NORMAL Ag
1	RAIN FOREST	IBADAN	442	4(0.9)	D2	6(1.4%)
2	SUDAN SAVANNA	KANO	267	0(0)	NONE	6(2.2%)
3	WOODED/GRASS SAVANNA	GOMBE	341	0(0)	NONE	14 (4.1%)
4	GRASS SAVANNA	ABUJA	281	1(0.36)	D2	7 (2.5%)
5	DELTAIC SAVANNA	CALABAR	317	3(0.1)	D2	1(0.1%)
6	SAHEL SAVANNA	MAIDUGURI	300	5 (1.67)	D1 AND D2	5 (1.67%)
	TOTAL		1948	13 (0.67)		39 (2.0%)
	* NO REACTION WITH NORMAL ANTIGEN					
	** REACTED WITH NORMAL ANTIGEN					

Table 2: The Result of RT-PCR ON A*edes species*

Aedes aegypti	female	27	1	2	0	4
Aedes aegypti	males	7	0	1	2	1
Aedes species	females	12	0	0	1	1
Aedes species	males	9	0	1	1	0
unidentified	not known	4	0	0	2	2
Total		59	1	4	5	4

.

4.0 Discussion

In Nigeria most febrile cases are routinely investigated for malaria and /or typhoid and not viruses. This study has revealed that, 13 (0.67%) of 1948 febrile patients in four of six ecological zones in Nigeria had DEN IgM antibodies. Although the prevalence rate of DEN infection as revealed in this study is low, it has confirmed the activities of this virus in Nigeria. Like Yellow Fever, a positive case of DEN virus infection in a community, is of epidemiological importance. This is because, if the mosquito vector feeds on the viremic blood of a DEN infected patient, it could also transmit the virus to a high proportion of susceptible population within the environment. A significant association between the prevalence of DEN virus infections and the ecology has been observed in this study in agreement with a previous report in Nigeria. (Fagbami et al.1977). In both studies, higher prevalence of DEN infections in the Rain forest but low in Guinea savanna was observed.

A report revealed that, a positive DEN IgM by MAC-ELISA on acute serum samples is an indication that infection must have occurred sometime in the previous one or two months before sample collection (World Health Organization, 2001**).** Another study revealed that, PRNT is more specific than ELISA because it shows a monotypic reaction to the infecting virus through the late convalescent phase of illness (Vorndam and Kuno 1997). This study has shown that, DEN virus infections among those studied, must have occurred within a one or two months before samples were collected.

The prevalence rate of DEN IgG antibodies and the ecological zones were significantly different with the highest in Sahel savanna (81.7%), followed by wooded savanna (69.2%), and Rain forest (69.0%). The least among them were Grass and Sudan savanna with 32.6% and 38.1% respectively. The low percentage of people with DEN IgG antibodies in the two zones is of epidemiological importance. This is because any introduction of an epidemic strain or serotypes of any of the Flaviviruses in these zones could result in epidemic due to the presence of high proportion of susceptible host.

Thein (2003) observed that, levels of anti dengue IgG in acute phase sera collected during a period of high dengue activity correlated with disease severity but low dengue activity showed no association. In this study, because there is no active surveillance for dengue or other arbovirus activities in Nigeria, it is difficult to differentiate periods of high and low virus activities. Also, because there was no follow-up on these cases, correlation of levels of IgG and disease severity was not applicable in this study. Nevertheless the clinical importance of IgG in diagnosis of DEN infections is its usefulness in distinguishing between primary and secondary dengue infections with 100% primary and 96% of secondary being correctly classified (Innis et al. 1989, Vauhgn et al. 1999). Based on these reports, from figure 1 of this study, samples 1, 4, 9, 12 and 13 could be described as suspected cases of anamnestic response to DEN infections. Moreover, these patients could be assumed to be at the risk of developing DSS because the risk of developing DSS following an anamnestic infection was from 82-103 times greater than that of developing DSS following a primary dengue infection (Thein 2003)**.** In addition this author observed a significantly higher rate of anamnestic infections with DEN-2 (which is the most prevalent serotype of DEN in Nigeria) in DSS compared with other serotypes. Lack of surveillance activities for these viruses in the country poses constrain to the precise status of these infections in the community. For instance, in 2003 two suspected cases of viral hemorrhagic fever (based on clinical manifestations) were reported in University of Maiduguri Teaching Hospital, Maiduguri (a Tertiary Health Institution in Northeastern Nigeria. (Personal communication). These patients died within few hours on the same day they sought medical attention. It could be assumed that, when the infection was at the prodromal phase (the phase at which the symptoms and signs mimic malaria or typhoid), the patients were receiving different malaria treatments (with the assumption that the drugs were resistant to the infecting parasites) till symptoms of haemorrhages appeared. Therefore, since the patients tested in this study were not followed up, associating these cases with DSS was beyond the scope of this study. The need for active surveillance and intensive education on arbovirus activities in the environment cannot be emphasized.

The detection of DEN RNA in *Aedes species* has demonstrated the important role of the vector in the epidemiology of dengue infections in the environment. The presence of DEN RNA in male *Aedes aegypti* and *Aedes Species* is evident of vertical transmission in Nigeria and this compared favorably with previous report in Mexico (Gunther et al. 2007). In agreement with Miagostovich et al. (1988), one of the DEN IgM negative serum was found positive (DEN-3) by RT-PCR, suggesting that, most of the IgM negative samples in this study could have been false. This probably contributed to the low prevalence rate of DEN infections obtained in this study. It could be speculated that, consideration of the time of onset of symptoms during sample collection would have given more precise information on the status of these patients with regards to recent DEN infections in Nigeria. This becomes necessary because specimens taken earlier than six days after onset would have a variable percentage of false negatives due to insufficient time for antibody development. To further support the speculation, a report showed that, a small percentage of patients had detectable IgM antibodies on the day that symptoms began and most patients became positive by the sixth day after onset (Vorndam and Kuno 1977). Therefore the few IgM positive sera in this study yielded no viral RNA probably because the time of sample collection did not favor RT-PCR result. It is therefore imperative to employ the two techniques (MAC-ELISA and RT-PCR) in proper diagnosis of DEN infections.

Similar to this study in the same environment, West Nile virus infections (1.3%) have been misdiagnosed for malaria/typhoid (Baba et al. 2006). Therefore, as the clinical symptoms associated with DEN infections are indistinguishable from those of many other viral, bacterial and parasitic infections, specific diagnostic tests assume critical importance in the unequivocal identification of DEN infections (Hapugoda et al. 2007). It is important to include this virus (and possibly other endemic arboviruses) in the differential diagnosis of febrile illnesses in Nigeria. Surveillance with good

laboratory services serve as an “early warning system” against any impending outbreak of arbovirus infections.

Acknowledgment
I wish to express my profound gratitude to TWOWS (Third World Organization for Women in Science) and Management of Institut Pasteur De Dakar, Senegal for sponsoring this project. Also the technical support of University of Maiduguri Teaching Hospital (UMTH) and University of Maiduguri is highly appreciated.

CORRESPONDENCE:
M. M. BABA,
DEPARTMENT OF MEDICAL SCIENCES
UNIVERSITY OF MAIDUGURI,
P.M.B. 1069, MAIDUGURI,
BORNO STATE, NIGERIA.
E-mail: marycelinb@yahoo.com
Tel : 234 80 23612573; 234 70 39027220

REFERENCES

1. Gunther J; Martinez-Munoz TP; Perez-Ishiwara D C; Salas-Benito J. Evidence of vertical transmission of Dengue virus in two endemic localities in the State of Oaxaca, Mexico *Intervirology*. 2007; **50, (5)**:347-352
2. *Morb Morta Wkly Rep.* Dengue hemorrhagic fever-US. Mexico border. 2007; **56 (31)** 785-917
3. Holmes E C.; Worobey M..and Rambaut A. Phylogenetic Evidence for Recombination in Dengue viru. *Mol. Biol. Evol*. 1999; **16 (3):** 405-409.
4. Gubler D.J. Dengue. In: Monath, T.P. (ed): *The Arboviruses: Epidemiol. EcolVol. II. CRC Press, Florida*. 1988: 223-260.
5. Vorndam A V and Kuno G.. Laboratory diagnosis of dengue virus infections. In: Gubler DJ and G. Kuno Editors. dengue and dengue hemorrhagic fever. New York: *CAB International.* 1977: *313-33*
6. Mangiafico JA; Sanchez J L; Figueiredo LT; LeDue J W; Peters C J.Isolation of newly recognized Bunyamwera sero-group virus from a febrile human in Panama. Am. J. Trop. Med. Hyg. 1988; **39**: 593-596..
7. Chungue E; Boutin J P and Roux. Significance of IgM titration by an immunoenzyme technic for the serodiagnosis and epidemiological surveillance of dengue in French Polynesia *Res. Virol.* 1989; **140**: 229-240.
8. Innis B L; Nisalak A; Nimmannitya S; Kusalerdchariya S; Chongwasdi V; Suntayakorn S P. and Hoke C H. An enzyme-linked immunosorbent assay to characterize dengue infections where dengue and Japanese encephalitis co-circulate. *Am. J. Trop. Med.Hyg.* 1989; **40:** 418-427.
9. Beckwith W. H; Sirpenski.S; French.R A; Nelson R and May O D: Isolation of Eastern Equine encephalitis virus and West Nile virus from crows during increased arbovirus surveillance in Connecticut, 2000 (2002) *Am. J. Trop. Med. Hyg*. **66(4):** 422-426
10. Lanciotti RS; Calisher C H; Gubler D J; Chang G J and Vorndam AV Rapid detection and Typing of Dengue Viruses from clinical samples by using reverse transcriptase-polymerase chain reaction *J. Clin. Microbiol.* 1992; **30**: 545-551.
11. Fagbami A H; Monath T P; Fabiyi A: Dengue virus infections in Nigeria: a survey for antibodies in monkeys and humans. *Trans. R. Soc. Trop. Med. Hyg*. 1977; **71 (1):** 60 –65.
12. World Health Organization. Regional guidelines on dengue 1 DHF prevention and control (*Regional publication 29/1999)* 2001; 1-5.
13. Thein S. Risk factors in dengue hemoorrhagic fever.A thesis submitted for the degree of Doctor of Philosophy in the Tropical Health program, the University of Queensland.
14. Vauhgn D W; Nisalak A; Solomon T; Kalayanarooj S; Nguyen M D; Kneen R; Cuzzubbo A; Devine P L. Rapid serologic diagnosis of dengue virus infection using a commercial capture ELISA that distinguishes primary and secondary infections. *Am. J. Trop.Med. Hyg*. 1999; **60(4):** 693-8**.**
15. Hapugoda M D; Batra G; Abeyewickreme W; Swaminathan S and Khanna N. A single antigen detects both IgM and IgG antibodies elicited by all four dengue serotypes): *Clin Vaccine Immunol.* 2007*:* 1789818.

Cultivation of Straw Mushroom (Volvariella volvacea) Using Some Agro-Waste Material

[1]Onuoha C.I., [2]Oyibo, G and [1]Ebibila Judith

[1]Department of Plant Science and Biotechnology Imo State University, P.M.B. 2000. Owerri Nigeria
[2]Department of Crop Science and Biotechnology Imo State University P.M.B. 2000 Owerri Nigeria.
onuohaci@yahoo.com

Abstract: Some agro-waste materials, like paddy straw, oil palm fibre and sawdust were screened for the cultivations of the straw mushroom volvariella volvacea. The experiment consisted of four treatments; paddy straw, oil palm fibre, sawdust, and a mixture of oil palm fibre and sawdust; in a Completely Randomized Design (CRD) replicated three times. The paddy straw served as the control as it is the traditional substrate for the growth of the mushroom. The results showed that the straw naturally supported the mycelial growth and production of fruitbodies. Growth and production of fruitbodies on oil palm fibre was similar to that of paddy straw. The production of fruitbodies on the mixture of oil palm fibre and sawdust was scanty. Sawdust alone as a substrate produced few fruitbodies that were comparatively small in size. [Journal of American Science 2009;5(5):135-138]. (ISSN: 1545-1003).

Key words: Cultivation straw mushroom, agro-waste materials

1. Introduction

Mushrooms are known to be among the largest of fungi that attracted the attention of naturalists before microscopes were invented. Chang and Milles (1991) defined mushroom as macrofungus with definitive fruiting body and large enough to be seen with the naked eyes. They extended this definition by adding that mushrooms do not need to be Basidionmycetes nor aerial nor fleshy. They can grow underground having a non fleshy texture and need not be edible. Davis and Aegertar (2000) defined mushroom as the fruit of certain fungi analogous to apple on a tree. Many fungi that form mushrooms exist in mycorrhizal relationship with trees, and this is one of the reasons why forests are often generous to mushroom hunters (Ogunlana, 1978). Some wild mycorrhizal mushrooms cannot be cultivated unless the tree is also cultivated. The mushrooms are sometimes taken to the market after being collected from the forest (Kuyper *et.al*.2002,Quimio, *et al* 1990) Mushrooms are now grown worldwide as they have been recognized as food (Munjal,1970)

Edible mushrooms like *Volvariella volvacea* have attracted much attention as source of food and medicine over the years. The paddy straw mushroom is a preferred type of mushroom by most consumers because of its aroma and taste (Tharun, 1993) It grows on almost all cellulosic agricultural waste material like rice straw, banana leaves dried paddy straw etc (Reyes and Abella, 1997) These substrates are used because they contain cellulose and also pose a problem of disposal to the environment (Onuoha, 2008) So the cultivation of mushroom using the agro-waste is a way of reducing environmental waste materials (Reyes and Abella, 1997). Mushroom in recent times has become a contemporary business enterprise because of its high nutritional and medicinal values, and consequently high societal demand. There is therefore, need to maintain a constant supply of mushroom by cultivating rather than depend on seasonal forest supplies.

It is, therefore, the aim of this study, to determine the suitability of some common agro-waste materials in the growth of *Volvariella volvacea*.

2. Materials and Methods

Sources of Materials: The spawn of the mushroom was collected from Imo State Agricultural Development Programme (ADP) Owerri. The substrates like paddy straw and oil palm fibre were also collected from Imo ADP while sawdust collected from the state timber shed, Owerri.

Species Selection: *Volvariella volvacea* was selected for study because it is particularly common in Nigeria (Zoberi, 1978) It is also mostly preferred by many consumers because of its aroma and taste (Tharum, 1993). The consumption of oyster mushroom and *Volvariella volvacea* has been reported to lower the cholesterol levels in the body (Poppe, 2000).

Growth Substrates: Four agrowaste materials were used as substrates in the study. They include paddy straw, oil palm fibre, sawdust and a mixture of sawdust and oil palm fibre.

Preparation of Substrates: The straw was chopped manually and soaked in water for 24 hours. The soaked straw was rinsed in distilled water twice and drained with a sieve. The oil palm fibre was soaked in distilled water overnight in order to melt the remaining oil in the fibre. Excess water was drained off. Five hundred grammes each of the prepared sawdust and oil palm fibre were mixed up properly. One kilogramme of each substrate was used. The mixture substrates were prepared in equal proportions by weight. This was done using a weighing balance. Sawdust was mildly sprinkled with sterile distilled water.

The four prepared substrates were separately packed into polythene bags and tied up for sterilization. Boiling drum containing stacks of sticks and water up to the level of the sticks was used for sterilization. The substrates were packed into the drum and covered with fresh plantain leaves in order to generate enough heat. The substrates were steam-sterilized for three hours and allowed to cool while still in the drum, they were taken to mushroom house and poured separately on sterile polythene sheets on a table. The spawn was sprinkled on the substrates covered with sterile polythene sheet and watered daily to maintain a high relative humidity of between 75 – 80%.

Data Collection

The following parameters of growth/yield were measured:

1. Number of fruiting bodies: This was done by directly counting the number of fruitbodies produced on each substrate
2. Diameter of the pileus: This was measured by placing a transparent plastic ruler across the centre of the pileus
3. Weight of fruitbodies: Electronic weighing balance was used to determine the average weight of the fruitbodies.

   The results obtained were recorded and subjected to statistical analysis. Analysis of variance (ANOVA)

3. Results

Fifteen days after planting and incubation, whitish mycelia colonized all the substrates. Few days later fruitbodies were observed firstly on the paddy straw (control), then oil palm fibre, then 3 days later on the mixture of oil palm fibre and lastly on the sawdust (plates 1 – 4).

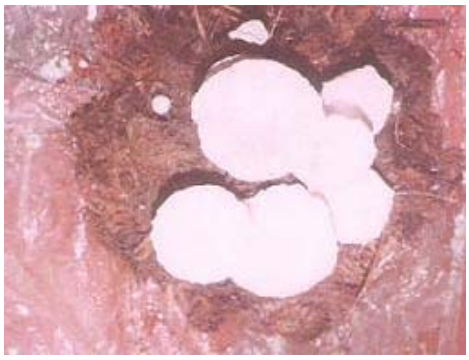

Plate 1: Showing *V. volvaceae* mushroom growing on Oil Palm fibre

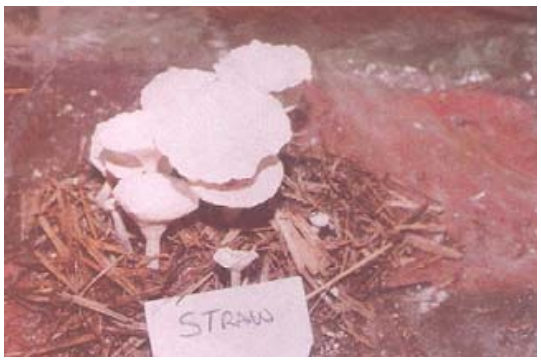

Plate 2: Showing *V. volvaceae* mushroom growing on Paddy Straw

Plate 3: Showing *V. volvaceae* mushroom growing on mixture of Oil Palm fibre and sawdust

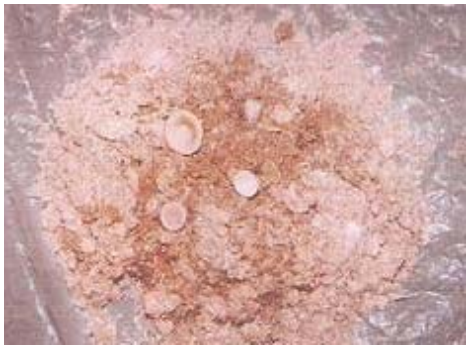

Plate 2: Showing *V. volvaceae* mushroom growing on Sawdust

Table 1: Yield parameters of the straw mushroom

Substrates	Mean no. of fruitbodies	Mean diameter of the pilens (cm)	Mean fresh weight of the fruitbodies (g)	Mean dry % water weight of the fruitbodies (g)	% of water Content of the fruitbodies
Paddy straw oil palm	13.3	3.7	16.3	10.2	37.4
fibre Saw dust	11.3	3.7	16.3	10.5	35.6
Oil palm fibre	5.6	1.8	8.0	5.3	33.8
sawdust					
	10.3	2.9	15.3	10.3	32.7

The yield parameters of the mushroom from each of the substrates are shown in table 1. While the mean number of fruitbodies produced was highest in the control (paddy straw) with 13.3, oil palm fibre and a mixture of oil palm fibre and sawdust equally produced good number of fruitbodies with 11.3 and 10.3 respectively. Sawdust yielded only 5.6

The mean fresh weight of the fruitbodies produced on paddy straw, oil palm fibre and a mixture of oil palm fibre and sawdust were high with 16.3g, 16.3g and 15.3g respectively. Also the mean fresh weight of the fruitbodies produced on sawdust was relatively low. The mean diameter of the pileus of the fruitbodies as well as the mean dry weight of the fruitbodies produced on the different substrates also appeared in the order of the earlier parameter mentioned. While the fruitbodies produced on paddy straw had the same mean diameter with those produced on palm fibre (3.7cm) the mixture of oil palm fibre and sawdust produced pileus with a mean diameter of 2.9 cm. Sawdust, however produced the smallest sized fruitbodies with a mean pileus diameter of 1.8 cm.

There is no significant difference ($P \leq 0.5$) between the mean dry weight of the fruitbodies produced on paddy straw, oil palm fibre and a mixture of oil palm fibre and sawdust. But there was a significant difference ($P \leq 0.05$) between these and those produced on sawdust.

The percentage of the moisture content of the fruitbodies produced on the different substrates showed slight variations but they are not statistically significant ($p>0.05$) except those produced on paddy straw against those produced on the mixture of oil palm fibre and sawdust.

4. Discussion

The four substrates screened, all supported the growth of the mushroom though to a varying degrees. This confirms the report of Keshari (2004) and Tricita (2005) that *Volvoriella volvacea* could be grown on agricultural waste. Apart from the paddy straw which is the traditional substrate for the cultivation of the mushroom, oil palm fibre was equally good. In terms of the number of fruitbodies produced, weight of the fruitbodies and diameter of the pileus it was as good as the control. This agrees with the findings of Isikhemhen (2004) who reported that *Volvoriella volvacea* can be cultivated on other unsupplemented agricultural waste. The duration of growth is very short and many fruitbodies could be produced within the period. It was also reported by Landford (2004) that they are not only excellent edible mushroom but also can colonize substrates and grow quickly on some unsuplemented agrowaste. There was statistically no significant difference between ($p>0.05$) the yield parameters of control (paddy straw) and oil palm fibre. This means that the oil palm fibre as an agrowaste, could be used to produce the mushroom as much as the paddy straw could produce. It might be a way of reducing agrowaste in the environment first as reported by Kuyper *et.al.*(2002) that the cultivation of *Volvariella volvacea* on local agricultural creates a way of reducing environmental pollution.

Correspondence to:

Dr. C. I. Onuoha
Department of Plant Science & Biotechnology
Imo State University, Owerri,
Imo State Nigeria.
Email: onuohaci@yahoo.com

References

Chang, S.T. and Milles, P.G. (1991) Recent trends in wood production of edible mushrooms. The mushroom Journ. 503: 15 – 18

Davis, R.A and Aegerter, B.J. (2000) Edible mushroom cultivation Scientific publishers Ladpur India 2 -5

Isikhemhen, O.S. (2004) Volunteer trainer to Imo ADP extension staff on mushroom production using locally available substrates (palm fibre, and

sawdust) A seminar 27th – 30th Dec. 2004. Owerri, Imo State, Nigeria.

Keshari, L.M. (2004) Center for Agricultural Technology Nepal Mushroom growing for a living worldwide

Kuyper, T.N., Vandigk, J.F.N and Onguene, N.A. (2002) Knowledge and utilization of edible mushroom by local population of mains forest of South Cameroun Abstract #365, IMC7 Oslo Norway pp 115.

Landlord, K.C (2004) Poverty alleviation by mushroom growing in Zimbabwe. University of Zimbabwe pp 408.

Munjal, R.A., Kapoon, J.N. and Bahl, N. (1970). Mushroom Cultivation. Advances in Mycology and Plant pathology 1: 83 – 84.

Ogunlana, S.K (1992) Studies on the cultivation of the edible mushroom Pleurotus tuber-regium (Fr) singer. Tropical Journ. Appl. Sci. 2: 56 – 60

Onuoha, C.I. (2007) Cultivation of the mushroom (pleurotus tuber-regium) using some local substrates Life Science Journ. 4(4): 58 – 61

Poppe, J. (200) Use of agricultural waste materials in the cultivation of mushroom in: Van Griensven ed.: proceedings 15th International congress on sciences and cultivation of edible mushroom Balkema Rotterdan, 2 – 23

Quimo, T.H., Chang S.T. Royse, D.J. (1990 Technical guidelines for mushroom growing in the tropics. Food and Agriculture Organisation of the United Nations Rome. 106

Reyes, R.G. and Abella, E.A. (1997) Myuhial and Basidiocamp performance of P. sayor-cajn on the mushroom spent of V. volvalea. Proceedings of international seminar on the Development of Agribusiness and its unpirt on Agricultural Production in South earth Asia. Tokoyo NODA1 Press. 491 – 497

Tharun, G. (1993) Promotion of mushroom production and Bioconversion of wastes for income generation in rural areas. CDG 3EAPO's Biotechnology Training Project. In Chang, St. Bussivell JA and Chril, S (eds) Mushroom Biology and Mushroom products. Hong Kong Chinese University Press. 307 – 318.

Tricita, H.O (2005) University of Philippines at Los Banos the Philippines Published by Mush world. Republic Korea.

Zoberi, M.H (1992) Tropical Macrofungi. Macmillan Press Ltd. Londong P 158.

Rooting of Stem Cuttings of *Ginkgo* Living Fossil Under Threat

[1]Vijay Kant Purohit*, [2]Prakash Chandra Phondani, [2]Lakhpat Singh Rawat, [2]Rakesh Kumar Maikhuri, [2]Deepak Dhyani and [1]Anant Ram Nautiyal

[1]High Altitude Plant Physiology Research Centre (HAPPRC), H.N. Bahuguna Garhwal University, Srinagar (Garhwal) - 246 174, Uttarakhand, India
[2]G.B. Pant Institute of Himalayan Environment and Development, Garhwal Unit, Srinagar (Garhwal) 246 174, Uttarakhand, India
vijaykantpurohit@rediffmail.com,pc.phondani@rediffmail.com,lsrawat@rediffmail.com,rkmaikhuri@rediffmail.com,deepak_smile@rediffmail.com, arnautiyal@gmail.com

Abstract: A systematic study were carried out to examine the rooting ability of male and female branch cuttings of *G. biloba* under different microclimatic conditions i.e. polyhouse, polypit, and open while using plant growth hormone (IBA) and a systematic fungicide (Bavistin; containing 50% Carbendazim) for raising maximum number of planting materials. Various concentrations 100, 250 & 500 µM of IBA and 0.1, 0.5 and 1.0% of a systemic fungicide Bavistin were applied to the cuttings. The higher concentration of IBA (500 µM) resulted maximum rooting (50.0%) in male cuttings and Bavistin (1.0%) produced maximum 41.66% in male and 58.33% in female cuttings, respectively, whereas no rooting was recorded in both male & female cuttings kept in all the microclimatic conditions as control. The highest number of roots (7.5) per male cuttings was formed in 500 µM IBA while 5.0 roots per female cuttings was formed in 100 µM IBA treatment. Cuttings planted inside polyhouse and in the open conditions did not survive and died after bud sprouting. Since this is a rare species and has got the status of living fossils being known from rocks as old as 200 million years, growing naturally and only few individuals are reported to exist and therefore vegetative propagation may be viable option for its multiplication and conservation to save this species from extinction. [Journal of American Science 2009;5(5):139-144]. (ISSN: 1545-1003).

Keywords: *Ginkgo biloba*/living fossil/ Rooting/ propagation/ Indole - 3 - butyric acid/ Bavistin/ medicinal tree/ conservation

1. Introduction

Unfortunately, due to legal and illegal exploitation of important plant species from wild, anthropogenic pressure and lack of knowledge about sustainable harvesting of useful bioresources particularly medicinal ones as many of them has been listed under the categories of rare, threatened, endangered or at the verge of extinction. Although the extinction of species is a natural process, the current speed of extinction of species through human interventions is approximately 100-1000 times faster than the natural speed of extinction. In many groups of organisms 5-20% of all species are already extinct (Chaplin et al. 2000). The species currently on earth are the result of a natural selection process over the last three billion years, which has lead to a large degree of specialization. Species diversity is therefore a prerequisite for ecosystem to function. But how important are species and ecosystems for society? This can be researched by investigating the functions and associated goods and services of ecosystems that are important for humans. A central problem is a continuing loss of biodiversity, but our knowledge about human dimension of biodiversity is still relatively limited. However, there are several plant species growing in this earth but has not still given priority for conservation due to lack of awareness about their usefulness, economic potential and applicable multiplication technology package.

The *Ginkgo biloba* Linn. (MAIDENHAIR TREE; family Ginkgoaceae) is worldôs oldest tree mostly known as living fossils and only surviving member of seed plant groups. It is found growing naturally in very limited localities in the central Himalayan mountain at an elevation of 6000 ft (Anonymous, 1999). It is a handsome, straight, up to 100 ft. high, sparsely branched when young, bearing clusters of fan shaped leaves and dioecious slow growing gymnosperm and known to have huge medicinal, spiritual and horticultural importance worldwide. The Leaves of this species is extensively used in the form of a concentrated, standardized Ginkgo biloba extract (GBE) in different countries (particularly China, Europe, France and Germany) as a source of herbal

on kg of purposes litionally

*G*inkgo is being used to treat circulatory disorders and enhance loss of memory. Its leaves contain two types of chemicals (flavonoids and terpenoids) have potent antioxident properties. It is also widely used for treating dementia, eye problems, intermittent claudicating, memory impairment, tinnitus and a variety of other ailments including altitude sickness, asthma, depression, disorientation, headaches, high blood pressure, erectile dysfunction, and vertigo (http://www.umm.edu/altmed/ConsHerbs/*GinkgoBilob*ach.html).

In central Himalayan Mountains of India, there are very few spots in Uttarakhand (i.e. Ranikhet, Nainital and Dehradun) where the individuals of this species are found growing naturally and require immediate conservation measures. However, countries like China, Europe, France, and Germany have already undertaken initiatives for large-scale propagation and plantation for its conservation so as to maintain its status and population on one hand and to make use of it properly in the field of herbal medicine in near future. Despite of having huge medicinal properties and ornamental value, this species still has not received much attention as far as conservation is concerned particularly in India. Due to poor regeneration, only few individuals exists in the nature particularly in diverse climatic conditions in different places and facing serious threat of extinction from central Himalayan mountains of India. Since this is a rare species and has got the status of oldest living tree fossils and therefore require urgent propagation protocol for large-scale multiplication. Rooting of stem cuttings provides the advantage of greater genetic uniformity and availability of superior stock in a short period of time for afforestation works. This method has been tried sufficiently in number of gymnosperms as well as angiosperms trees (Nandi et al. 1996, Tamta et al. 2000, Nandi et al. 2002, Purohit et al. 2005). The vegetative propagation studies on *Ginkgo biloba* has been reported by Dirr et al. 1987, Doran, 1954 and Natalia, 1994). Using auxins, but there are very few studies or reports available in Indian Himalayan region where phenolic compounds either alone or in combination with auxins were applied (Prakash et al. 2002 and Gopichand et al. 2006). In view of this, an experiment on vegetative propagation using rooting of branch cuttings was carried out to examine the effect of IBA and Bavistin under different microclimatic conditions.

2. Material and methods

The experiments were carried out inside the polyhouse, polypit and in the open conditions (details given below) established in the G. B. Pant Institute of Himalayan Environment & Development, Garhwal, Unit, Srinagar, Garhwal, Uttarakhand, India, (30° 13' 05.8" N and 78° 46' 24.5" E; 584 m amsl). Branch cuttings (semi - hardwood) were excised in the morning and brought to the laboratory in polythene bags in order to prevent desiccation, during the first week of January 2006 from mature single male and female tree of *G.biloba* (of more than 50 years old trees) growing in Kalika (1750 m amsl) and Chaubatia (1850 m amsl) areas of Ranikhet (Distt. Almora, Uttarakhand, India), respectively. The final cuttings (average length 10.52 ±0.88 cm male and 11.14 ±0.32 cm female, dia. 8.82±0.34 mm male and 9.21±0.41mm female, with atleast 3-4 nodes per cutting) were clipped from the branches. The basal 2.0 cm portion of cuttings was dipped in various concentrations of test solutions for 24 h at 22°C. The treatments consisted of Indole - 3 - butyric acid, IBA 100, 250 & 500 µM; HiMedia Laboratories Pvt. Ltd, Mumbai) and Bavistin (0.1, 0.5, 1.0%; a systemic fungicide; containing 50% Carbendazim, a. i.; from BASF India Ltd., Mumbai, India); one untreated set served as control. The IBA was dissolved in 1.5% (v/v) aqueous ethanol; control cuttings were dipped in aqueous ethanol (1.5%, v/v). In each treatment only 24 cuttings were applied.

Following treatment, cuttings were planted vertically in polythene bags (16.0 cm h x 8.0 cm dia; one cutting per bag) containing sieved rooting mixture (equal parts of sand, soil and farmyard manure) and placed in following microclimatic conditions.

2.1. Polyhouse: A small polyhouse of 20 ft length x 9.0 ft width and 7.0 ft height (in the middle) was erected with the help of bamboo poles and covered with a thin semi-transparent polyethylene sheet (thickness: 162.5 µM, UV stabilized) from all the sides. The door could be opened at the front end to access the polyhouse.

2.2 Polypit: A pit dug in the ground (size 10.0 ft L x 6.0 ft W x 3.0 ft D), covered on the top with a semi ï transparent polyethylene sheet (thickness: 162.5 µM, UV stabilized) supported by a bamboo frame. On one side, a small mud wall (about 30 cm high from the ground level, sloping on the two sides) was raised. The polyethylene sheet was sealed on higher side with mud, leaving three sides

could be
ll as the
o form of plastering (even with mud) was carried out. As a routine polyethylene covers from the top of the polypit were partially opened during the daytime after midday for a few hours (see Vyas et al. 1999 for details about its function and benefit).

2.3 Open: Open field space without any cover or modifications.

Observations were taken six months after treatment and planting for estimation of percent rooting, number of roots formed per cutting, root diameter and the length of individual roots. Only those cuttings with one or more clearly visible root initials (≥ 2 mm) and/ or roots were classified as having rooted (Nandi et. al. 1996). Following this the well rooted cuttings were again planted in polybags and moved into the shade house, receiving 50% sunlight for hardening and the plants were watered periodically (Fig. 1E).
Least significant differences (LSD), standard error (SE) were calculated for comparison among the treatments following the methods as described by (Snedecor and Cochran, 1967). Analysis of variance (ANOVA) was performed using the Microsoft excel programme.

3. Results

Rooting ability of male and female branch cuttings of *G.biloba* was examined inside polyhouse, polypit and in the open conditions. Cuttings planted in all the conditions exhibited 70-80% bud sprouting (Figure 1A and B). Based on the random observations, cuttings planted in polyhouse and in the open were dried up after four months of planting, therefore, details data of both the conditions are not presented. The first root initiation was observed at six months in majority of the cuttings planted inside polypit (average temperature and relative humidity (RH) during experiment period; 25-30°C, with 60 to 80%). The cuttings under control sets failed to root in both male & female even planted under polypit condition. LSD (P = 0.05) indicates significant differences in all the attributes measured for different treatments. IBA (500 µM) and Bavistin (1.0%) were found very effective for root formation. A maximum 50.0% rooting success was achieved in male cuttings (Table 1 and Figure 1C) with the application of 500µM IBA treatment on an average of 6.71 roots per cuttings and average root length of 3.27 cm, while Bavistin 1.0% treatment produce maximum rooting success 41.66% (with an average of 4.83 roots per cuttings and average root length 3.19; Table 1) in male cuttings and 58.33% (with an average of 4.66 roots per cuttings and average root length 4.0 cm) in female cuttings of *G. biloba* (Table 2 and Figure 1D). Other concentration tried 100 µM IBA was found to be slightly effective with rooting success of 33.33% in female cuttings with an average of 5.0 roots per cuttings and average root length of 3.25 cm. In male cuttings average length of longest root 7.5 cm and 7.32 cm while in female cuttings 6.83 cm and 6.72 cm was recorded with 500µM IBA and 1.0% Bavistin treatment, respectively. The maximum root diameter was recorded 1.26 mm for male (Table 1) and 1.53 mm for female cuttings (Table 2).

Table 1. Effect of IB on rooting respons male cuttings insic condition **Treatments**	**% Rooting**	**No. of roots/ cutting (mean ±SE)**	**Avg. Root length (mean ±SE, cm)**	**Length of longest root (mean±SE, cm)**	**Avg. root diameter (mean ±SE, mm)**
IBA (100 µM)	20.83	3.77±0.88	2.61±0.57	5.0±0.73	1.22±0.26
IBA (250 µM)	25.00	2.5±0.35	3.48±1.03	5.35±1.52	0.94±0.21
IBA (500 (µM)	50.00	6.71±1.30	3.27±0.36	7.5±1.02	1.26±0.06
Bavistin (0.1%)	-	-	-	-	-
Bavistin (0.5%)	29.0	5.28±0.37	2.90±0.39	5.41±0.33	1.04±0.15
Bavistin (1.0%)	41.66	4.83±0.60	3.19±0.41	7.32±1.25	1.08±0.08
LSD (p = 0.05)	**30.67**	**4.18**	**2.08**	**4.63**	**0.73**

SE = Standard error of mean. All values are an average of 24 cuttings.
A dash (-) indicates cuttings did not root.

Source of variation	DF	Mean Square	F-ratio
Treatments	5	112.6579	2.194888^{ns}
Parameters	4	742.7473	14.47077**
Error	20	51.32741	

**Level of significance at 0.05; ns: not significant

Table 2. Effect of IBA and Bavistin on rooting response of *G. biloba* female cuttings inside the polypit condition

Treatments	% Rooting	No. of roots/ cutting (mean ±SE)	Avg. Root length (mean ±SE, cm)	Length of longest root (mean±SE, cm)	Avg. root diameter (mean ±SE, mm)
IBA (100 µM)	33.33	5.0±2.0	3.25±0.76	4.96±1.56	1.46±0.12
IBA (250 µM)	20.83	2.8±0.86	3.77±1.13	4.96±1.56	1.46±0.12
IBA (500 (µM)	12.5	4.0±1.52	5.14±1.13	6.83±1.96	1.35±0.13
Bavistin (0.1%)	12.5	4.33±1.85	3.33±0.63	4.83±1.58	1.12±0.13
Bavistin (0.5%)	20.83	1.5±0.35	1.56±0.23	2.0±0.0	1.34±0.22
Bavistin (1.0%)	58.33	4.66±1.33	4.0±0.58	6.72±0.84	1.53±0.11
LSD (p = 0.05)	**30.67**	**2.35**	**1.83**	**2.94**	**0.24**

SE = Standard error of mean. All values are an average of 24 cuttings.

ANOVA Summary Table

Source of Variation	DF	Mean Square	F-Ratio
Treatments	5	72.14717	1.216312^{ns}
Parameters	4	643.7649	10.85308**
Error	20	59.31633	

**Level of significance at 0.05; ns: not significant.

Figure 1. Propagation of *Ginkgo biloba*: (A) A mature tree of *G. biloba*, (B) A sprouted male and female cuttings, (C&D) well rooted male and female cuttings and (E) Cuttings raised plants kept inside shade house for hardening.

4. Discussion

The stimulation of adventitious root formation in stem cuttings with auxins and commercial rooting mixtures is well known in many species those are difficult-to-root (Morsink and Smith, 1974, Blazich, 1998, Nandi et al. 1996, Purohit, 2002). The effect of growth hormone and fungicide on adventitious root formation in semi - hardwood cuttings of *G.biloba* in different microclimatic conditions, was examined for the first time. Although there are several studies available on the propagation of gymnosperms and angiosperms trees using stem cuttings (Nandi et al. 1996, 1997, 2002, Tamta et al. 2000, Purohit et al. 2005). The rooting efficiency observed in *G. biloba* showed satisfactory result within six months of planting inside the polypit conditions whereas reports available reveals that cuttings taking two years to root in natural conditions (Annonymous, 1999),

under
results
te that in the present study the application of IBA (500µM) significantly improved the rooting up to 50.0% in male cuttings whereas the application of Bavistin (1.0%) was found more effective in both the cuttings (male and female) with highest rooting response was observed in female cuttings (58.33%). However, on the other hand, the application of growth regulators (catechin and gallic acid) produced 53.3% and 56.7% rooting respectively, in the semi hard woodcuttings of *G. biloba* (Gopichand et al. 2006). Besides, the applications of different phenolic compounds were applied to assess the rooting response in *G.* biloba (Prakash et al. 2002) and they reported that the combination of IBA (500 mg/l) and catechin (5 mg/l) enhanced the rooting upto 96.0%.

IBA and Bavistin have also been reported to be more effective in inducing rooting in stem cutting of *Taxus baccata* (Nandi et al. 1996, 1997) and *Cedrus deodara* (Nandi et al. 2002). The rooting percentage displayed a positive trend with increasing concentrations of chemicals in this study. Applications of auxins enhanced rooting and root quality in many tree species (Hartman and Kester, 1983). The application of IBA may have an indirect influence by enhancing the speed of translocation and movement of sugar to the base of cuttings and consequently stimulate rooting (Haissig, 1974). Treatments with a systematic fungicide, Bavistin were also found effective in this study, however, the mechanism of stimulation of rooting by Bavistin is not clear. It may be related to auxin ï like activity of benomyl, which is known to be converted into carbendazim in water and in contact with plants (Thurston et al. 1979). Application of 500µM IBA and 1.0% Bavistin also enhanced the number of roots developed on each rooted cuttings as compared with another concentrations applied. This may have an advantage by enhancing good anchorage when planted in the field. Besides the effect of IBA and Bavistin, the diameter of cuttings may also have influenced the root formation on the cuttings whereas most of the thin cuttings either dried up or could not develop root even after six months.

In the present study rooting of stem cuttings was carried out in the months of January to June because of the deciduous nature of tree, best sprouting of dormant buds, active growth season which has been reported to favor rooting of cuttings (Loach, 1988). High humidity environments created by means of mist systems or plastic covers are commonly used in vegetative propagation experiments to reduce the risk of water stress (Hartmann et al.1990). Generally, spring season when the fresh flush starts is considered to be the best period for rooting.

5. Conclusions

The results of this study are important and low natural regeneration as reported in this species can be supplemented with clonally propagated plants raised through rooting of stem cuttings. Moreover, it is important to note that the cuttings were taken from mature trees from different sources; further trials in different seasons may result in better rooting efficiency and genetically specific-differences. Due to poor economic condition and tough terrain in the mountains the construction of Green houses are difficult, therefore, a low cost polypit (poor man growth chamber) can meet out the requirement of rooting of cuttings and raising maximum number of plants. Keeping in view the present status, importance and conservation value of *G. biloba* a multi-faceted efforts is required while involving local communities, scientific institutions and NGOs for its nursery raising and afforestation programmes. Further, well-rooted plants could be obtained within a short time; the method is also inexpensive and easy to perform. It is hoped that it will be acceptable to the involved in the forestry sector.

Acknowledgements:
Financial support from the Department of Science and Technology (DST-SERC division), and Ministry of Environment and Forest, Govt. of India is gratefully acknowledged.

***Correspondence to:**
Dr. Vijay Kant Purohit, Ph.D.
Scientist
Herbal Biotechnology & Extension Research
High Altitude Plant Physiology Research Centre (HAPPRC), H.N. Bahuguna Garhwal University (A Central University), Srinagar (Garhwal) - 246 174, Uttarakhand, India
Email: **vijaykantpurohit@rediffmail.com**
Phone: 01346:253760, Ext: 211

References

[1] Anonymous. The wealth of India - Raw Materials, Council of Scientific and Industrial Research, New Delhi. 1999; Vol. IV, pp. 1 -287.
[2] Blazich FA. Chemicals and formulation used to promote adventitious rooting. In: Davis TD, Haissig B. E. & Sankhla N. (eds.), Adventitious root formation in cuttings. Dioscorides Press, Portland, USA. 1998; pp. 132-149.

uences
: 234-

[4] Dirr MA, Heuser CW Jr. *The* reference manual of woody plant propagation: from seed to tissue culture. Athens G.A. Varsity Press. 1987; 239 p.

[5] Doran WL. The vegetative propagation of *Ginkgo*. Journal of Forestry 1954;52(3): 176-177.

[6] Gopichand, Rakesh N, Ramjee LM, Singh RD, Ahuja PS. Effect of Different Growth Regulators on Vegetative Propagtion of *Ginkgo biloba*. Indian Scientific and Industrial Research Bulletin 2006; 14 (1).

[7] Haissig BE. Influences of auxin synergists on adventitious root primordium initiation and development. NZ Journal of Forest Science 1974; 4: 311-323.

[8] Hartman HT, Kester DE. Plant propagation-Principles and Practices. Prentice Hall, Englewood Cliffs, New Jersy1983; p. 662.

[9] Hartmann HT, Kester DE, Davis FT. Plant Propagation: Principles and Practices. 5th ed. Prentice-Hall publishers, Englewood Cliff, NJ, USA 1990; p. 647.

[10] Loach K. Controlling environmental conditions to improve adventitious rooting. In: Davis, TD, Haissig BE, Sankhla N (eds.), Adventitious root formation in cuttings. Dioscorides Press, Portland, USA 1988; pp. 248ï 273.

[11] Morsink WAG, Smith VG. Root and shoot development on cuttings of basswood (*Tilia Americana* L.) as affected by auxin treatments and size of cuttings. Canadian Journal of Forest Research 1974; 4: 246-249.

[12] Nandi SK, Palni LMS, Rikhari HC. Chemical induction of adventitious root formation in *Taxus baccata* cuttings. Plant Growth Regulation 1996; 19: 117-122.

[13] Nandi SK, Rikhari HC, Nadeem M, Palni LMS. Clonal propagation of *Taxus baccata* L.- A Himalayan asset under threat. Physiology and Molecular Biology of Plants 1997; 3: 15-24.

[14] Nandi SK, Tamta S, Palni LMS. Adventitious root formation in young shoots of *Cedrus deodara*. Biologia Plantarum 2002; 45(3): 473-476.

[15] Natalia SS. A unique mode of the natural propagation of *Ginkgo biloba* L. ï A key to the problem of its ñsurvivalò. Acta Palaeobotanica 1994; 34(2): 215-223.

[16] Prakash O, Nagar PK, Brij L, Ahuja PS. Effect of auxins and phenolic acids on adventitious rooting in semi-hardwood cuttings of *Ginkgo biloba*. Journal of Non-Timber Forest Products 2002; 9(1/2): 47-49.

[17] Purohit VK. Mass propagation of Banj, Tilonj and Phaniyat oaks. Ph.D. Thesis submitted to H.N.B. Garhwal University, Srinagar (Garhwal), 2002; 180 p.

[**18]** Purohit VK,Palni LMS, Nandi SK. Root formation in stem cuttings of *Quercus glauca* Thunb. and *Q. floribunda* Lindl. : Oaks from the Indian Central Himalaya. National Academy of Science Letters 2005; 28 (No. 7 & 8): 5-6.

[19] Snedecor GW, Cochran WG. Statistical methods, oxford and IBH Publishing, New Delhi, India1967.

[20] Tamta S, Purohit VK, Nandi SK, Palni, LMS. Chemical induction of root formation in *Quercus leucotrichophora* L. stem cuttings. Indian Journal of Forestry, 2000;23(2): 135-138.

[21] Thurston KC, Spencer SJ, Arditti J. Phytotoxicity of fungicides and bactricides in orchid culture media. American Journal of Botany 1979; 66: 825-835.

[22] Vyas P, Bisht MS, Bhuchar S, Sharma S, Palni LMS. Polypit: An improved technique for raising nursery plants. Journal of Sustainable Forestry, 1999; 8 (1): 43-59.

[23] WWF Journal. Apotheke Wildnis: Naturmedizin boomt ï auf Kosten der Natur. 2000; P. 25, issue 4/2000, WWF-Germany.

The Role Played By Azores High in Developing of Extratropical Cyclone Klaus

Yehia Hafez

Astronomy and Meteorology Department, Faculty of Science, Cairo University, Giza, 12613, Egypt

d_hafez@hotmail.com

Abstract: On 24 January 2009 southern France and northern Spain were affected by a severe windstorm associated with extratropical cyclone Klaus. This paper investigates the role played by Azores high in developing of extratropical cyclone Klaus. The 6-hour and daily NCEP/NCAR reanalysis data composites for meteorological elements (surface pressure, sea surface temperature , surface wind, surface relative humidity, and geopotential height and wind fields at 500 mb level) over the northern hemisphere for the period of 20-25 January 2009 were used in this study. In addition, satellite images for cyclone Klaus and its damage have been used. The results revealed that, the Azores high pressure system extended strongly and rapidly to the east direction towards the North Africa and it was accompanied with an eastward extension of a deep low pressure system over the northern Atlantic region. The combination of the two opposite pressure systems together over Atlantic Ocean creates a very strong pure westerly air current moving toward the eastward direction. This huge westerly winds set aside the air over the eastern Atlantic region and western European coasts and forced it to sweep and to circulate westward direction and develop cyclonic circulation system which originating in the west of Bay of Biscay, extratropical cyclone Klaus. The development theory and the life cycle of Klaus model are uncovered. Uncover of the life cycle model of cyclone Klaus conduct to a new theory of cyclones development which so called the cyclonic circulation theory. [Journal of American Science 2009;5(5):145-163]. (ISSN: 1545-1003).

Keywords: Azores high; cyclone Klaus; air mass; cyclonic circulation theory

1. Introduction

On the early morning of Friday January 23, a strong low pressure system, extratropical cyclone Klaus was developed over the northern Atlantic region with a minimum central pressure of 1000 mb. On Friday night, it moved eastward across the Bay of Biscay towards southern France bringing damaging winds to the southwest of France and to northern Spain. Klaus landfall strongly crossing southern France and northern Spain and entered the Bordeaux region of France early Saturday morning with a minimum central pressure of 966 mb and intense wind gusts on the order of 150 kph and higher. Surface wind speeds were recorded at 180 kph, and even at 200 kph on the first inland higher ground. These wind speeds correspond to those experienced in Hurricanes Category (III) according to the (Safir-Sampson) scale of hurricane intensity. The storm swept in from the Atlantic Ocean and continued to track east causing significant damage across northern Spain and waves as high as 21 meters off of the Basque coast. However, this storm wreaking havoc across the region. Klaus caused the death of 21 people and left a path of heavy destruction stretching from approximately Bordeaux to the Mediterranean coast and all along northern Spain. Besides expected substantial damages to property, life lines and electricity networks have also been hit hard. Similarly hard hit have also been forests in south-western France, with reported losses of up to 70% of stock in certain areas. An estimated 60 to 70 percent of the pine trees in Lands Forest, one of Europe's largest, had been uprooted. Storm Klaus caused widespread destruction: building damage, power outages, flooding and travel disruption, and the landscape of the Department of Les Lands was changed for perhaps the next hundred years. Recent assessments by catastrophe modeling firms estimate are ranging as high as €5 billion in respect of this storm. However, this storm was weakening in the afternoon of 24 January 2009.

There are several scientific literatures challenges the developing and life cycle of midlatitude cyclones and extratropical marine cyclones e.g. (Bjerknes (1919); Bjerknes and Solberg (1922); Bottger, et al., (1975); Hadlock and Kreitzberg (1988); Shapiro and Keyser (1990); Davies, et al., (1991); Wakimoto et al., (1992);

Neiman and Shapiro (1993); Neiman et al., (1993); Evans et al., (1994); Schultz et al., (1998) Nielsen and Sass (2003)). These literatures were refereed the development and life cycle of cyclones to the models of Norwegian frontal- cyclone model (Bjerknes 1921; Bjerknes and Solberg 1922) and Shapiro-Keyser life cycle model (Shapiro-Keyser 1990) for extratropical marine cyclones. Cyclonic development in midlatitudes was based on the concept of the polar front theory of atmospheric circulation (Bjerknes and Solberg 1922). In one hand, there are valuable researches challenge the field of hurricanes formation and hazards (e.g. Gray (2001); Zebrowski and Judith (2005); Asbury et al., (2006) and Hafez (2008)). In other hand, the effect of the geopotential height anomalies and blocking systems in the upper atmospheric levels upon the European climate studied by (Rex (1950a, 1950b, and 1951); Cohen et al., (2001); Hafez (2007 and 2008)…etc.). However, the present work aims to uncover the role played by Azores high in the developing of extratropical cyclone Klaus.

2. Data and Methodology

The 6-hour and daily NCEP/NCAR reanalysis data composites for meteorological elements (surface pressure, sea surface temperature, surface wind, surface relative humidity , and geopotential height at the 500 mb level) over the northern hemisphere for the period 20 to 25 January 2009 (Kalnay et al., 1996) were used in this study. In addition, satellite images for extratropical cyclone Klaus and its damage were used. Satellite images were obtained from Dundee Satellite Receiving Station and NOAA. In the present work, these datasets were analyzed using the anomalies methodology. The track of the center of the cyclone, labeled with passing dates, UTC times and minimum MSLP's analyzed by HIRLAM-AEMET numerical model, has been used. In addition to that the 6 hours time step air mass RGB composite satellite images through the developing stages in the life cycle of the cyclone Klaus has been analyzed.

3. Results

3.1 Analysis of synoptic situation of extratropical cyclone Klaus

The current study presents the synoptic regime analysis of the development and life cycle of extratropical cyclone Klaus that exited over middle of the North Atlantic Ocean, west of Bay of Biscay, on 23 - 24 January 2009. The available meteorological data sets as mentioned above in the section of data and methodology had been used in this analysis. Extratropical cyclone Klaus developed as a system with a clear surface pressure signal approximately started on day 23 about 0000 UTC, in the middle of the Atlantic, at position shown in Figure (1), with a minimum mean sea level pressure (MSLP) value of 1000 mb. Rapidly, reaching its explosive development rates as high as 34 mb in 24 hours, and registered maximum surface wind gusts of the order of 200 km/h. This cyclone moved eastward and its track was purely zonal and its speed was markedly high, reaching values above 100 km/h. A minimum surface pressure of about 964 mb at cyclone center took place on day 24 at about 0000 UTC. Figure (1) shows an approximate 6- hour track of the center of the cyclone, labeled with passing dates, UTC times and minimum [Source; High Resolution Limited Area Model, (HIRLAM-AEMET) Spain Agency of Meteorology]. However, the intensity of cyclone Klaus reached the intensity of hurricanes of category (3), according to Safir - Sampson hurricane scale (Zebrowski and Judith (2005)). However, Klaus formation may be is the start point that Atlantic hurricanes invade Western Europe.

Analysis of the wind field at the surface and at 500 mb level illustrates that the flow of air current is completely from west to east (purely zonal flow) over the northern Atlantic region through the period of 23-24 January. Analysis of the geopotential height at 500mb shows that the flow aloft over the northern Atlantic Ocean is completely westerly flow, and the Rossby wave was completely disappears on the synoptic charts over the northern Atlantic region through the period of 23-24 January 2009 see Figure (2). However, Rossby wave zonal phase propagation is always westward relative to the mean zonal flow, furthermore, the Rossby wave phase speed depends inversely on the square of the horizontal wavenumber. Therefore, Rossby waves are dispersive waves whose phase speeds increase rapidly with increasing wavelength, Holton (2004). Absents of Rossby wave stopped the westward motion of the air currents and this leads to increase of the phase speed of the air current to be completely the mean zonal wind flow. In addition to that, the analysis of the mean sea level pressure and geopotential height at 500mb illustrates that, the Azores high pressure system extended strongly and rapidly to the east direction towards the North Africa and it was accompanied with an eastward extension of a deep low pressure system over the northern Atlantic region through the period of 23-24 January 2009 as shown in Figure (2). The combination of the two opposite pressure systems together over Atlantic Ocean creates a very strong pure westerly air current moving toward the eastward direction. This huge westerly winds set aside the air over the eastern Atlantic region and western European coasts to forced to swept and to circulate

westward direction and initiate the cyclonic circulation system which originating in the west of Bay of Biscay, extratropical cyclone Klaus, not only that but also to pushing Klaus itself to landfall strongly crossing southern France and northern Spain. Analysis of the 6-day mean anomaly of the geopotential height at 500 mb for the northern hemisphere for January 2009 revealed that there was an outstanding positive anomaly of more than +175 m over Eastern Atlantic region simultaneously with negative anomalies of less than -200 m over North Atlantic Ocean during the six days from 20 to 25 of January 2009 as clear from Figure (3a). In contradicting to that, the analysis of sea surface temperature over the northern Atlantic region shows no any significant variation of SST through that period, also, there were no positive or negative anomalies in SST temperature over this region through that period as shown in Figures (5 and 4a). Meanwhile, it is clear that, from surface relative humidity analysis that there are outstanding positive anomalies in relative humidity over the northern Atlantic Ocean through that period. See Figures (3b and 6). In addition to that, there are remarkable positive anomalies in the surface wind reached (+ 12 m/sec) at the surface, see Figure (4d).The advection of the different types of air mass over the northern Atlantic Ocean through the period 23-24 January 2009 can be noticed in the RGB satellite images (Figure 7). The composite satellite image is obtained by water vapors and infrared channel differences. The infrared channel is used in determining the temperature of satellite-observed surface. For this reason, the RGB is useful for observing the air mass type. Analysis of The 6 hours time step air mass RGB of the develop and life cycle of cyclone Klaus from 0000 UTC on 23 to 1800 UTC on 24 January 2009 shows clearly the development stages, whereas there is a two different air masses, air mass (1) and air mass (2), and fast moving nature of the cyclonic system, and the nearly zonal path that it followed, as it is illustrated in Figure (7).

3.2. The role of Azores high in developing of extratropical cyclone Klaus

The results from the above mentioned synoptic study revealed that, the Azores high pressure system aloft becomes stronger than usual and was extended rapidly to NE direction towards the north Africa at 35° N and supply the north Atlantic region by westerly air current. This high pressure accompanied with an eastward extension of low pressure system over the northern east of Atlantic Ocean at higher latitudes 65° N through the period of 23-24 January 2009, that supply too the north Atlantic region by westerly air current; see Figures (2 and 3a). The combination of the two distinct pressure systems existed over the middle of Atlantic Ocean creates together a very strong purely westerly air current which moved toward the eastward direction causing of a wind storm. This huge completely westerly air current set aside the air over the eastern Atlantic region to forced to swept and to circulate westward direction and develop the cyclonic circulation system which originating in the west of the Bay of Biscay, extratropical cyclone Klaus, not only that but also to pushing Klaus itself to landfall strongly crossing southern France and northern Spain, reaching northern Italy and even the Adriatic Sea with intensity of hurricanes. It is clear from 500 mb level charts that the Rossby wave completely disappears over the northern Atlantic Ocean whereas, the not exist of Rossby wave add eastward wind to the phase air current speed through the two days 23 and 24 January 2009. In addition to that, analysis of the 6-day mean anomaly of the geopotential height at 500 mb for the northern hemisphere for January 2009 shows that there was an outstanding positive anomaly of more than +175 m over eastern Atlantic region near 30° N simultaneously with negative anomalies of less than -200 m over North Atlantic Ocean at higher latitudes near 65° N during the six days from 20 to 25 of January 2009, see Figures (2 and 3a). However, the strong of Azores high and its rapidly movement toward the north eastward direction creates a circulation between mild and humid air mass (1) in the northern Atlantic to the south and the other (mild to cold) and humid air mass (2) in the middle Atlantic region to the north. This circulation of the two different air masses (1and 2) formed the cyclonic circulation of extratropical cyclone Klaus. Figures (12 and 13) show constructs of the six phases of Klaus development of 6 hour intervals. Throughout six phases starting from phase (I) at 0000 UTC on 23 January 2009 ended by phase (VI) at 0600 UTC on 24 January 2009, the life cycle of cyclone Klaus has been occurred. Phase (I) is the initiation stage of Klaus, whereas, there were two different air masses (1 and 2) in the north Atlantic region, air mass (1) in the north meanwhile second air mass was in the south of it. See Figure (7a). Phase (II) is considered as the first circulation stage between the two air masses. At this stage, the air mass (2) jumped to the north and second air mass circulated to the west. See Figure (7b). Phase (III) represented second circulation stage; through it the air mass (2) moved to the westward direction and circulated toward air mass (1). Meanwhile the first air mass (I) was continued to circulate southward direction. See Figure (7c). Phase (IV) is the phase of developing of the cyclone, whereas, the two air masses touch each other and started to circulate together. See Figures (7d and 9a). Phase (V) is the cyclonic phase, through this stage the air mass (2) moved faster to the North West direction and going into the air mass (I). Simultaneously air mass (1) moved to the south east direction and all of them becomes a one moving system

and create a cyclonic circulation. Figure (7e) shows the cyclonic circulation of the two air masses. The last phase is the other explosive phase at which the two air masses become circulated faster inside each with a cyclonic circulation. Through this stage, the eye of cyclone Klaus formed. See Figures (7f and 9b). However, the source of the developing of this cyclone was the huge westerly zonal air current aloft over the North Atlantic Ocean which mainly due to the strong and rapidly north east extension of the Azores high. See Figures (4c and 8).

Certainty, the life cycle model of cyclone Klaus is investigated thorough the present work. This Model is innovated as a result of the analysis of the air mass RGB satellite maps, wind field distribution and a satellite perspective of cyclone Klaus evaluation over the northern Atlantic region respectively, through the period of 0000 UTC on 23 to 1800 UTC on 24 January 2009; see Figures (7, 8, 9, 12 and 13). Whereas, the results revealed that the developing and life cycle model of Klaus, is a unique model which completely differ than both of Norwegian frontal- cyclone model (Bjerknes 1921; Bjerknes and Solberg 1922) and Shapiro-Keyser life cycle model (Shapiro-Keyser 1990) for extratropical marine cyclones. These two models for midlatitude cyclones development and life cycle had a principle concept of their development on the polar front theory of atmospheric circulation by (Bjerknes and Solberg 1922), see Figures (10 and 11) respectively. Meanwhile, Figures (12 and 13) illustrates the six phases of Klaus development theory from incipient phase, phase (I), to its explosive phase, Phase (VI) which called as; the cyclonic circulation theory. According to this theory, the cyclone developed as a result of the circulation between two different air masses (not from the conversions of the two different air masses in a front like the polar front theory by Bjerknes and Solberg (1922).

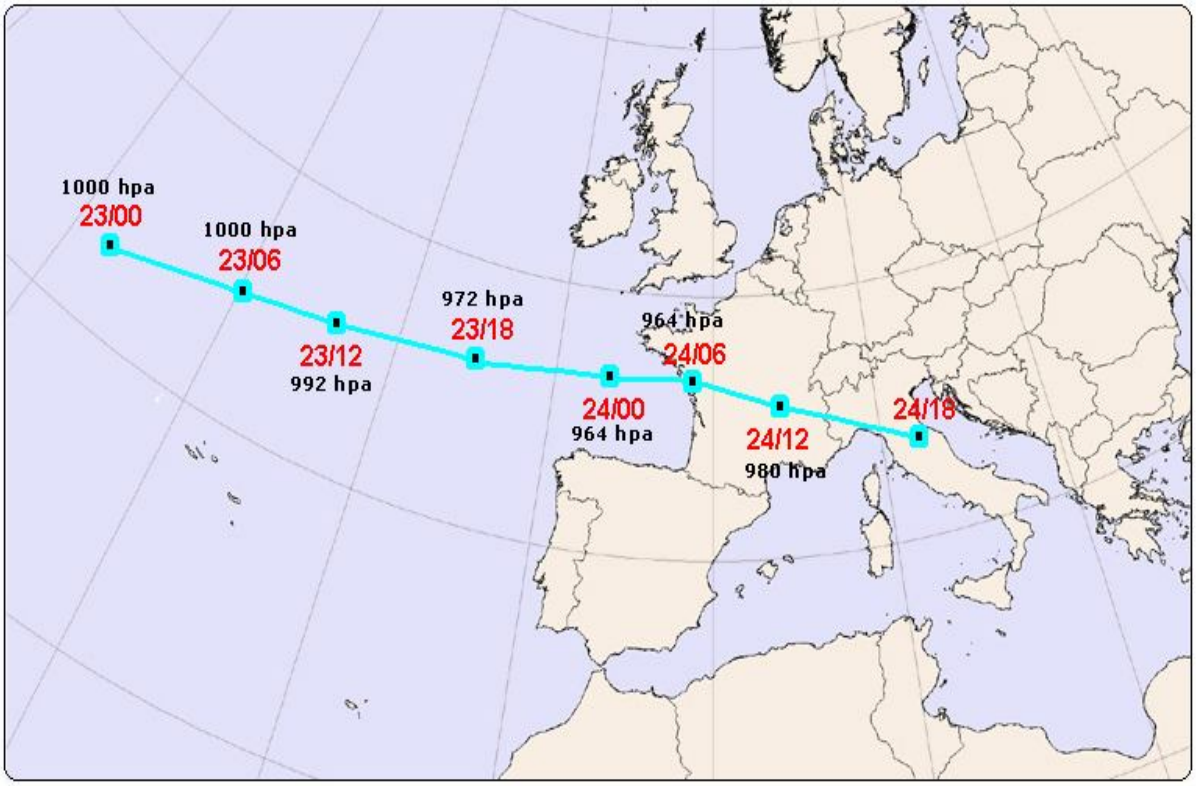

Figure 1: An approximate 6 hour track of the center of extratropical cyclone Klaus, labeled with passing dates, UTC times and minimum MSLP's analyzed by HIRLAM-AEMET numerical model. [Source; High Resolution Limited Area Model, (HIRLAM-AEMET) Spain Agency of Meteorology].

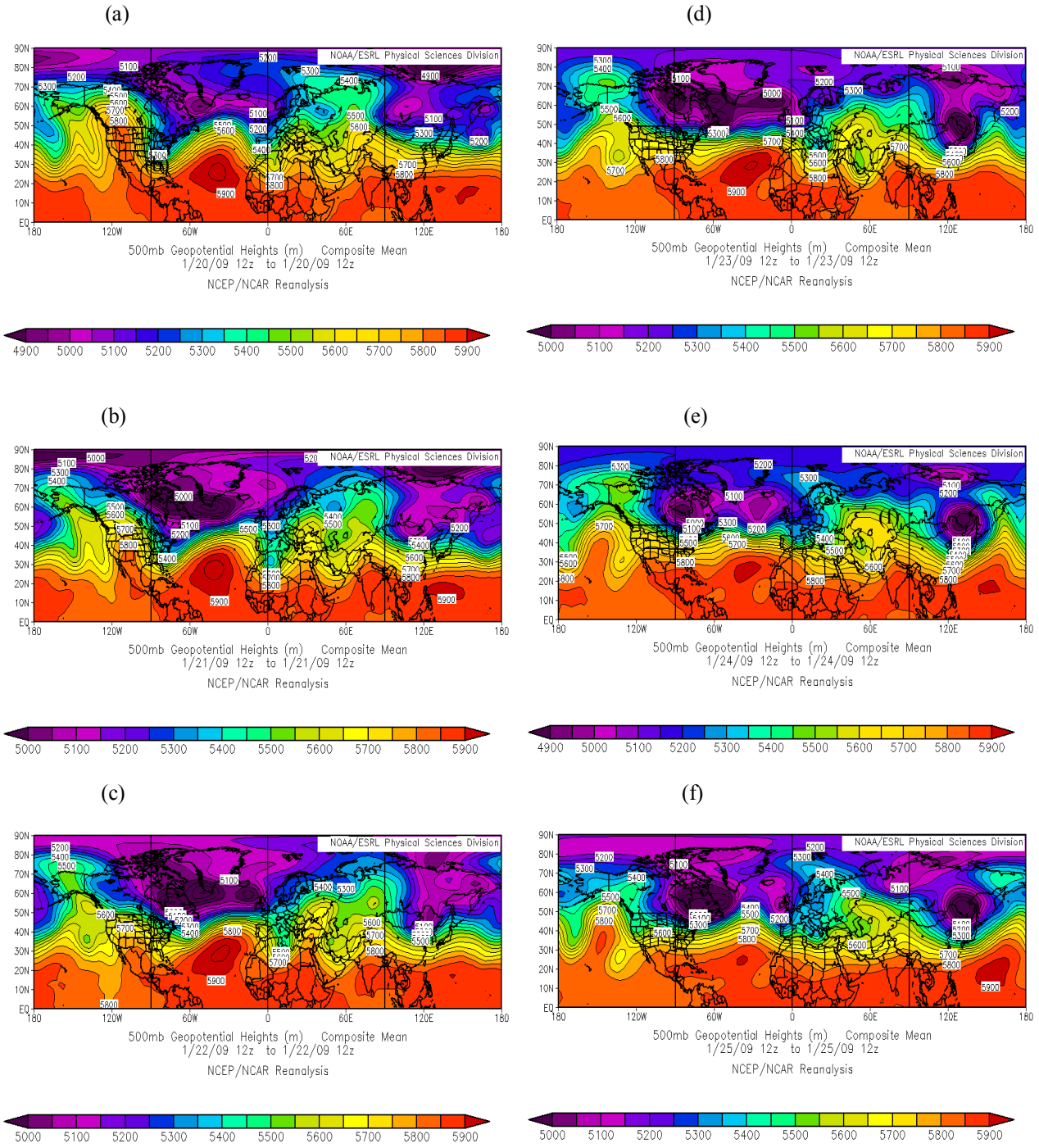

Figure 2: The daily mean of geopotential height (m) at level 500 mb for 1200 UTC over the northern hemisphere through the six days from 20 to 25 January 2009, (a, b, c, d, e, and f, respectively).

(a)

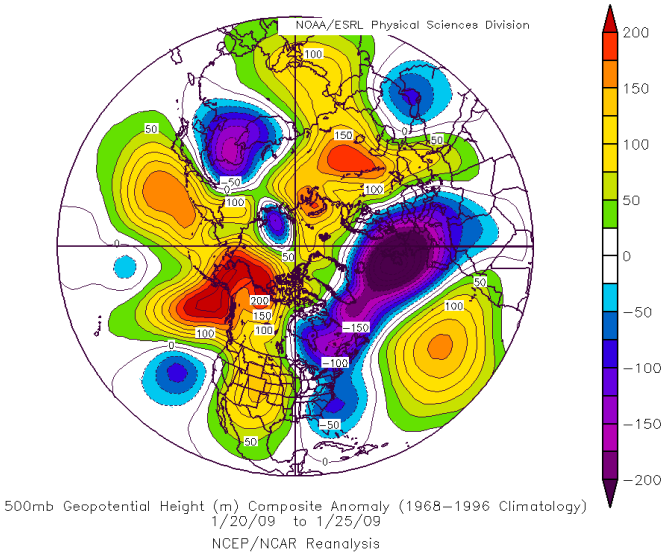

(b)

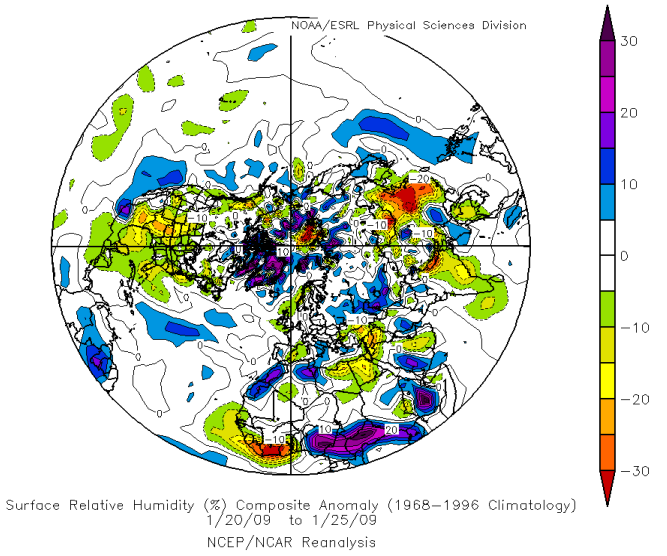

Figure 3: The six days mean composite anomaly over the northern hemisphere through the days from 20 to 25 January 2009. (a) for 500 mb geopotential height (m), and (b) for surface relative humidity.

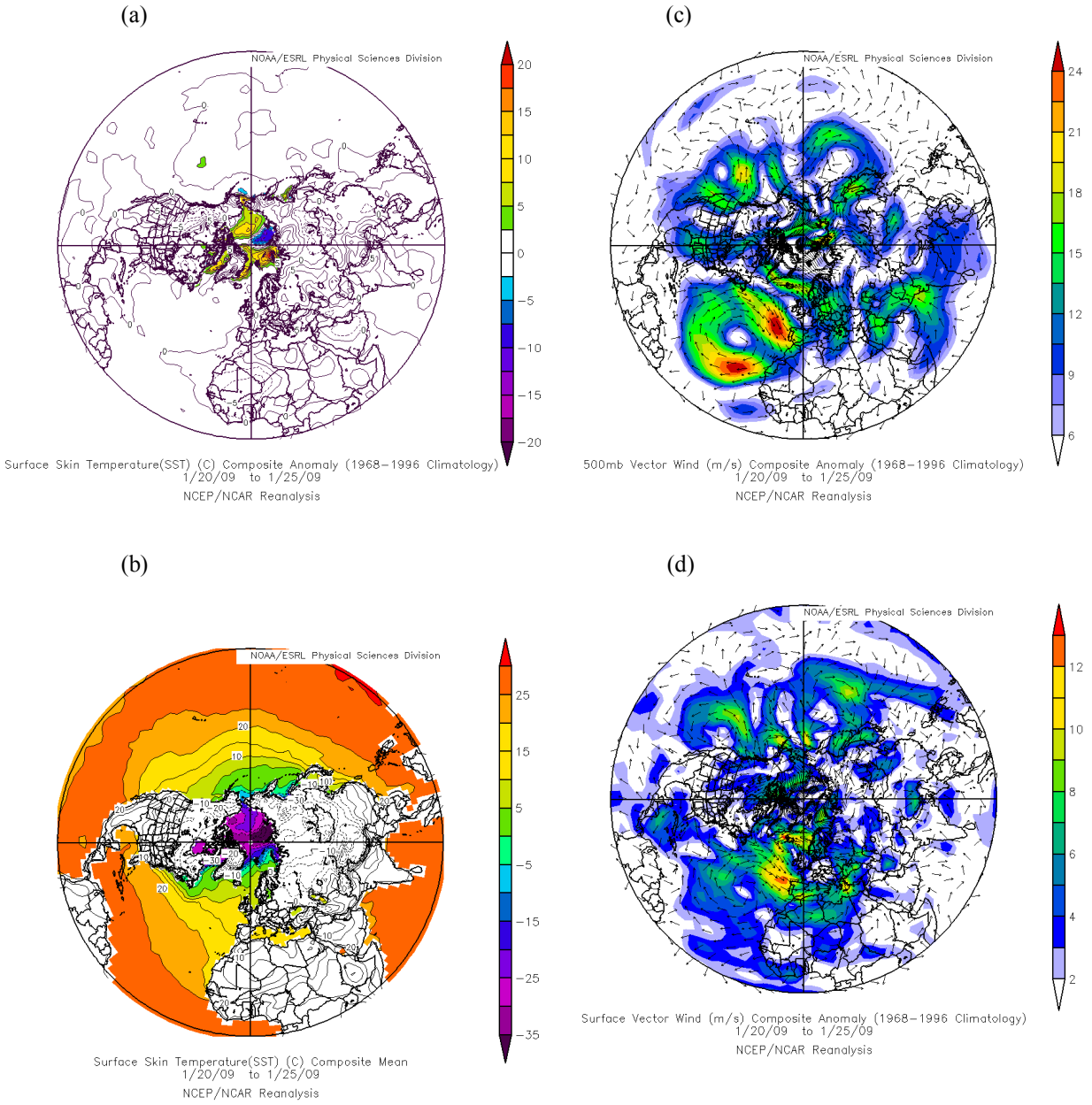

Figure 4: The six days mean composite over the northern hemisphere through the days from 20 to 25 January 2009. (a) for surface air temperature anomaly, (b) for surface air temperature, (c) for surface wind anomaly, and (d) for surface wind.

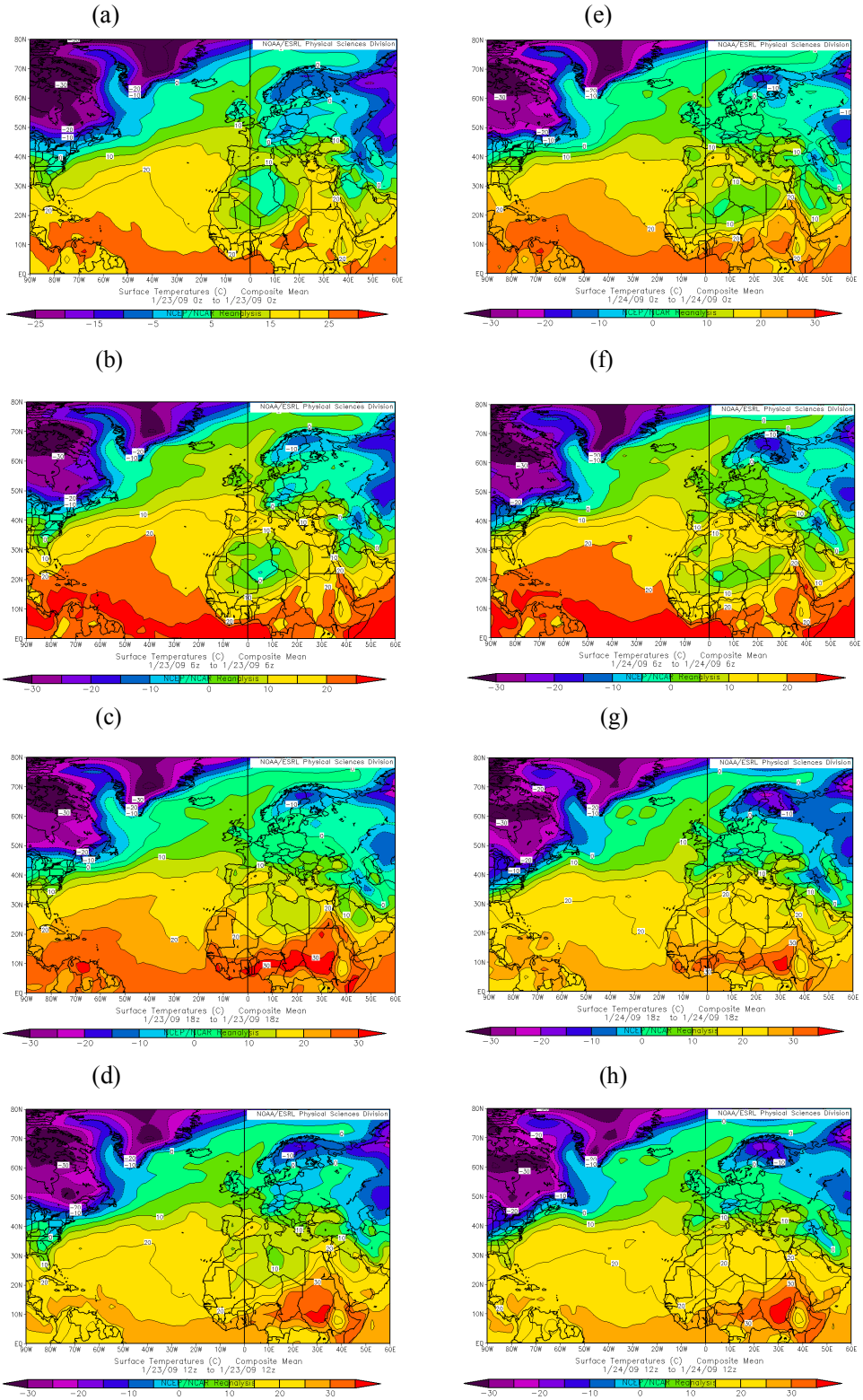

Figure 5: The 6 hour mean surface air temperature (°C) composite mean over the north Atlantic region through the period 23-24 January 2009.

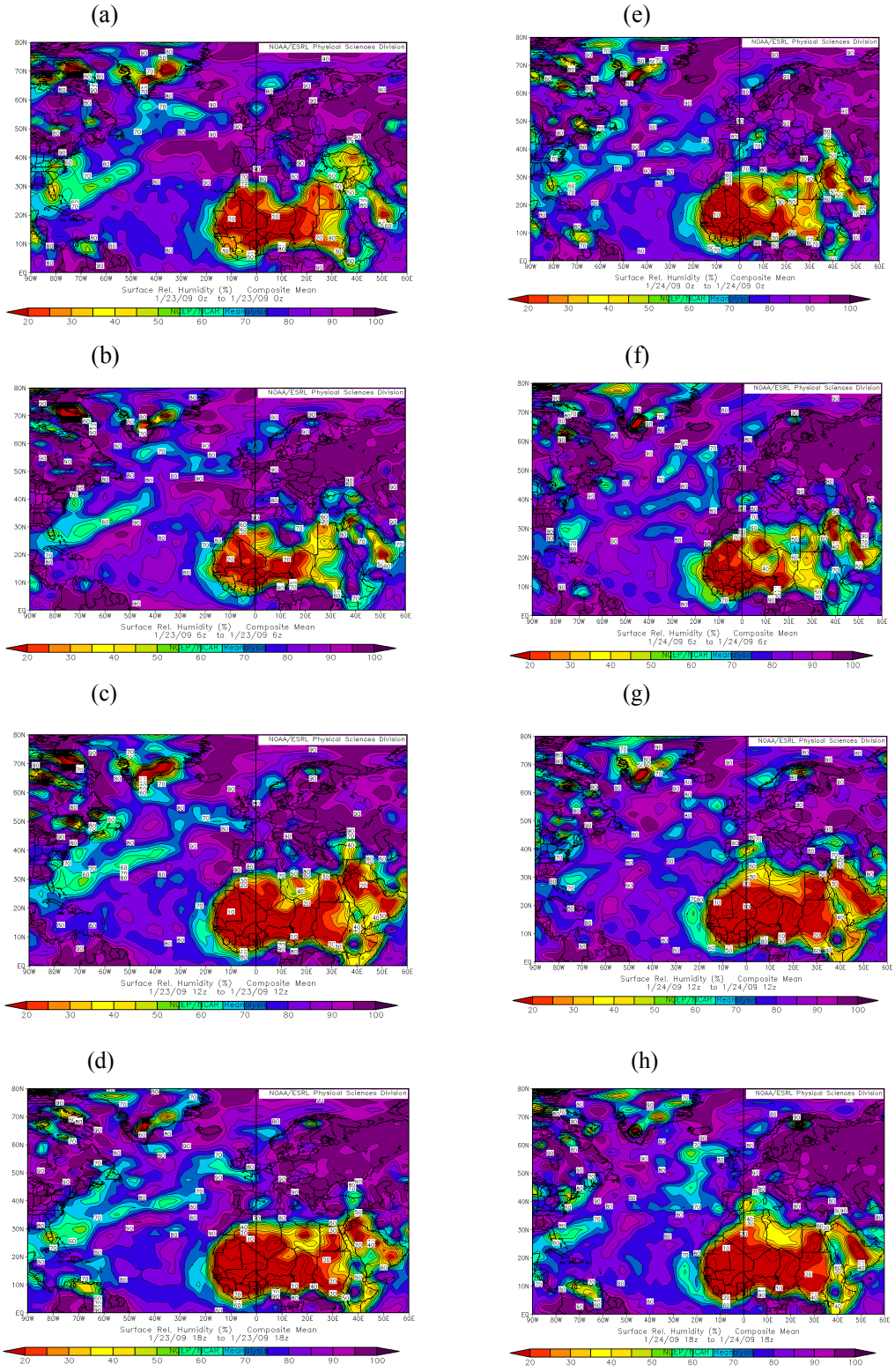

Figure 6: The 6 hour surface relative humidity (%) composite mean over the north Atlantic region through the period 23-24 January 2009.

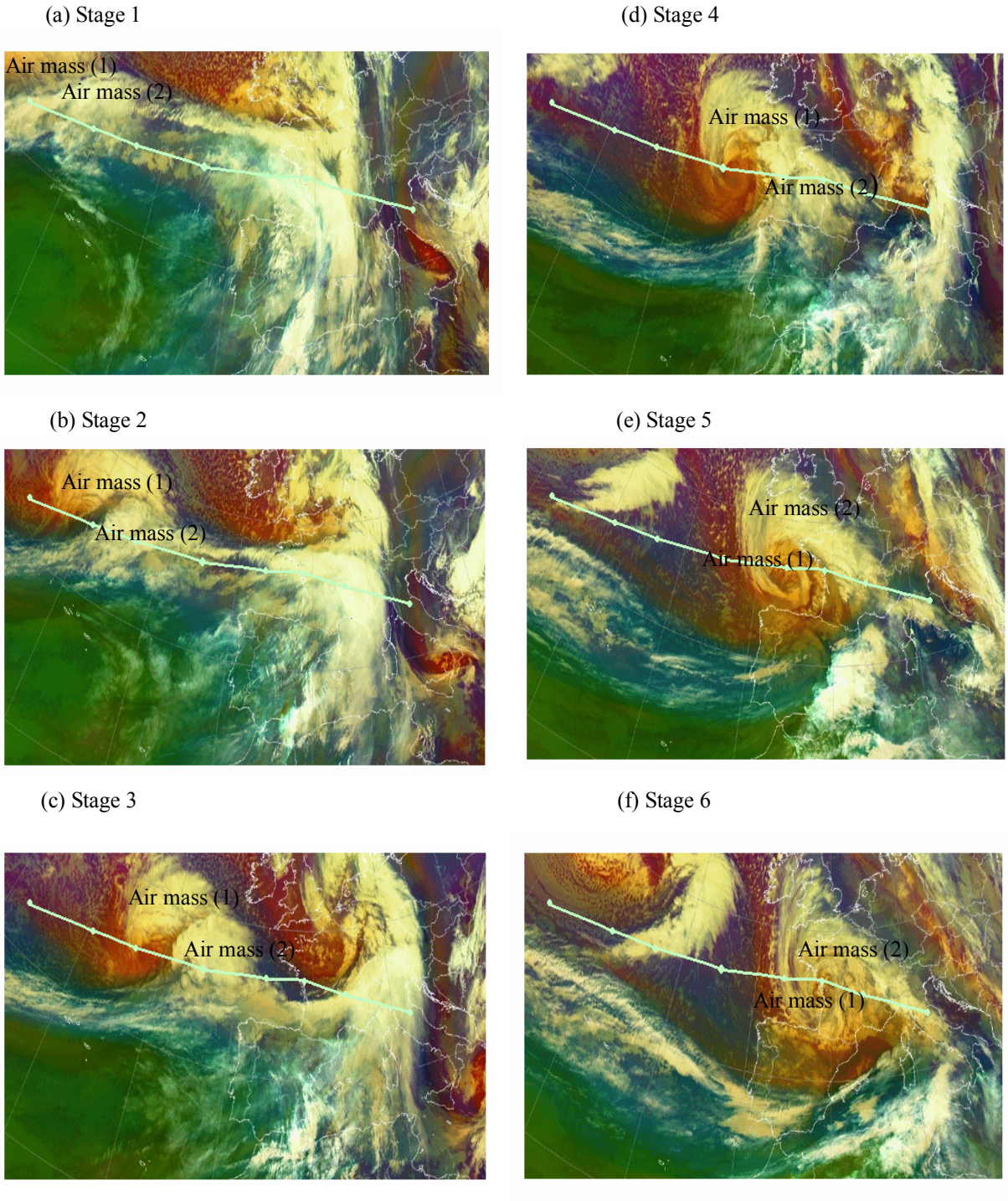

Figure 7: The 6 hours time step air mass RGB composites satellite images show clearly the developing stages in the life cycle, type of two air masses of the system, and the nearly zonal path of extratropical cyclone Klaus.

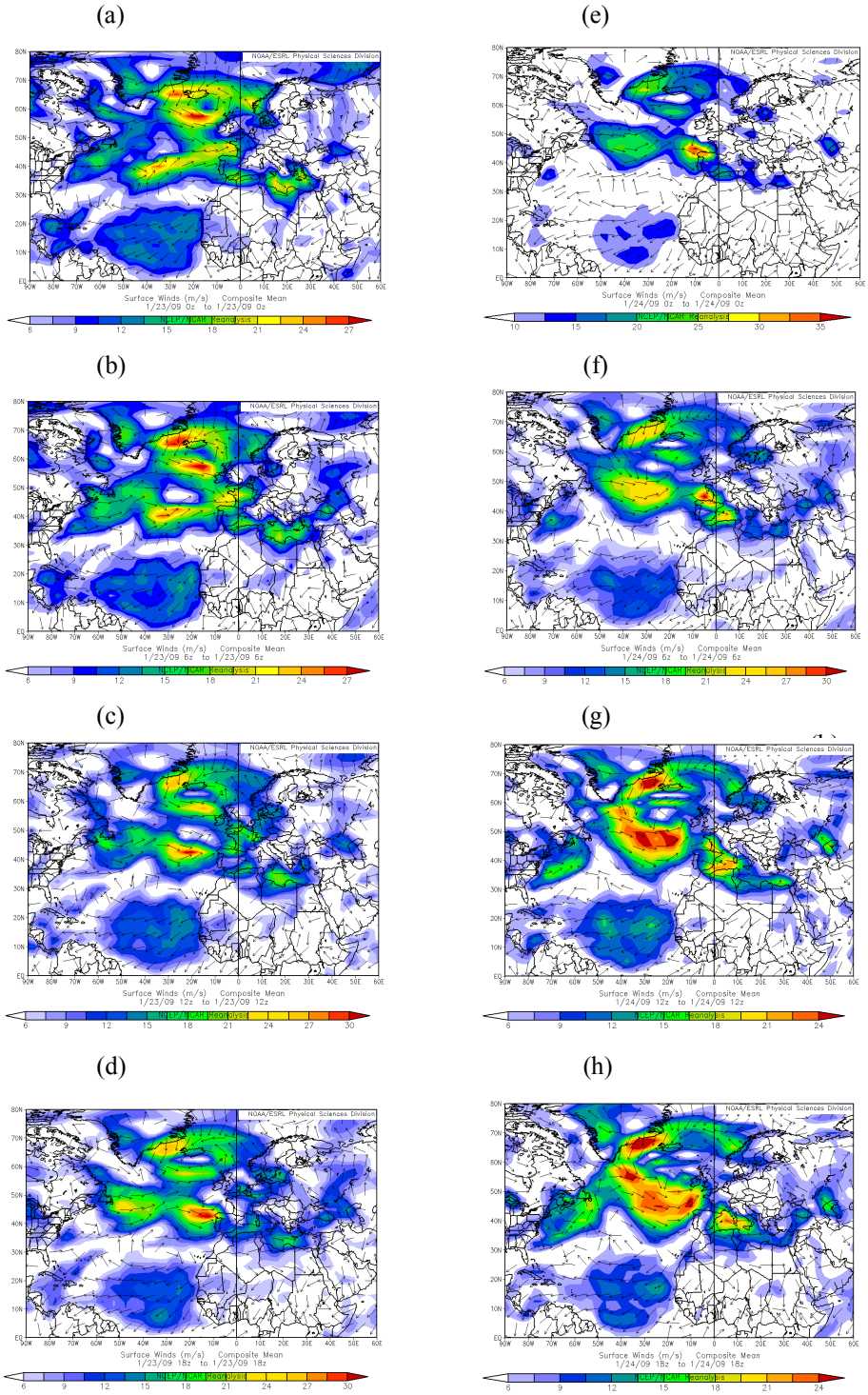

Figure 8: The 6 hour surface wind (m/s) composite mean over the north Atlantic region through the period 23-24 January 2009.

(a)

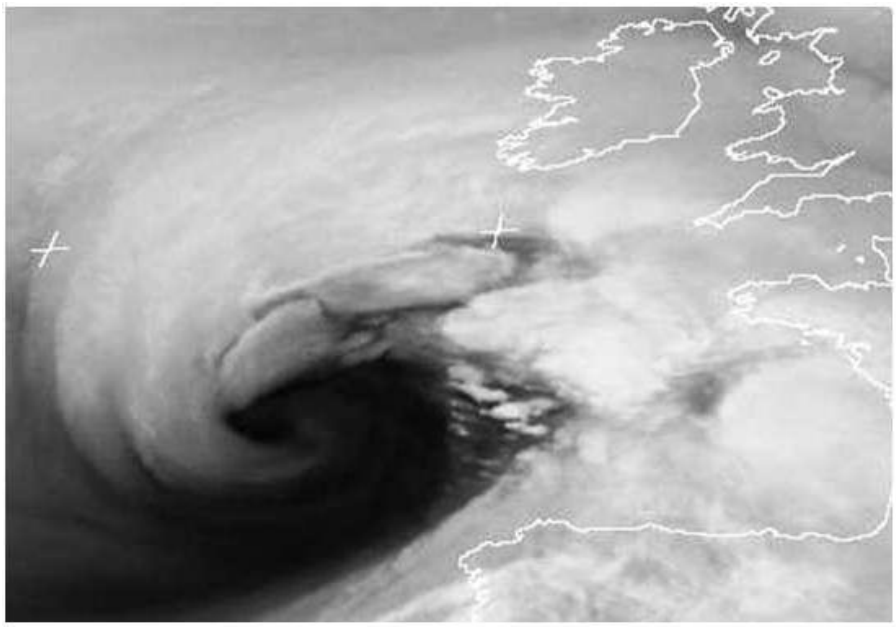

(b)

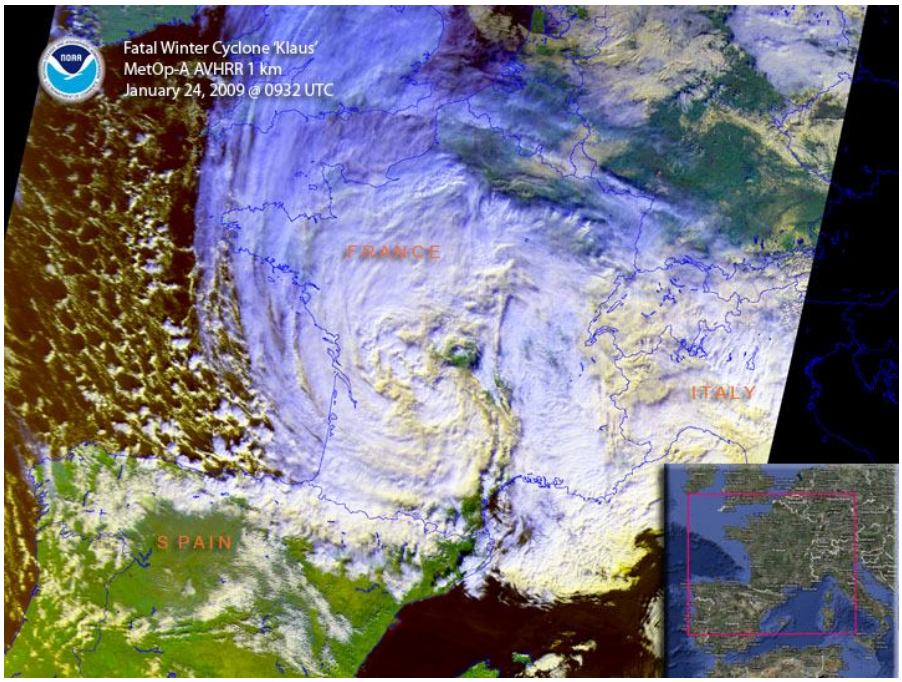

Figure 9: (a) Extratropical cyclone Klaus at 1800 UTC on 23 January 2009 as represented in satellite imagery (Source: Dundee Satellite Receiving Station and NOAA), and (b) Satellite image showing the location of Klaus over France and northern Spain at 0932 UTC 24 January 2009. (Source: MetOp-A AVHRR 1 Km, NOAA).

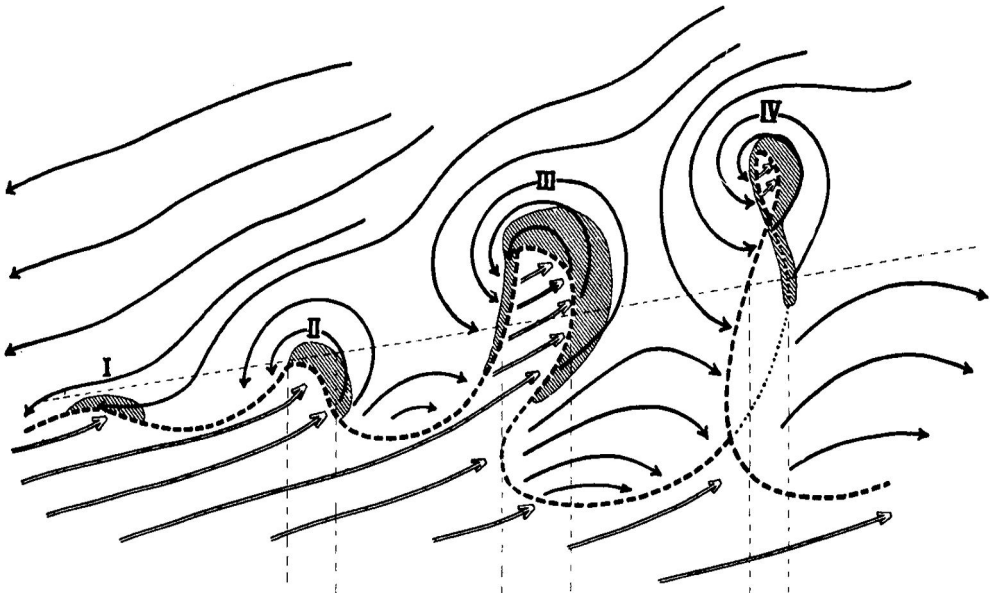

Figure 10: The Norwegian frontal-cyclone model (Bjerknes 1921; Bjerknes and Solberg 1922) describing the amplification of a frontal wave from initiation (I), through cyclogenses, (II, III), to frontal occlusion (IV). (Neiman and Shapiro, 1993)

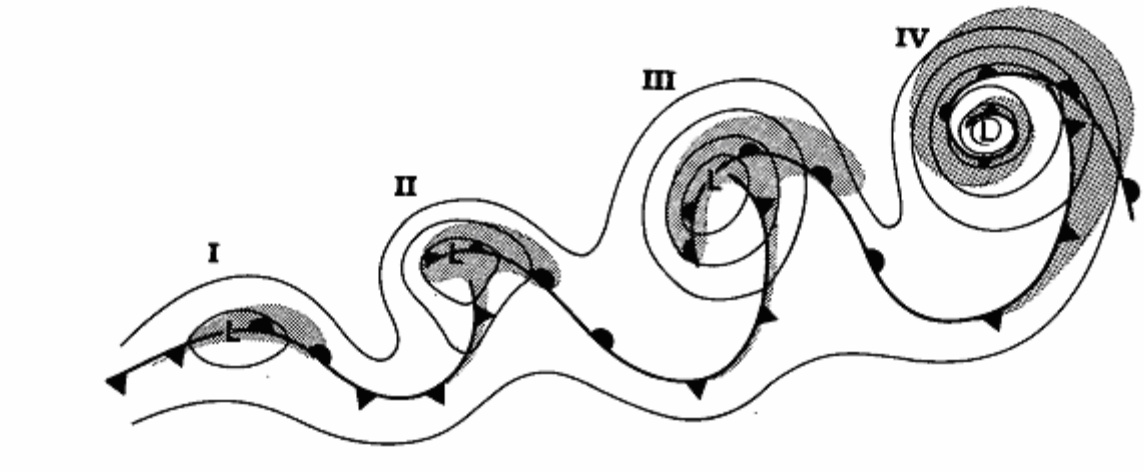

Figure 11: An alternative model of frontal-cyclone evaluation (Shapiro, and Keyser, 1990): incipient broad-baroclinic phase (I), frontal fracture (II), bent-back front and frontal T-bone (III), and warm-core frontal seclusion (IV). Sea level pressure, fronts and cloud signature. (Neiman and Shapiro, 1993).

PHASE (I): At 0000UTC 23 January 2009

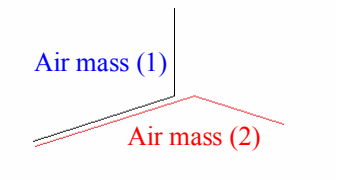

PHASE (II): At 0600UTC 23 January 2009

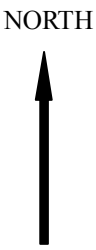

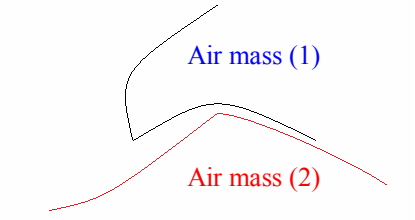

PHASE (III): At 1200UTC 23 January 2009

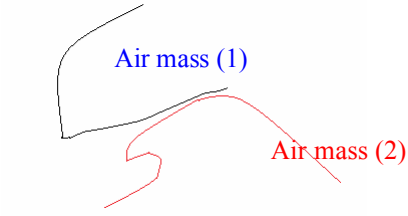

PHASE (IV): At 1800UTC 23 January 2009

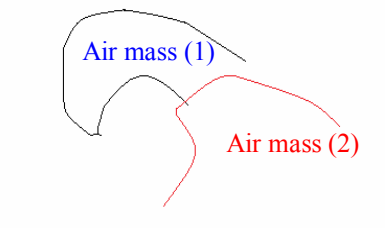

PHASE (V): At 0000UTC 24 January 2009

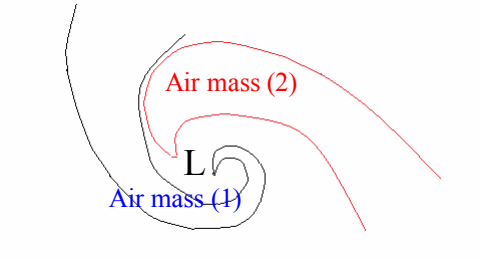

PHASE (VI): At 0600UTC 24 January 2009

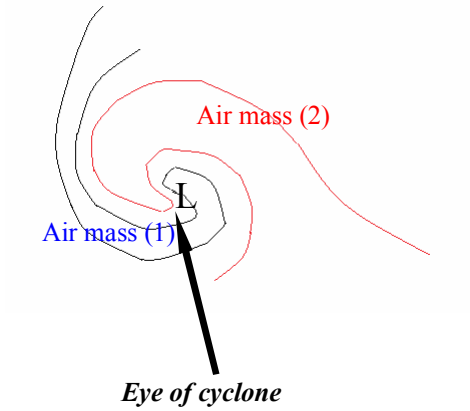

Figure 12: The six development phases and the life cycle model of extratropical cyclone Klaus (the development building upon the air masses). [The cyclonic circulation theory]

PHASE (I): At 0000UTC 23 January 2009

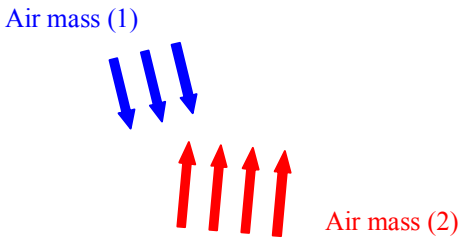

PHASE (II): At 0600UTC 23 January 2009

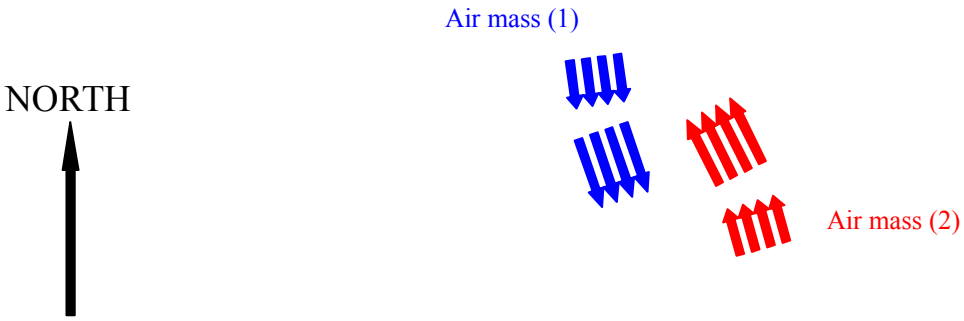

PHASE (III): At 1200UTC 23 January 2009

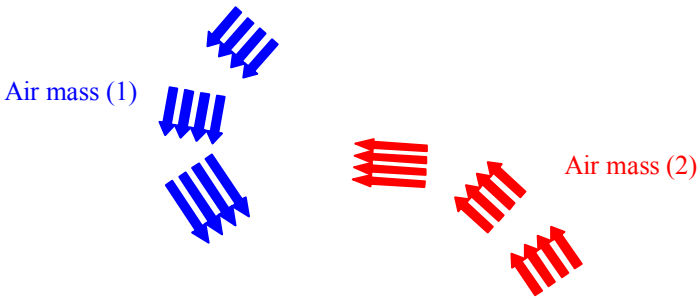

PHASE (IV): At 1800UTC 23 January 2009

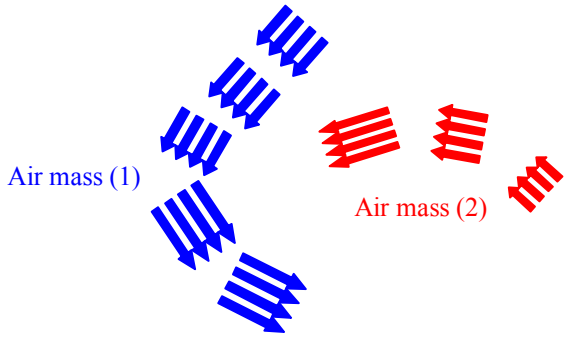

PHASE (V): At 0000UTC 24 January, 2009

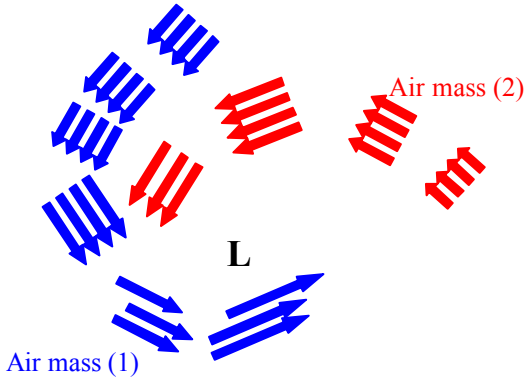

PHASE (VI): At 0600UTC 24 January 2009

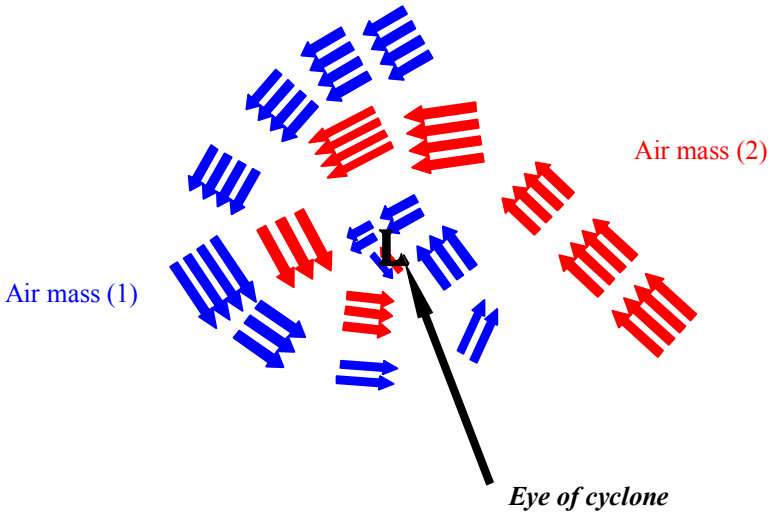

Figure 13: The six development phases and the life cycle model of extratropical cyclone Klaus (the development building upon the circulation of wind field (arrows)). [The cyclonic circulation theory]

4. Conclusions

On 23-24 January 2009, southern France and northwestern Spain were subjected to hurricane-force winds over the weekend, leaving a trail of destruction and disruption. The strong winds, combined with heavy rain, were the result of a deep low pressure system of extratropical cyclone Klaus. At least 23 people were killed during the passage of this storm which caused damage from the Dordogne area to the Pyrenees. Klaus moved across the Bay of Biscay on 23 January and into the Bordeaux region of France on 24 January, bringing powerful winds and torrential rain to southern France and northwestern Spain. Wind gusts of around 160 kmph were recorded in various locations across the region (with gusts reaching 184 kmph in the eastern Pyrenees near Perpignan). Klaus continued to track eastwards across southern France before moving into the Mediterranean Sea. Hundreds of thousands of trees had been flattened by the storm in the Gironde and Landes departments. The Landes forest is reported to have sustained severe damage while the Gironde region in southwestern France has also seen vast forest areas flattened by the storm. The synoptic analysis of the situation over the Atlantic Ocean and the northern hemisphere using of the available meteorological data and using of anomalies methodology was done. The role played of Azores high on the formation of Klaus had been studied. Through the present work there are remarkable results had been achieved.

1. The results revealed that the strong and north eastward movement of the Azores high through the period 23-24 January 2009 causing of a huge westerly air current over the middle of the northern Atlantic region. This huge completely westerly air current set aside the air over the eastern Atlantic region to forced to swept and to circulate westward direction and made the cyclonic circulation that develop extratropical cyclone Klaus.

2. The 6-day mean anomaly analysis of the geopotential height at 500 mb for the northern hemisphere for January 2009 shows that there was an outstanding positive anomaly of more than +175 m over eastern Atlantic region near 30° N simultaneously with negative anomalies of less than -200 m over North Atlantic Ocean at higher latitudes near 65° N during the six days from 20 to 25 of January 2009.

3. Anyalysis of the 6 hour geoptential height and wind fields for 500 mb level appears that the Rossby wave was completely absents over the north Atlantic region through the period of 23-24 January 2009, whereas this absence of Rossby wave push the westerly phase speed, over the north Atlantic region, eastward toward western Europe by the eliminates of westward wind speed of Rossby wave, which also leads to the strong wind storm.

4. The analysis of the 6 hours time step air mass RGB satellite images, wind field distribution, and a satellite perspective of cyclone Klaus evaluation over the northern Atlantic region through the period of 0000 UTC on 23 to 1800 UTC on 24 January 2009 leads to uncover the development six phases of extratropical cyclone Klaus and to construct its life cycle model.

5. The life cycle model of Klaus is a unique model which completely differs than both of Norwegian frontal- cyclone model (Bjerknes 1921; Bjerknes and Solberg 1922) and Shapiro-Keyser life cycle model (Shapiro-Keyser 1990) for extratropical marine cyclones.

6. Knowing of the life cycle model of Klaus is conduct to innovate a new theory of cyclonic formation is so called; the cyclonic circulation theory.

7. According to the cyclonic circulation theory, the cyclone is develop as a result of the circulation between two different air masses, through a six phases from incipient phase , phase (I), to its explosive phase, phase (IV). See Figures (12 and 13). However, there is no a front between the two air masses or a warm sector existed here.

Finally, one can conclude that the Azores high pressure system played a great role in the developing of the extratropical cyclone Klaus on 23-24 January 2009 over the middle of the northern Atlantic Ocean, west of the Bay of Biscay, by supporting the north Atlantic with a strong westerly air current and swept the air over the eastern north Atlantic Ocean and western Europe to move toward the westward direction and creates the cyclonic circulation over the east of the northern Atlantic region. After a one hundred years since the polar front theory made by Bjerknes, (1919, 1921 and 1922), there is another theory of midlatitude cyclonic formation, the cyclonic circulation theory. The analysis of the development stages of extratropical cyclone Klaus is considered as the practical application which leads to this theory.

Acknowledgment:

It is a pleasure to the author to thank the Climate Diagnostics Centre for supporting the data used throughout this study. Plots and images were provided by the NOAA-CIRES Climate Diagnostics Centre, Boulder, Colorado, USA from their Web site at http://www.cdc.noaa.gov. Also, thanks to Meteo-France, the French meteorological agency, Spain Agency of Meteorology and (EUMeTrain Wiki) for reports for Klaus meteorological information. Great thanks for, NOAA, and the Dundee Satellite Receiving Station. Whereas, Satellite images were obtained from Dundee Satellite Receiving Station and NOAA.

Correspondence to:

Yehia Yehia Hafez

Professor of Meteorology

Astronomy and Meteorology Department
Faculty of Science , Cairo University
Giza 12613, Egypt
Telephone: 0020235676845
Cellular phone: 0020103719523
Emails: d_hafez@hotmail.com

References

[1] Bjerknes J. On the structure of moving cyclones. Geofys Publ 1919;1:1-8.

[2] Bjerknes J, Solberg H. Life cycle of cyclones and the polar front theory of atmospheric circulation. Geofys Publ 1922; 3:1-18.

[3] Bottger H, Eckardt M, Katergiannakis U. Forecasting Extratropical storms with Hurricane intensity using satellite information. J Appl Meteor 1975;14(7): 1259-65.

[4] Hadlock R, Kreitzberg CW. The experiment on rapidly Intensifying cyclones over the Atlantic (ERICA) field study-objectives and plans. Bull Amer Meteor Soc 1988;69:1309-20.

[5] Shapiro MA, Keyser D. Fronts, jet streams and the tropopause. extratropical cyclones, The Erik Palmén Memorial Volume, C. W. Newton and E. O. Holopainen, Eds., Amer Meteor Soc 1990:167-91.

[6] Davies HC, Schär C, Wernli H. The palette of fronts and cyclones within a baroclinic wave development. J Atmos Sci 1991;48:1666-89.

[7] Wakimoto RM, Blier W, Liu C. On the frontal structure of an explosive Oceanic cyclone: Airbrone radar observations of ERICA IOP 4. Mon Wea Rev 1992;120:1135-55.

[8] Neiman PJ, Shapiro M. The life cycle of an extratropical marine cyclone. Part I: Fontal-cyclone evolution and thermodynamic air-sea interaction. Mon Wea Rev 1993;121,2153-76.

[9] Neiman PJ, Shapiro M, Fedor L. The life cycle of an extratropical marine cyclone. Part II: Mesoscale structure and diagnostics. Mon Wea Rev 1993;121:2177-99.

[10] Evans MS, Keyser D, Bosart LF, Lackmann GM. A satellite-derived classification scheme for rapid maritime cyclogenesis. Mon Wea Rev 1994;122, 1381-416

[11] Schultz DM, Keyser D, Bosart LF. The effect of large-scale flow on low-level frontal structure and evolution in midlatitude cyclones. Mon Wea Rev 1998;126:1767-91.

[12] Nielsen N, Sass B. A numerical, high-resolution study of the life cycle of the severe storm over Denmark on 3 December 1999.Tellus A, 2003;55(4):338-51.

[13] Bjerknes V. On the dynamics of the circular vortex with applications to the atmosphere and atmospheric vortex and wave motion. Geofys Publ 1921; 2:1-88.

[14] Gray, The recent increase in Atlantic hurricane activity: Causes and implications. Science 2001;293:474-9.

[15] Zebrowski Jr, Judith AH. Category 5: The story of Camille – lessons unlearned from American's most violent hurricane.2005, ISBN 0472115251,Hardcover:304.

[16] Asbury HS, Hilary FS, Laura, F, Mark H, David T, Wayne W, Jeff L. Hurricanes 2004: An overview of their characteristics and coastal change. Estuaries and Coasts 2006; 29(6A): 880-8.

[17] Hafez YY. The role played by blocking over the Northern Hemisphere in hurricane Katrina. The J Amer Sci 2008;4(2): 10-25.

[18] Rex DF. Blocking action in the middle troposphere and its effect upon regional climate. (I) An aero logical study of blocking action. Tellus 1950a;2:196-211.

[19] Rex DF. Blocking action in the middle troposphere and its effect upon regional climate. (II) The climatology of blocking action. Tellus 1950b;2:275-301.

[20] Rex DF. The effect of Atlantic blocking action upon European climate. Tellus 1951;3:100-11.

[21] Cohen J, Saito K, Entekhabi D. The role of the Siberian high in Northern Hemisphere climate variability. Geophys Res Lett 2001;28(2):299-302.

[22] Hafez YY. The teleconnection between the global mean surface air temperature and precipitation over Europe. I J Meteorology UK 2008;33(331):230-6.

[23] Hafez YY. The connection between the 500 hpa geopotential height anomalies over Europe and the abnormal weather in eastern Mediterranean during winter 2006. I J Meteorology UK 2007;32(324):335-43.

[24] Kalnay E, et al., The NCEP/NCAR 40-year reanalysis project. Bull Amer Meteor Soc 1996;77: 437-70.

[25] Holton JR. An Introduction to Dynamic Meteorology. Elsevier Academic Press,2004:216.

Persistent Organic Pollutants (POPs) in Sea food of China- A review

Mangala Yatawara*, N.Linthoingambi Devi, Qi Shihua

Key Laboratory of Biogeology and Environmental Geology of Ministry of Education, Wuhan, Hubei 430074, P.R.China

*mmkyat@yahoo.com

Abstract: The coastal zone of China has been undergoing rapid economic growth in the past few years. Large quantities of persistent organic pesticides have been either used in agriculture and public health or released from manufacturing plants in this region. Weak environmental management framework has over the years permitted improper waste disposal use and disposal of pesticides have caused serious environmental problems. This paper attempts to review the state of sea food contamination and evaluate its risk to consumers in China using recent research data. The daily intake of Organochlorine pesticides (OCPs) and Polychlorinated biphenyles (PCBs) ingested by people living in coastal cities in China through fish and shellfish was also estimated. Risk assessment against various standards showed that seafood products have been contaminated by Dichlorodiphenyltrichloroethane (DDTs) and may pose health threat to local residents and the consumers due to the fact that China has been a major producer and consumer of DDTs in the past, and also uses DDT for vector control, resulting in higher background levels of DDTs in different ecological compartments. It is recommended to impose a tighter control on the use of DDT for vector control as well as for agricultural application, conduct regular monitoring of DDT concentrations in different ecological compartments. However, most research in coastal area is limited to a few kinds of POP compounds. [Journal of American Science 2009; 5(5):164-174]. (ISSN: 1545-1003).

Key words: POPs, Risk Assessment, Coastal Zone

1. Introduction

Organochlorinated substances are listed as Persistent Organic Pesticides (POPs) by the United Nations Environment Program (UNEP) in the 1995 Stockholm Convention. Twelve POPs were identified of which, nine are pesticides (aldrin, endrin, dieldrin, heptachlor, chlordane, mirex, toxaphene, Dichlorodiphenyltrichloroethane (DDT) and hexa chlorobenzene (HCB) (Wei et al. 2007). The other substances are industrial chemical products or byproducts including Hexachlorocyclohexane (HCH), Polychlorinated biphenyles (PCBs) and Polychlorinated dibenzo-p-dioxins and furans. Due to their persistence, bioaccumulation, and adverse effects on wildlife and human, production and use of these chemicals were banned in the early 1970s in developed countries (Loganathan and Kannan, 1994).

Large amounts of Organo Chlorine Pesticides (OCPs) were used in past decades to obtain high yield to sustain overpopulation in China. Even after the ban of technical HCH and DDT in 1983, 3200 t of lindane (almost pure γ-HCH) was still in use between 1991 and 2000, and DDT production also continues due to export demand and dicofol production (Zhang et al. 2002; Qiu et al. 2004; Tao et al. 2005).During past few years, a number of surveys and studies on OCPs and PCBs in various environment phases has been conducted in China (Wu et al. 1999; Zhou et al. 2000; Zhou et al. 2001; Bi et al. 2002 ; Monirith et al. 2003). The foodstuffs, especially meat, fish and dairy products are important routes of exposure to organic contaminants for human (Yang et al. 2006; Harrison et al. 1996; Dougherty et al. 2000).

The rapid socio-economic development during the past two decades in China, especially the coastal area has given rise to severe economic, environmental and health problems (Wong et al. 2005). According to Wong et al. (2005) and National Implementation Plan (2007), the most pesticide application areas belong to eastern and southern area of China. Many investigation reports have been documented that these contaminants might be transported widely through aquatic environment. Fisheries and Aquaculture activities have been successfully done along the coastal zone of P.R.China. China has been the world's largest producer and exporter of fishery products since

2002(Guo et al. 2007). Fish and shellfish are important food for supplying essential trace elements and certain vitamins; moreover, the polyunsaturated *n*-3 fatty acids in fatty fish species are biologically important and have been associated with a decreased risk for cardiovascular disease (Svensson et al. 1995; Kromhout et al. 1985). This is more important in China, where human dietary habits are changing and widening with the ongoing rapid economic development and changing facets in life-styles. While consumption of grains and vegetables decreased from 1989 to 1997, consumption of meat, fish and dairy products increased during this period. In 1997, consumption of meat, fish and dairy products accounted for about 21% of foodstuffs consumed by Chinese and fish consumption was an important portion of them (Du et al. 2004). Given the importance of China's seafood products to the human health, information regarding the state of OCPs and PCBs contamination in seafood products is needed in order to evaluate risk of exposure to the contaminants on consumers. Therefore, this paper attempts to review the production, exploitation of pesticidal POPs and PCBs in China and the distribution and the fate of them in marine matrix based on recent research findings in coastal zone in China with emphasis on potential human health risk related to sea food consumption.

2. Production and Exploitation of POPs in China

Being one of the largest agricultural production countries, China has been a major producer and consumer of organochlorine pesticides, until their ban on production and agricultural use were enforced (Yang et al. 2004). In China ten pesticidal POPs were recorded. Seven of them were DDT, HCH, toxaphene, hexachlorbenzene (HCB), chlordane, heptachlor and mirex and they were produced at an industrial scale , and the other three (aldrin, dieldrin and endrin) were produced, only at a pilot plant level, or in research phase during 1950s to 1980s.

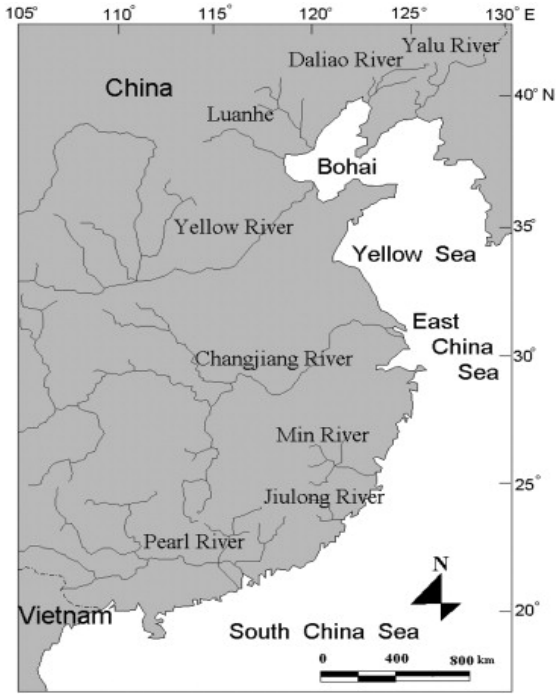

Figure 1. The map showing the coastal zone in China

2.1 Dichlorodiphenyl trichloroethane (DDTs)

The Organochlorine Pesticide DDT was one of the first synthetic chemicals to be produced in large quantities in China for the purpose of agricultural and disease vector control and dispersed widely in the environment (Li et al., 2005). It was first produced and mainly used in agriculture in 1951 (Wong et al. 2002) for controlling army worm, ball worm, pink ball worm, apple tortrix moth, greenish brown hawk moth on wheat, maize, cotton, orchard, soybean and sorghum (Cai et al. 1992).

The total production of commercial DDT was more than 430 kilo tons (Wong et al. 2002) until its agricultural use was banned in 1983 (Cheng, 1990). Before the ban, China was the third largest consumer of DDT for agricultural purposes (Figure 2) after US and Former Soviet Union and fifth consumer country for overall usage of the chemical (Figure 3). The importation of DDT has also been banned in China since 1994 (Wei et al. 2007). Since 1995, the output of technical grade DDT in China has been maintained at the level of 5,000 - 6,000 tons/year, and the output in 2004 was 3,945 tons (NIP, 2007).However, there remain only two enterprises producing technical grade DDT and one enterprise producing DDT preparations.

Small amount of DDT currently produce in China under the exemption of Stockholm Convention is to use as the intermediate in dicofol production, to export for disease vector control in the tropical regions where malaria breaks out heavily such as Southeast Asia and Africa, and to use in antifouling paint.

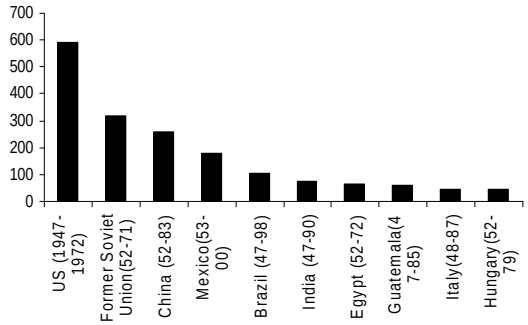

Figure 2. The top 10 countries with historical highest DDT use in agriculture (Source: Li, 2003a, 2003b)

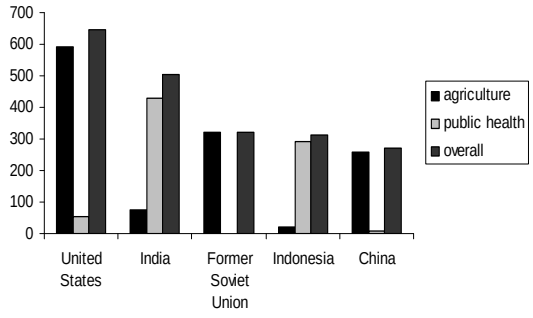

Figure 3. Top 5 countries for overall DDT use (Source: Li et al. 2004)

2.2 Hexachlorohexane (HCHs)

The Organochlorine Pesticide HCH has two formulations as technical hexachlorocyclohexane (HCH) and lindane. Technical-grade HCH consists principally of five isomers, α-HCH (60–70%), β-HCH (5–12%), γ- HCH (10–15%), δ-HCH (6–10%) and ε -HCH (3–4%) (Walker et al.1999).

China has consumed the highest amount of technical HCH (Figure 4), accounting for almost half of the total global usage, followed by India to kill pests on rice, wheat, maize, cotton, soybean, sorghum, orchards and some vegetables. Among them, more than half of HCH was used in rice paddies, 25% on wheat, and 10% on each of soybean/sorghum and maize (Cai et al. 1992). China started to produce and use technical HCH in 1952 and its use was banned in 1983. The total amount of technical HCH produced in China was 4.5 million tons by 1983 (Li et al. 1998b). Although technical HCH is no longer used, applications of lindane continue in many countries including China. The total lindane usage between 1970 and 1993 was 720 kilo tons (Voldner and Li, 1995).

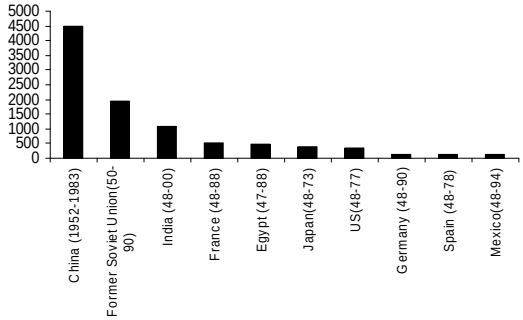

Figure 4. Top 10 countries with highest technical HCH use (Li et al., 1999a, 2004a)

2.3 Chlordane and Mirex

Chlordane and Mirex were used in China due to a lack of highly efficacious and low cost termiticites. China started to produce and use Chlordane in 1950s and the highest production could observe in 1999 accounting 520.6 tons (NIP, 2007). The production of mirex started in 1960s and the highest production could observe in 2000 accounting 31 tons (NIP, 2007).

From 1995 to 2003, about 5000 tons of chlordane and 140 tons of mirex were produced, especially, within 5 years from 1997 to 2001, 2300 tons t of chlordane and 14 tons of mirex was used in China (WB, 2005). Most of these pesticides may have been used in the south and south east China, as most of termites severely affected areas belong to these areas.

2.4 Hexachlorbenzene (HCB)

China began to produce HCB in 1958 and in total there were six enterprises. These enterprises used HCHs to produce HCBs and lindane. Due to control of HCH production, the production of HCB was reduced drastically. In 1990, the maximum HCB output of the whole country was 7365 tons. Production was reduced year by year after 2000 and completely stopped in 2004 (NIP, 2007).HCB has not been used as a direct pesticide in China, but as an intermediate for the production of other chlorinated substances such as Na-PCP which used to be employed for schistosomiasis prevention and control.

2.5 Toxaphene, heptachlor and other OCPs

Toxaphene was broadly used for cotton pests, fruit trees pests and maize borer prevention **(**Wei et al. 2007). The production was started in 1970. The highest production was in 1973 accounting 3740 tons (NIP, 2007).

Heptachlor was mainly used for soil pests, controlling termites in railway crossties and vector pests' prevention. The production was started in 1967 and it was stopped in 1982 (UNEP, 2002). The maximum amount used (20 tons) identified between 1967 and 1978. However, these two chemicals have not been produced or consumed because they were banned in 1982.No production carried out for aldrin, dieldrin and endrin at large scale in China, and the research or trial production has been stopped (NIP, 2007).

2.6 Polychlorinated biphenyles (PCB)

Polychlorinated biphenyls (PCBs) are amongst the more dangerous environmental contaminants due to their persistence, bioaccumulative properties and toxicity. PCBs have been used worldwide as plasticizers, hydraulic and dielectric fluids, fire retardants and paint additives (Kennisch, 1996). The production of PCBs oils began in 1965 in China (NIP, 2007). During the 1950's and the 1980's, China used to import PCBs-containing electrical equipment from other countries without being informed, most of which were specific transformers and capacitors for large facilities. (Jiang et al. 1997) reported that approximately 8000 tons of PCBs were produced under trade name 1 PCB and 2 PCB during period of 1960s–1970s. Most of them were used as dielectric fluids in electrical appliances and a small portion was used as additives in paints. Even today, large proportion of the original amounts of PCBs, still remain in old transformers and capacitors (Jiang et al. 1997). In January 1974, the Chinese government promulgated the decree on stopping production of capacitors with PCBs, as well as the decree on restricting import of electrical equipment containing PCBs.

3. Sources of OCPs and PCBs in Coastal Zone in China

The coastal zone of China comprises an area of more than three million square kilometers covering, four major Seas; Bohai, Yellow, East China and South China Sea (Figure 1)**.** The area possesses an 18000-km coastline stretching across tropical, subtropical and temperate zones (Cao et al. 2007). The coastal zone is an interface between the land and sea, which comprises of a continuum of coastal land, intertidal area, aquatic systems including the network of rivers and estuaries, islands, transitional and intertidal areas, salt marshes, wetlands, and beaches. Fifty seven per cent of China total population comprise in East, Central and South China (NIP, 2007). Rapid industrialization, urbanization, and conversion of massive agricultural lands to commercial use have accelerated environmental deterioration in coastal region (Guo et al. 2007). Large amount of electrical waste are being carried from many other places to coastal areas in China (Zhao et al. 2007). Since China has been a major producer of seafood, coastal area consists of considerable amount of boats and they are being used antifouling chemicals. Hence, the major sources of OCPs and PCBs in the coastal zone in China are riverine exports of agricultural chemicals from coastal catchments, high shipping activities, heavy manufacturing effluent discharge, and municipal and industrial sewage disposal practices of low standard, used electrical items and atmospheric deposition.

Once discharged into the ocean, these chemicals disperse into three phases, namely water, sediment and biota (Pandit et al. 2002). These contaminants then accumulate in the sediment-dwelling organisms which may be transferred to higher trophic levels through the food chain (Lee et al. 2001).

4 Contamination levels of sea food in coastal zone

4.1 Increasing trend of DDTs towards Pearl River Delta, South China Sea

Many research activities have been carried out in China to investigate the OCPs in marine organisms (Table1). The results showed that the fish/shell fish species in Chinese coastal zone is contaminated by OCPs. DDTs were at the top level. A recent report launched in Asian countries revealed that the contents of DDTs in the marine benthos along the coastal areas of China were at the top level (Monirith et al. 2003). The highest DDTs could observe in the South China Sea. Results from (Monirith et al. 2003; Chen et al. 1996, 2000, 2002; Fang et al. 2001; Phillips, 1985; Tanabe et al. 1987) also showed that South China is the most contaminated coastal sea among the major seas in China. There are possible reasons behind this observation. The coastal area of Guangdong province in South China has 60,000 fishing ships, which is above 1/5 of the total number in China. It can be estimated that about 30–60 tons of DDT may be introduced to the coastal environment of Guangdong, including the Pearl River Delta. According to Fu et al. 2003, the Pearl River is believed to carry a considerable load of chlorinated pesticides, up to 863 tones per annum, which is the highest amongst China's rivers. High ratio of DDT/(DDD+DDE) in sediment (Hong et al. 1995; Zhang et al. 2001 ; Mai et al. 2002), as well as water (Zhou et al. 2001; Luo et al. 2004) samples indicated the relatively recent releases of DDT. Previous studies from (Zhang et al. 2002; Luo et al. 2004; Zhou, 2004; Chen et al. 2006) also showed that there were new inputs of DDTs in the PRD. However, comparatively lower level of DDTs found in marine organisms collected from East coast. But the survey of the National Bureau of Coastal Zone Protection during 1980–1987 showed that the organochlorines flux just carried by Yangtze River (the longest river in China) was 239.3 tons per year, which accounted for 19.8% of the total flux by Chinese river catchments into the marine coastal sites. Bohai Sea, Northern China collects pollutants from major rivers namely, Yalu, Daliao, Luanhi and Yellow (Figure 1) and showed comparatively intermediate levels of DDTs among the recent researches. Wu et al. (1999) noted high concentrations of DDTs in the river sediments from Northern China where a factory with high manufacturing capacity of DDT is located.

Table 1. The concentrations of OCPs and PCBs in marine organisms in ng/g (wet weight basis, dry weight basis in parenthesis; Wet weight = 0.16 * Dry weight (Ramesh et al. 1990)) in China.

Coastal region	DDTs	HCHs	CHLs	HCBs	PCBs	Reference
east Xiamen Island, South Eastern China	(75.2 - 2143)	(0.18 – 345)			(n.d. – 234)	Chen et al. (2002)
Minjing Estuary, South Eastern China	(21.5– 2396)	(n.d.-5.07)			(n.d.-6.78)	Chen et al. (2002)
South coast, China	(150–200)					Klumpp et al. (2002)
South China Sea	65.70	< 1.5				Guo et al. (2007)
PRD	(4.1 - 7840)	(10.8)				Guo et al. (2008)
East coast, China	(14.4–640)	(0.17– 9.91)	(0.13– 1.86)		(1.34–13)	Fung et al. (2004)
Bohai Sea	29.40	1.27				Yang et al. (2004)
Dalian, Tianjin and Shanghai	28.9	0.92	0.47	0.38		Yang et al (2006)
northeast coast	(54.8– 2680)	(1.42– 25.5)	(n.d.–2.28)		(3.27– 25.4)	Jin et al., 2008

4.2 Reasons for the different levels of other OCPs and PCBs

The results indicate that the HCHs concentrations were below than concentrations of DDTs. Historically, the usages of technical HCHs were much more (Figure 4) than those of DDTs in China. The discrepancy between the usages of HCHs and DDTs and their accumulative levels in seafood products may be due to the difference in physicochemical and biochemical properties between HCHs and DDTs, where in HCHs have higher biodegradability and lower lipophilicity compared to DDTs (Guo et al. 2007). The PCB levels in some areas showed high levels while other places had low levels. The physicochemical properties of PCBs vary

widely and depend on the number and position of chlorine atoms in biphenyl rings. Vapor pressure, water solubility and biodegradability decrease with increasing number of chlorine atoms. In contrast, lipophilicity and adsorption capacity show a reverse trend (Loganathan, 1994). Therefore, high levels of PCBs in body tissues explained by accumulation of low chlorinated PCB congeners. PCBs were banned in 1983, yet a large proportion still remains in use at present in older transformers and capacitors. The high assimilative and self-purification capabilities of the estuary against anthropogenic activities and pollution impact via large runoff discharge during wet season and enormous sediment loads might be the major abating factors for high PCBs. However, (Jiang et al. 1997) reported that in the previous decades, only about 8000 tons of PCBs were produced in China. The chlordanes were also observed in marine organisms but the level was low. It was reported that technical chlordane is still being used in China against termites (Xu et al. 2004; Nakata et al. 2005), and trans-chlordane, cis-chlordane, trans-nonachlor are dominant constituents in technical chlordane (Kawano et al. 1988; Kawano et al. 1992 ; Xu et al. 2004).

4.3 Comparison the OCPs and PCBs in Chinese seafood with different countries

Table 2 summarizes the OCPs and PCBs analyzed in fish/shell fish species in different countries. P.R.China shows the highest DDT value among the sea foods in different countries. The reason behind this statement is high back ground levels in history. A substantial number of studies have focused on the contamination by POP pesticides in different ecological compartments in China, with pesticide residues remaining highly abundant in soils and crops (Wong et al. 2005). These contaminants ultimately reach to coastal environment through water bodies. In contrast, studies on the levels of POPs in the global environment show that emission sources of a number of POPs (including DDT) in the last 20 years have shifted from industrialized countries of Northern Hemisphere to less developing countries in tropical and sub-tropical regions including India and China (Wong et al. 2005). This may be due to the late production ban otherwise DDT is still being used in agriculture and for the control of disease such as malaria, typhus and cholera (Iwata et al. 1994 ; Loganathan and Kannan, 1994). But in tropical environment, these POPs compounds biodegrade and volatilize soon due to high temperatures. Therefore, the levels become reduced (Table 2). Hong Kong also shows comparatively high DDT and those values are implying that South China Sea is receiving DDT residues. Li et al. (2006) reported that higher concentrations of HCHs and DDTs in water, sediment, fish, and human breast milk in Hong Kong where no HCHs and DDTs were presently in use. This may due to the dispersion of OCPs in marine matrices and in turn to the uptake of OCPs via aquatic food chain.

The highest PCBs, HCHs, CHLs and HCBs concentrations in Table 2 are in the samples collected from Russia, India, Japan and Malaysia respectively. In the former USSR, technical PCBs mixtures have been used and produced as a dielectric fluid in the manufacture of power capacitors and transformers (Ivanov and Sundell, 1992). Therefore high PCBs level could explain by the presence of local PCB sources. In history, China was the top in use of HCHs. But in the present, the reason for the high level of HCHs in the marine organisms of India may be the usage of certain amount of technical HCHs for public health purposes and on certain food crops after its ban for agriculture in 1983 (Li et al. 1998). The chlordanes had been used largely for termite control until in 1986 in Japan (Loganathan et al. 1993) and high levels in marine organisms implied that they may be still discharged into the marine environment. HCB is not only used as a fungicide, but also generated as a byproduct during the production of agrochemicals and industrial chemicals (Monirth et al. 2003). Furthermore the HCB has been released to the environment by waste incineration (Van-Birgelen, 1998). Those reasons could account to the high levels of HCBs in Malaysia. However, the low residual levels of these pesticides and their low frequency of detection in Chinese coastal environment may be attributed to their relatively low residual levels in coastal environment and in seafood products in China or their relatively low potential for bioaccumulation in the species under consideration.

Table 2. The concentrations of OCPs and PCBs in marine organisms in $ng^{-1}g$ (wet weight basis, dry weight basis in parenthesis; Wet weight = 0.16 * Dry weight (Ramesh et al. 1990)) in different coastal regions in the world.

Country/coastal region	DDTs	HCHs	CHLs	HCBs	PCBs	References
China	240	0.80	3.0	1.3	2.5	Monirith et al. (2003)
Perth (western Australia)	0.2					Sericano et al. (1993)
Taiwan (China)	(0–121)	(0–7)				Ling and Teng (1997)

The marine coastal (USA)	(0.51–27.9)					O'Connor and Beliaeff (1998)
The coast of north Vietnam	(12.0 - 23.3)				(5.1- 25.3)	Nhan et al. (1999)
Taiwan- Machu	(340)					Cheng Han et al. (2000)
Kim-man	(337)					
Coastal water of Thailand	0.05–5.7		0.22–12.0			Boonyatumanond et al. (2002)
Korea entire coast	3.13	0.98	0.62	0.04	3.90	Kim et al. (2002)
Japan	3.5	0.32	6.0	0.08	30	Monirith et al. (2003)
India	4.2	2.0	0.6	0.02	3.8	Monirith et al. (2003)
Black sea coast	<0.12-14			0.364		Ozcok et al. (2007)
Egypt	98.1-629.8					Khalid et al. (2004)

5. Health Risk Assessment

Human epidemiological surveys have been proven that the exposure to chlorinated pesticides make adverse effects on human health (Ribas-Fito et al. 2003 ; Longnecker et al. 2001; Cooper et al. 2004). Table 3 summarizes the acceptable daily intakes of these pesticides issued by some authorities. The results revealed that the DDTs are the predominant contaminant. Most of the studies showed higher levels of DDTs than the Chinese government's first level criterion (10 ng/g) for marine biological quality (GB-18421-2001) (Chen et al. 2002) but conformed to the first level criterion (20 ng/g and 50 ng/g) for HCHs and PCBs respectively. DDT is highly persistent in the environment with a half life of 2–15 years (USEPA, 1989). In human fatty tissue, the half life of DDT has been reported to be 7–8 years (NACEC, 2001). To assess the human health risk, the estimated daily intakes (EDI) were calculated using the average values per each pollutant and the value for the consumption of fish and seafood in China (30.5 g/person/day) in 1997 (Du et al. 2004). The results (Table 4) reveal that the estimated daily intakes (EDI) for DDTs in South China Sea exceed the maximum admissible DDTs concentration established by the European Union which is more feasible value from the farmer's point of view. Hence, the sea food in South China could consider overloaded with DDTs. However, the exposure levels depend on the lipid content of the fish and on the amount of seafood consumed.

Table 3. The acceptable limit of certain POPs pesticides for humans (ng/g wet weight)

Authority	DDTs	HCHs	PCBs	Reference
Food and Agricultural Organization, World Health Organization	20	8		FAO/WHO (1993)
European Union	50	10		Binelli and Provini, 2003

Table 4. Estimated daily intakes (EDI) of PCBs, DDTs and HCHs through sea food by human (average body wt. 60 kg) in China. EDI (ng /kg /day) = [daily fish consumption (g /day)] × [mean OCP concentration (ng/g wet wt.)]/ [human body weight (kg)].

Pollutant	Average concentration (ng/g wet wt.)	EDI (ng/kg body wt./day)	ADI (FAO/WHO) (ng/kg body wt./day)
PCBs	China : 2.5	1.27	
DDTs	South China: 65.70	33.39	20
	Bohai Sea : 29.40	14.94	
HCHs	South China : < 1.5	0.76	8
	Bohai Sea : 1.27	0.64	

The results confirm that the concentrations of HCHs and PCBs in sea foods are far below to all the maximum admissible limits establish by different authorities. (Nakata et al. 2002) reported that the levels of HCHs in foodstuffs (including aquatic products) dramatically declined during the last 30 years. Moreover, low residual levels of HCHs suggest that HCHs are no longer an environmentally significant organic contaminant in seafood products from China.

Conclusion

Sea foods in Chinese coastal zone are contaminated with OCPs. Risk assessment against various standards clearly showed that seafood products in South China Sea are contaminated by DDTs and may pose health threat to local residents and the consumers if they totally rely on sea foods as their prime animal proteins. A national wide survey is needed to investigate the intake of OCPs, due to dietary differences, with a strong focus on the more sensitive populations, e.g., coastal residents who consume a large amount of fish.

Correspondence to: Mangala Yatawara,
China University of Geoscience of Wuhan,
P.R.China
Telephone: +8613476245770
Email: mmkyat@yahoo.com

References

[1]Bi X, Chu S, Meng Q, Xu X. Movement and retention of polychlorinated biphenyls in a paddy field of WenTai area in China, Agriculture**.** Ecosystems and Environment 2002; 89: 241–252.

[2]Binelli A, Provini A. POPs in edible clams from different Italian and European markets and possible human health risk. Marine Pollution Bulletin 2003; 46:879–886.

[3]Boonyatumanond R, Jaksakul A, Puncharoen P, Tabucanon M S. Monitoring of organochlorine pesticides residues in green mussels (*Perna viridis*) from the coastal area of Thailand. Environmental Pollution 2002; 119: 245–252.

[4]Cai D J, Sun L J, Ke J L, Tang G C. Technical report RP032: pesticide usage in China, Ontario, Environment Canada, Canada. 1992.

[5]Cao W, Wong M H. Current status of coastal zone issues and management in China: A review. Environment International 2007; 33(7): 985-992.

[6]Chen L G, Mai B X, Bi X H, Ran Y, Luo X J, Chen S J, Sheng G Y, Fu J M, Zeng E Y. Concentration levels, compositional profiles, and gas-particle partitioning of polybrominated diphenyl ethers in the atmosphere of an urban city in South China. Environmental Science and Technology 2006; 40: 709–714.

[7]Chen W, Zhang L, Xu , Wang X, Hong L, Hong H. Residue levels of HCHs, DDTs and PCBs in shellfish from coastal areas of east Xiamen Island and Minjiang Estuary, China. Marine Pollution Bulletin**.** 2002; 45(1-12): 385-390.

[8]Chen W, Hong H, Zhang L, Xu L, Wang X, Hong, L. Residue levels and distribution features of organochlorine pollutants in the surface sediments of the sea areas between Minjiang Estuary and Mazu. Marine Science Bulletin. 2000; 19: 53–58 (in Chinese).

[9]Chen W, Zhang L, Xu L, Wang X, Hong H. Concentrations and distributions of HCHs, DDTs and PCBs in surface sediments of sea areas between Xiamen and Jinmen. Journal of Xaimen University (Natural Science). 1996; 35: 936–940 (in Chinese).

[10]Cheng Han, B, Lih Jeng W, Chang Hung T, Chien Ling Y, Jer Shieh M, Chu Chien L. Estimation of metal and organochlorine pesticide exposures and potential health threat by consumption of oysters in Taiwan. Environmental Pollution. 2000; 109(1): 147-156.

[11]Cheng, X. The pesticides production of China going to a period of higher efficient and more secure. Pesticides (in Chinese). 1990; 29 (1): 15–19.

[12]Cooper G S, Martin S A, Longnecker M P, Sandler D P, Germolec D R. Associations between plasma DDE levels and immunologic measures in African-American farmers in North Carolina. Environmental Health Perspectives. 2004; 112: 1080–1084.

[13]Dougherty C P, Holtz S H, Reinert J C , Panyacosit L, Axelrad D A, Woodruff T J. Dietary exposures to food contaminants across the United States. Environmental Research. 2000; 84:170–185.

[14]Du S, Zai F, Yang X. Report on nutritional and physical status of Chinese population. Databank of nutritional and physical status of Chinese population. 2004. Available from: http://www.in fh.ac.cn/database.htm.

[15]Fang Z Q, Cheung R Y H, Wong M H. Concentrations and distribution of organochlorinated pesticides and PCBs in green-lipped mussels, *Perna viridis* collected from the Pearl River estuarine zone. Acta Scientiae Circumstantiae 2001; 21**(**1): 113–116 (in Chinese).

[16]FAO/WHO. Food Standards Programme vol. 9 (4). Codex Alimentarius Commission, 1993;149–158.

[17]Fu J M, Mai B X, Sheng G Y, Zhang G, Wang X M, Peng P A, Xiao X M, Ran R, Cheng F Z, Peng X Z, Wang Z S, Tang U W. Persistent organic pollutants in environment of the Pearl River Delta, China: An overview. Chemosphere. 2003 ; 52:1411–1422.

[18]Fung C N, Lam J C W, Zheng G J, Connel D W, Monirith I, Tanabe S, Richardson B J, Lam P K S. Mussel based monitoring of trace metal and organic contaminants along the east coast of China using *Perna viridis* and *Mytillus edulis.* Environmental Pollution. 2004; 127: 203-216.

[19]Guo Y, Meng X Z, Tang H L, Zeng E Y. Tissue distribution of organochlorine pesticides in fish collected from the Pearl River Delta, China: Implications for fishery input source and bioaccumulation. Environmental Pollution. 2008; 155(1): 150-156.

[20]Guo J Y, Zeng E Y, Wu F C, Meng X Z, Mai B X, Luo X J. Organochorine Pesticides in Sea Food Products from Southern China and Health Risk Assessment. Environmental Toxicology and Chemistry. 2007; 26 (6): 1109–1115.

[21]Harrison R M, Smith D J T, Luhana L. Source apportionment of atmospheric polycyclic aromatic hydrocarbons collected from an urban location in Birmingham, U.K. Environmental Science and Technology1996; 30: 825–832.

[22]Hong H, Xu L, Zhang L, Chem J C, Wong Y S, Wan T S M. Environmental fate and chemistry of organic pollutants in the sediment of Xiamen and Victoria Harbours. Marine Pollution Bulletin.1995; 31: 229–236.

[23]Ivanov V, Sundell E N. Characterization of polychlorinated biphenyl isomers in Sovol and trichlorobiphenyl formulations by high resolution gas chromatography with electron capture detection and high resolution gas chromatography mass spectrometry technique. Environmental Science and Technology 1992; 26: 2012-2017.

[24]Iwata H, Tanabe S, Sakai N, Nichimura A, Tatsukawa R. Geographical distribution of persistent organochlorines in air, water and sediments from Asia and Oceania and their implications for global redistribution from lower latitudes. Environmental Pollution. 1994; 85: 15–33.

[25]Jiang K, Li L, Chen Y, Jin J. Determination of PCDD/Fs and dioxin-like PCBs in Chinese commercial PCBs and emissions from a testing PCB incinerator, Chemosphere.1997 ; 34: 941–950.

[26]Jin Y, Hong S H, Li D, Shim W J, Lee S S. Distribution of persistent organic pollutants in bivalves from the northeast coast of China Marine Pollution Bulletin. 2008; 57(6-12): 775-781.

[27]Kawano M, Inoue T, Wada T, Hidaka H, Tatsukawa R. Bioaccumulation and residue patterns of chlordane compounds in marine animals: Invertebrates, fish, mammals, and seabirds. Environmental Science and Technology. 1988; 22: 792–797.

[28]Kawano M, Ramesh A, Thao V D, Tatsukawa R, Subramanian A N. Persistent organochorine insecticide residues in some paddy, upland and urban soils of India. International Journal of Environmental Analytical Chemistry. 1992; 48: 163–174.

[29]Kennisch M J. Practical handbook of estuarine and marine pollution. Boca Raton, NY: CRC Press, Marine Science Series. 1996.

[30]Khalid A, Nemr A E, Said T O, El-Sikaily A, ABD-Alla A M A. Polychlorinated biphenyls and chlorinated pesticides in mussels from the Egyptian Red Sea Coast. Chemosphere. 2004; 54: 1407-1412.

[31]Kim S K, Oh J R, Shim W J, Lee D H, Yim U H, Hong S H, Shin Y B, Lee D S. Geographical distribution and accumulation features of organochlorine residues in bivalves from coastal areas of South Korea. Marine Pollution Bulletin. 2002; 45(1-12): 268-279.

[32]Klumpp D W, Hong H, Humphrey C, Wang X, Codi, S. Toxic contaminants and their biological effects in coastal waters of Xiamen, China. I. Organic pollutants in mussel and fish tissues. Marine Pollution Bulletin. 2002; 44: 752–760.

[33]Kromhout D, Bosschieter E B, Lezenne Coulander C. The inverse relation between fish consumption and 20-year mortality from coronary heart disease. New England Journal of Medicine. 1985; 312: 1205–1209.

[34]Lee K T, Tanabe S, Koh CH. Distribution of organochlorine pesticides in sediments from Kyeonggi Bay and nearby areas, Korea. Environmental Pollution. 2001; 114: 207–213.

[35]Li J, Zhang G., Qi S, Li X, Peng, X. Concentrations, enantiomeric compositions, and sources of HCH, DDT, and chlordane in soils from the Pearl River Delta, South China. Science of the Total Environment. 2006; 372:215–224.

[36]Li YF, Macdonald R W. Sources and pathways of selected organochlorine pesticides to the Arctic and the effect of pathway divergence on HCH trends in biota: a review. Science of the Total Environment. 2005; 342(1-3): 87-106.

[37]Li YF, Li D C. Global emission inventories for selected organochlorine pesticides. Internal report, meteorogical service of Canada, Environment Canada, Toronto, Canada. 2004.

[38]Li YF, Zhulidov JAV, Roberts R D, Korotova LG. Hexachlorocyclohexane use in the Former Soviet Union. Archives of Environmental Contamination and Toxicology. 2004a.48: 10–15.

[39] Li YF, Bidleman TF. Correlation between global emissions of hexachlorocyclohexane and its concentrations in the Arctic Air. Journal of Environmental Informatics. 2003a; 1: 52–57.

[40]Li YF Bidleman TF. Usage and emissions of organochlorine pesticides, Canadian Arctic contaminants assessment report II, Indian and Northern Affairs Canada, Ottawa, 2003b:49–70 Chap. A.2.

[41]Li YF. Global technical hexachlorocylohexane usage and its contamination consequences in environment: from 1948 to 1997. Science of the Total Environment 1999a; 232**:** 123–160**.**

[42]Li YF, Cai DJ, Singh A. Technical hexachlorocyclohexane use trends in China and their impact on the environment. Archives of Environmental Contamination and Toxicology1998b; 5: 688–697.

[43]Li YF, Cai DJ, Singh A. Technical hexachlorocyclohexane use trends in China and their impact on the environment. Archives of Environment Contamination Toxicology1998; 35**:** 688–697.

[44]Ling YC, Teng HC. Supercritical fluid extraction and cleanup of organochlorine pesticides and polychlorinated biphenyls in mussel. Journal of Chromatography. 1997; 90: 153–160.

[45]Loganathan BG, Kannan K. Global Organochlorine Contamination Trends: An Overview. Ambio1994; 23 (3): 187–191.

[46]Loganathan BG, Tnabe S, Hidaka Y, Kawano M, Hidaka H, Tatsukawa R. Temporal trends of persistent organochlorine residues in human adipose tissue from Japan, 1928-1985. Environmental Pollution1993; 81: 31-39.

[47]Longnecker MP, Klebanoff MA, Zhou H, Brock JW. Association between maternal serum concentration of the

DDT metabolite DDE and preterm and small-for-gestational-age babies at birth. Lancet2001; 358: 110–114.

[48]Luo XJ, Mai BX, Yang QS, Fu JM, Sheng GY, Wang ZS. Polycyclic aromatic hydrocarbons (PAHs) and organochlorine pesticides in water columns from the Pearl River and the Macao harbor in the Pearl River Delta in South China. Marine Pollution Bulletin2004; 48:1102–1115.

[49]Mai BX, Fu JM, Sheng GY, Kang YH, Lin Z, Zhang G, Min YS, Zeng EY. Chlorinated and polycyclic aromatic hydrocarbons in riverine and estuarine sediments from Pearl River Delta, China. Environmental Pollution2002; 117: 457–474.

[50]Monirith I, Ueno D, Takahashi S, Nakata H, Sudaryanto A, Subramanian A, Karuppiah S, Ismail A, Muchtar M, Zheng JJ, Richardson B, Prudente M, Due Hue N, Tana TVS, Tkalin A, Tanabe S. Asia-Pacific mussel watch: monitoring contamination of persistent organochlorine compounds in coastal waters of Asian countries. Marine Pollution Bulletin2003; 6 (3): 281–300.

[51]NACEC.Actions for eliminating DDT in Mexico and Central America. Q & A: NACEC, NARAP on DDT. North America Commission for Environmental Cooperation, 2001. (6/4/01)

[52]Nakata H, Hirakawa Y, Kawazoe M, Nakabo T, Arizono K, Abe S, Kitano T, Shimada H, Watanabe I, Li W, Ding X. Concentrations and compositions of organochlorine contaminants in sediments, soils, crustaceans, fishes and birds collected from Lake Tai, Hangzhou Bay and Shanghai city region, China. Environmental Pollution2005; 133 (3): 415–429.

[53]Nakata HM, Kawazoe K, Arizono S, Abe T, Kitano H, Shimada W, Li XD. Organochlorine pesticides and polychlorinated biphenyl residues in foodstuffs and human tissues from China: Status of contamination, historical trend, and human dietary exposure Archives of Environmental Contamination and Toxicology2002; 3: 473–480.

[54]Nhan D D, Am N M, Carvalhoc FP, Villeneuve JP, Cattini C. Organochlorine pesticides and PCBs along the coast of North Vietnam. The Science of the Total Environment1999; 237/238: 363-371.

[55]NIP; The People's Republic of China National Implementation Plan for the Stockholm Convention on Persistent Organic Pollutants. 2007.

[56]O'ConnorTP, Beliaeff B. Recent Trends in Coastal Environmental Quality (Result from the Mussel atch Project, NOAA Silver Spring, MD, 40) 1998.

[57]Ozkoc B, Bakan G Ariman S. Distribution and bioaccumulation of organochlorine pesticides along the Black Sea coast. Environmental Geochemistry and Health2007; 9(1):59-68.

[58]Pandit G G, Sahu S K, Sadasivan S. Distribution of HCH and DDT in the coastal marine environment of Mumbai, India. Journal of Environmental Monitoring2002; 4: 431–434.

[59]Phillips DJH. Organochlorine and trace metals in green-lipped mussels *perna viridis* from HongKong waters: a test of indicator ability. Marine Ecology Progress Series1985; 21:252–258.

[60]Qiu X, Zhu T, Li J, Pan H, Li Q, Miao G, Gong J. Organochlorine pesticides in the air around the Taihu Lake, China. Environmental Science and Technology2004; 38: 1368–1374.

[61]Ramesh A, Tanabe S, Subramanian AN, Mohan D, Venugopalan VK, Tatsukawa R. Persistent organochlorine residues in green mussels from coastal waters of South India. Marine Pollution Bulletin1990; 21: 587–590.

[62]Ribas-Fito N, Cardo E, Sala M, Eulàlia de Muga M, Mazón C, Verdú A, Kogevinas M, Grimalt JO, Sunyer J. Breastfeeding, exposure to organochlorine compounds, and neurodevelopment in infants. Pediatrics2003; 111: 580–585.

[63]Sericano JL, Wade TL, Brooks JM, Elliot LA, Fay RR, Wilkinson DL. National status and trends and mussel watch program: chlordane-related compounds in Gulf of Mexico oysters. Environmental Pollution1993; 82: 23–32.

[64]Svensson BG, Nilsson A, Josson E, Schütz A, Åkesson B, Hagmar L. Fish consumption and exposure to persistent organochlorine compounds, mercury, selenium and methylamines among Swedish fishermen. Scandinavia Journal of Work Environmental Health 1995; 21: 96–105.

[65]Tanabe S, Tatsukawa R, Phillips DJH. Mussels as bioindicators of PCB pollution: a case study of uptake and release of PCB isomers and congeners in green-lipped mussels (*perna viridis*) in Hong Kong waters. Environmental Pollution1987; 47: 41–48.

[66]Tao S, Xu FL, Wang XJ, Liu WX, Gong ZM, Fang JY, Zhu LZ, Luo YM. Organochlorine pesticides in agricultural soil and vegetables from Tianjin, Environmental Science and Technology2005; 39: 2494–2499.

[67]UNEP (United Nations Environment Programme), Central and North East Asia regional report, regionally based assessment of PTS, UNEP/GEF. 2002.

[68]USEPA. Pesticide Environmental Fate on Line Summary: DDT (*p*, *p*′). Environmental Fate and Effects Division, USEPA, Washington, DC. , 1989.

[69]Van-Birgelen APJM. Hexachlorobenzene as a possible major contributor to the dioxin activity of human milk. Environmental Health Perspectives1998; 106: 183-188.

[70]Voldner EC, Li YF. Global usage of selected persistent organochlorines. Science of the Total Environment1995; 60/161: 201–210.

[71]Walker K, Vallero DA, Lewis RG. Factors influencing the distribution of lindane and other hexachlorocyclohexanes in the environment. Environmental Science and Technology1999; 33:4373–8.

[72]WB (World Bank) Demonstration of alternatives to chlordane and mirex in termite control, GEF-2359, Document of World Bank. 2005.

[73]Wei D, Kameya T, Urano K. Environmental management of pesticidal POPs in China: Past, present and future. Environment International2007; 07: 894-902.

[74]Wong MH, Choi K, Grosheva E, Sakai S, Shibata Y, Suzuki N, Wang J, Zhou H, Leung A. Central and North East Asia

regional report-Regionally based assessment of persistent toxic substances, UNEP/GEF. 2002.

[75]Wong MH, Leung AOW, Chan JKY, Choi MPK. A review on the usage of POP pesticides in China, with emphasis on DDT loadings in human milk. Chemosphere2005; 60(6): 740-752.

[76]Wu Y, Zhang J, Zhou Q. Persistent orgnochlorine residues in sediments from Chinese river/estuary systems. Environmental Pollution1999; 105: 143–150.

[77]Xu D, Zhong W, Deng L, Chai Z, Mao X. Regional distribution of organochlorinated pesticides in pine needles and its indication for socioeconomic development. Chemosphere2004; 54: 743–752.

[77]Yang N, Matsuda M, Kawano M, Wakimoto T. PCBs and organochlorine pesticides (OCPs) in edible fish and shellfish from China. Chemosphere2006; 63(8):1342-1352.

[78]Yang N, Matsuda M, Kawano M, Wakimoto T. PCBs and organochlorine pesticides (OCPs) in edible fish and shellfish from China. Chemosphere2006; 63(8): 1342-1352.

[79]Yang R Q, Yao Z W, Jiang G B. Zhou Q F, Liu J Y. HCH and DDT residues in molluscs from Chinese Bohai coastal sites. Marine Pollution Bulletin2004; 48(7-8): 795-799.

[80]Zhang G,Parker A, House A, Mai B, Li X, Kang Y, Wang Z. Sedimentary records of DDT and HCH in the Pearl River Delta, South China. Environmental Science and Technology2002; 36:3671–3677.

[81]Zhang G, Qi S, Parker A, Li X, Li J, Wang X, Distribution of organochlorine pesticides and polycyclic aromatic hydrocarbons in soils from the Pearl River Delta, South China. Abstract on the 3rd Asia–Pacific Sym. Environmental Geochemistry Guangzhou, China.2001; 93.

[82]Zhao G, Xu Y, Li W, Han G, Ling B. PCBs and OCPs in human milk and selected foods from Luqiao and Pingqiao in Zhejiang, China. Science of the Total Environment2007; 378(3):281-292.

[83]Zhou HY, Wong MH. Screening of organochlorines in freshwater fish collected from the Pearl River Delta, People's Republic of China. Archives of Environmental Contamination and Toxicology2004; 46: 106–113.

[84]Zhou K, Maskaoui Y, Qiu W, Hong HS, Wang ZD. Polychlorinated biphenyl congeners and organochlorine insecticides in the water column and sediments of Daya Bay, China. Environmental Pollution2001; 113: 373–384.

[85]Zhou, J., Hong, H., Zhang, Z., Maskaoui, K., and Chen, W. 2000. Multi-phase distribution of organic micropollutants in Xiamen Harbour, China. Water Research. 34 (7): 2132–2150.

Thermodynamic simulation of performance of an endoreversible Dual cycle with variable specific heat ratio of working fluid

Rahim Ebrahimi *

Department of Agriculture Machine Mechanics, Shahrekord University, P.O. Box 115, Shahrekord, Iran
Rahim.Ebrahimi@gmail.com

Abstract: An endoreversible Dual heat engine model is established and used to investigate the influence of the variable specific heat ratio of the working fluid on the performance of the cycle. The net work output and thermal efficiency of the cycle are derived and optimized with respect to the specific heat ratio of the working fluid. The results shows that that if compression ratio is less than certain value, the increase of specific heat ratio of the working fluid makes the net work output bigger; on the contrary, if compression ratio exceeds certain value, the increase of specific heat ratio of the working fluid makes the net work output less. The thermal efficiency increases with the increase of specific heat ratio of the working fluid throughout the compression ratio range. One can see that the maximum net work output, the working range of the cycle and the optimal compression ratio corresponding to maximum net work output decrease when specific heat ratio of the working fluid increases. However, the effects of the specific heat ratio of the working fluid on the performance of the cycle are obvious and they should be considered in practice cycle analysis. The results obtained in this paper may provide guidance for the performance evaluation and improvement of real reciprocating heat engines. [Journal of American Science 2009;5(5):175-180]. (ISSN: 1545-1003).

Key words: Finite time thermodynamics; Dual cycle; Variable specific heat ratio; Performance analysis

1. Introduction

Traditional thermodynamics is a theory about equilibrium states and about limits on process variables for transformations from one equilibrium state to another. In order to obtain more realistic limits to the performance of real processes, thermodynamics is extended to finite-time thermodynamics to deal with processes which have explicit time or rate dependencies (Bejan 1996; Aragon-Gonzalez et al. 2006; Zhao and Chen, 2006; Parlak et al., 2008). Thus, significant achievements have ensued since finite-time thermodynamics was developed in order to analyze and optimize the performances of real heat-engines (Chen et al., 1998; Aragon-Gonzalez et al., 2000; Chen et al., 2004). Blank and Wu (1994) analyzed the effect of combustion on the performance of an endoreversible dual cycle. Lin et al. (1999) derived the relations between the net power and the efficiency for the Dual cycle with due consideration of the heat-transfer losses. Wang et al. (2002) modeled Dual cycle with friction-like term loss during a finite time and studied the effect of friction-like term loss on cycle performance. Sahin et al. (2002a, 2002b) optimized the performance of a new combined power cycle based on power density analysis of the dual cycle and made a comparative performance analysis of an endoreversible dual cycle under a maximum ecological function and maximum power conditions. Hou (2004) studied the effect of heat transfer through a cylinder wall on the performance of the dual cycle. Chen et al. (2004) determined the characteristics of net work and efficiency for Dual cycle with heat transfers and friction losses. It is found that there are optimal values of the cut-off ratio at which the net work output and efficiency attain their maxima. Parlak et al. (2004) optimized the performance of an irreversible Dual cycle: the predicted behavior was corroborated by experimental results. Ust et al. (2005) performed an ecological performance analysis for an irreversible Dual cycle by employing the new thermo-ecological criterion as the objective function. Parlak et al. (2005) optimized the performance of irreversible Dual cycle, gave the experimental results, and compared the performance of Dual and Diesel cycles under the maximum power output. Parlak and Sahin (2006) defined the internal irreversibility by using entropy production, and analyzed the effect of the internal irreversibility on the performance of irreversible Dual cycle. Zhao et al. (2007) defined the internal irreversibility by using compression and expansion efficiencies and analyzed the performance of Dual cycle. The above work was done without considering the variable specific heats of working fluid,

so Ghatak and Chakraborty (2007) and Chen et al. (2006) analyzed the effect of variable specific heats and heat transfer loss on the performance of the dual cycle when variable specific heats of working fluid are linear functions of its temperature. Furthermore, Ge et al. (2009) analyzed the performance of an air standard Dual cycle with nonlinear relation between the specific heats of working fluid and its temperature, by using finite-time thermodynamics.

All of the above mentioned research, the specific heats at constant pressure and volume of working fluid are assumed to be constants or functions of temperature alone and have the linear and or the non-linear forms. But when calculating the chemical heat released in combustion at each instant of time for internal combustion engine, the specific heat ratio is generally modeled as a linear function of mean charge temperature (Gatowski et al., 1984; Ebrahimi, 2006). The model has been widely used and the phenomena that it takes into account are well knows (Klein, 2004). However, since the specific heat ratio has a great influence on the heat release peak and on the shape of the heat release curve (Brunt, 1998), many researchers have elaborated different mathematical equations to describe the dependence of specific heat ratio from temperature (Gatowski et al., 1984; Brunt, 1998; Egnell, 1998; Klein, 2004; Klein and Erikson, 2004; Ceviz and Kaymaz, 2005). It should be mentioned here that the most important thermodynamic property used in the heat release calculations for engines is the specific heat ratio (Ceviz and Kaymaz, 2005). So, Ebrahimi (2009) modeled the dual cycle with considerations the variable specific heat ratio during a finite time and only studied the effect of cut-off ratio on cycle performance. Therefore, the objective of this study is to examine the effect of variable specific heat ratio on the net work output and the thermal efficiency of air standard Dual cycle.

2. Thermodynamic analysis

The temperature entropy diagram of a Dual heat engine is shown in figure 1. The compression process is an isentropic process ($1 \to 2$); the heat additions are an isochoric process ($2 \to 3$) and an isobaric process ($3 \to 4$); the expansion process is an isentropic process ($4 \to 5$) and the heat rejection is an isochoric process ($5 \to 1$).

As mentioned above, it can be supposed that the specific heat ratio of the working fluid is function of temperature alone and has the following linear form:

$$\gamma = \gamma_o - k_1 T \tag{1}$$

where γ is the specific heat ratio and T is the absolute temperature. γ_o and k_1 are constants.

The heat added to the working fluid, during processes ($2 \to 3$) and ($3 \to 4$) is

$$Q_{in} = \int_{T_2}^{T_3} c_v dT + \int_{T_3}^{T_4} c_p dT = \int_{T_2}^{T_3} \left(\frac{R_{air}}{\gamma_o - k_1 T - 1} \right) dT + \int_{T_3}^{T_4} \left(\frac{R_{air}\left(\gamma_o - k_1 T\right)}{\gamma_o - k_1 T - 1} \right) dT = \frac{R_{air}}{k_1} \ln\left(\frac{\gamma_o - k_1 T_2 - 1}{\gamma_o - k_1 T_4 - 1} \right) + R_{air}\left(T_4 - T_3\right) \tag{2}$$

where M is the molar number of the working fluid which is function of engine speed. R_{air} and c_p are molar gas constant and molar specific heat at constant pressure for the working fluid, respectively.

The heat rejected by the working fluid during the process ($5 \to 1$) is

$$Q_{out} = \int_{T_1}^{T_5} c_v dT = \int_{T_1}^{T_5} \left(\frac{R_{air}}{\gamma_o - k_1 T - 1} \right) dT = \frac{R_{air}}{k_1} \ln\left(\frac{\gamma_o - k_1 T_1 - 1}{\gamma_o - k_1 T_5 - 1} \right) \tag{3}$$

where c_v is the molar specific heat at constant volume for the working fluid.

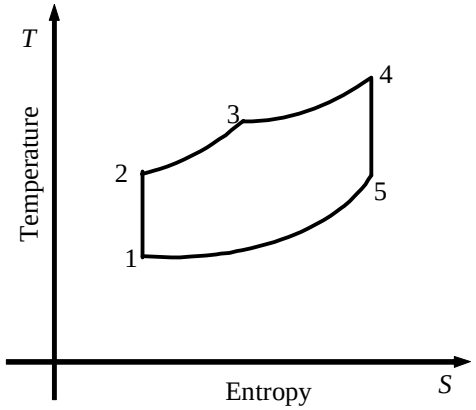

Figure 1. Diagram for the air standard Dual cycle

According to references (Ge et al., 2008a; Al-Sarkhi, 2007), the equation for a reversible adiabatic process with variable specific heat ratio can be written as follows:

$$TV^{\gamma-1} = \left(T + \mathrm{d}T\right)\left(V + \mathrm{d}V\right)^{\gamma-1} \tag{4}$$

From Eq. (4), we get the following equation

$$T_i\left(\gamma_o - k_1 T_j - 1\right) = T_j\left(\gamma_o - k_1 T_i - 1\right)\left(V_j / V_i\right)^{\gamma_o - 1} \tag{5}$$

The compression, r_c, and cut-off, β, ratios are defined as

$$r_c = V_1/V_2 \quad (6)$$

and

$$\beta = V_4/V_3 = T_4/T_3 \quad (7)$$

Therefore, the equations for processes $(1 \to 2)$ and $(4 \to 5)$ are shown, respectively, by the following:

$$T_1\left(\gamma_o - k_1 T_2 - 1\right)\left(r_c\right)^{\gamma_o - 1} = T_2\left(\gamma_o - k_1 T_1 - 1\right) \quad (8)$$

$$T_4\left(\gamma_o - k_1 T_5 - 1\right) = T_5\left(\gamma_o - k_1 T_4 - 1\right)\left(\frac{T_3}{T_4} r_c\right)^{\gamma_o - 1} \quad (9)$$

The energy transferred to the working fluid during combustion is given by the following linear relation (Zhao and Chen, 2007; Chen et al., 2008).

$$Q_{in} = A - B\left(T_2 + T_4\right) \quad (10)$$

where A and B are two constants related to combustion and heat transfer which are function of engine speed. From equation (10), it can be seen that Q_{in} contained two parts: the first part is A, the released heat by combustion per second, and the second part is the heat leak loss per second, $Q_{leak} = B\left(T_2 + T_4\right)$.

Thus, the net work output of the Dual cycle engine can be written as

$$W_{out} = \frac{R_{air}}{k_1} \ln\left(\frac{\left(\gamma_o - k_1 T_2 - 1\right)\left(\gamma_o - k_1 T_5 - 1\right)}{\left(\gamma_o - k_1 T_4 - 1\right)\left(\gamma_o - k_1 T_1 - 1\right)}\right) + R_{air}\left(T_4 - T_3\right) \quad (11)$$

The thermal efficiency of the Dual cycle engine is expressed by

$$\eta_{th} = \frac{\frac{1}{k_1}\ln\left(\frac{\left(\gamma_o - k_1 T_2 - 1\right)\left(\gamma_o - k_1 T_5 - 1\right)}{\left(\gamma_o - k_1 T_4 - 1\right)\left(\gamma_o - k_1 T_1 - 1\right)}\right) + T_4 - T_3}{\frac{1}{k_1}\ln\left(\frac{\gamma_o - k_1 T_2 - 1}{\gamma_o - k_1 T_4 - 1}\right) + T_4 - T_3} \quad (12)$$

When the values of r_c, β and T_1 are given, T_2 can be obtained from Eq. (8) and T_3 can be found from Eq. (7), then, substituting Eq. (2) into Eq. (10) yields T_4, and the last, T_5 can be worked out using Eq. (9). Substituting T_1, T_2, T_3, T_4 and T_5 into Eqs. (11) and (12), respectively, the net work output and thermal efficiency of the Dual cycle engine can be obtained. Therefore, the relations between the net work output, the thermal efficiency and the compression ratio can be derived.

3. Results and discussion

The following constants and parameter values have been used in this exercise: $T_1 = 300\,K$, $k_1 = 0.00003 - 0.00009\,K^{-1}$, $\gamma_o = 1.31 - 1.41$, $A = 60000\,J.mol^{-1}$, $\beta = 1.1$ and $B = 28\,J.mol^{-1}K^{-1}$ (Chen et al., 2006; Ghatak and Chakraborty, 2007; Ge et al., 2007; Ebrahimi, 2009). Using the above constants and range of parameters, the characteristic curves of the net work output and efficiency, varying with the pressure ratio, and the net work output versus efficiency can be plotted.

The variations in the temperatures T_2, T_3, T_4 and T_5 with the compression ratio are shown in figure 2. It is found that T_2, T_3 and T_4 increase with the increase of compression ratio, and T_5 decreases with the increase of compression ratio. In figure 2, there are two special states: one is the state with $T_5 \geq T_4$, the another is the state with $T_2 \geq T_3$. In the two special states, the cycle cannot work.

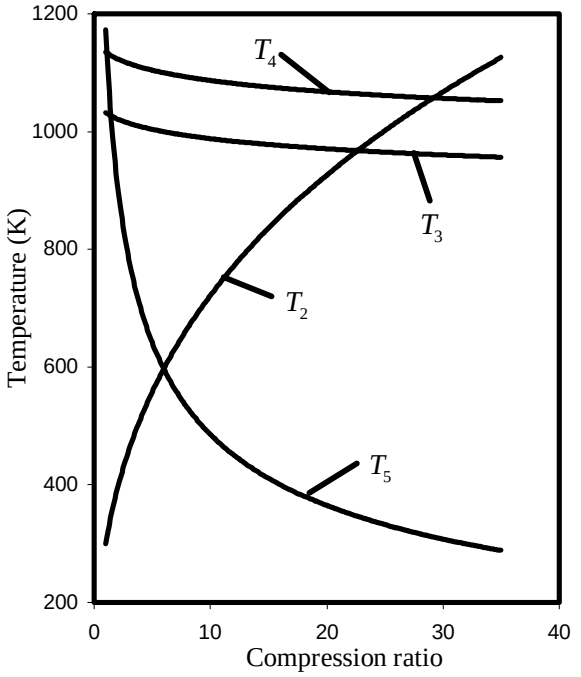

Figure 2. The temperature versus compression ratio for $\beta = 1.1$

Figures. 3-6 display the influence of the parameters γ_o and k_1 related to the variable specific heat ratio of the working fluid on the Dual cycle performance with considerations of heat transfer. From these figures, it can be found that γ_o and k_1 play a key role on the work output and the thermal efficiency. It should be noted that the heat added and the heat rejected by the working fluid decrease with increases of γ_o, while increase with increasing k_1. (see Eqs. (2) and (3)). It can be seen that the effect of γ_o is more than that of k_1 on the net work output and thermal efficiency. It should be mentioned here that for a fixed k_1, a larger γ_o

corresponds to a greater value of the specific heat ratio and for a given γ_o, a larger k_1 corresponds to a lower value of the specific heat ratio. It can also be found from these figures that the net work output versus compression ratio characteristic is approximately parabolic like curves. In other words, the net work output increases with increasing compression ratio, reach their maximum values and then decreases with further increase in compression ratio. But, the thermal efficiency increases with increasing compression ratio. It is also clearly seen that the effects of γ_o and k_1 on the work output and thermal efficiency are related to compression ratio. They reflect the performance characteristics of an endoreversible Dual cycle engine.

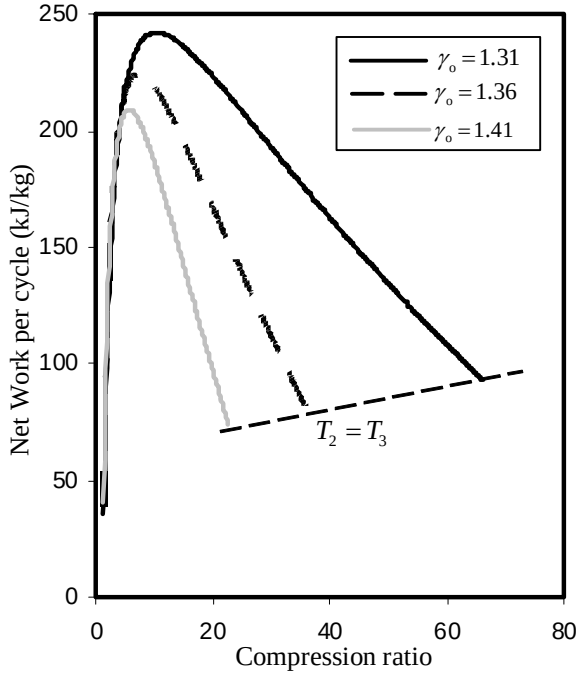

Figure 3. Effect of γ_o on the variation of the net work per cycle (per unit mass of gas) with compression ratio $\left(k_1 = 0.00006\,K^{-1}\right)$

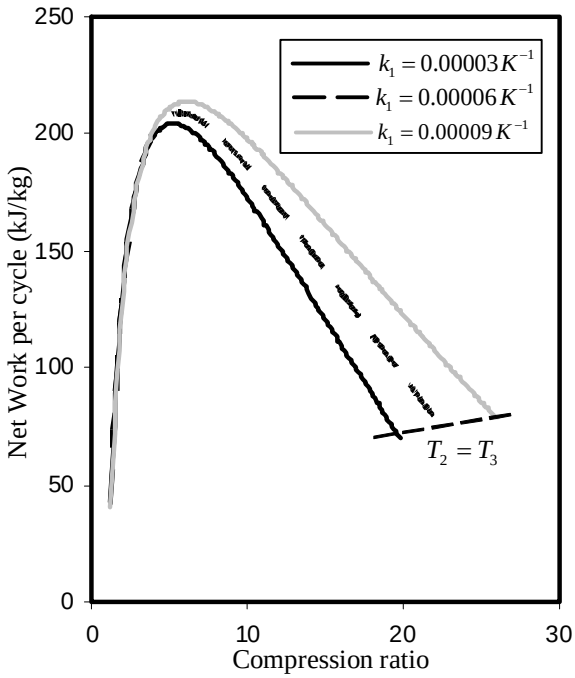

Figure 4. Effect of k_1 on the variation of the net work per cycle (per unit mass of gas) with compression ratio $\left(\gamma_o = 1.41\right)$

It can also be found from the figures 3 and 4 that if compression ratio is less than certain value, the increase (decrease) of γ_o (k_1) will make the net work output bigger, due to the increase in the ratio of the heat added to the heat rejected. In contrast, if compression ratio exceeds certain value, the increase (decrease) of γ_o (k_1) will make the net work output less, because of decrease in the ratio of the heat added to the heat rejected. One can see that the maximum net work output, the working range of the cycle and the optimal compression ratio corresponding to maximum net work output decrease (increase) about 13.7% (4.5%) and 67% (33%), 50.5% (21.4%) when γ_o (k_1) increases (increases) 7.6% (200%). This is due to the fact that the ratio of heat added to heat rejected increases (decreases) with increasing γ_o (k_1) in this case. It should be noted here that both the heat added and the heat rejected by the working fluid decrease with increasing γ_o (see Eq. (4)), and increase with increase of k_1 (see Eq. (5)). Referring to Figures 5 and 6, it can be seen that the efficiency increases with the increase of γ_o and the decrease of k_1 throughout the compression ratio range. On average, the thermal efficiency increases (decreases) by about 23% (6.2%) when γ_o (k_1) increases (increases) 7.6% (200%) over a range of compression ratios from 1.1 to 19.8.

4. Conclusion

In this paper, the effects of specific heat ratio of the working fluid on the performance of an endoreversible Dual cycle during the finite time are investigated. The analytical formulas of work output versus compression ratio and thermal efficiency versus compression ratio of the cycle are derived. The effects of variable specific heat ratio of working fluid on the performance of the cycle are analyzed. The results obtained herein show

that the effects of variable specific heat ratio of working fluid on the work output and thermal efficiency of the cycle are significant and should be considered in the design of practical Diesel engines. The detailed effect analyses are shown by one numerical example. The results can provide significant guidance for the performance evaluation and improvement of real Dual engines.

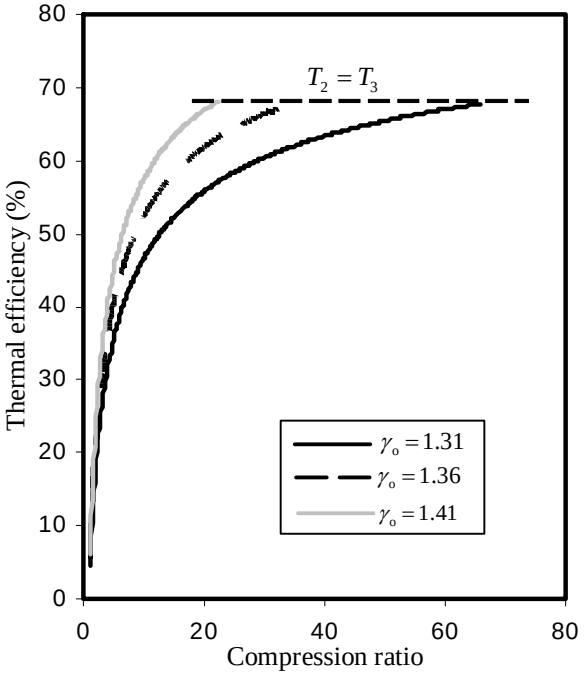

Figure 5. Effect of γ_o on the variation of the thermal efficiency with compression ratio $\left(k_1 = 0.00006 K^{-1}\right)$

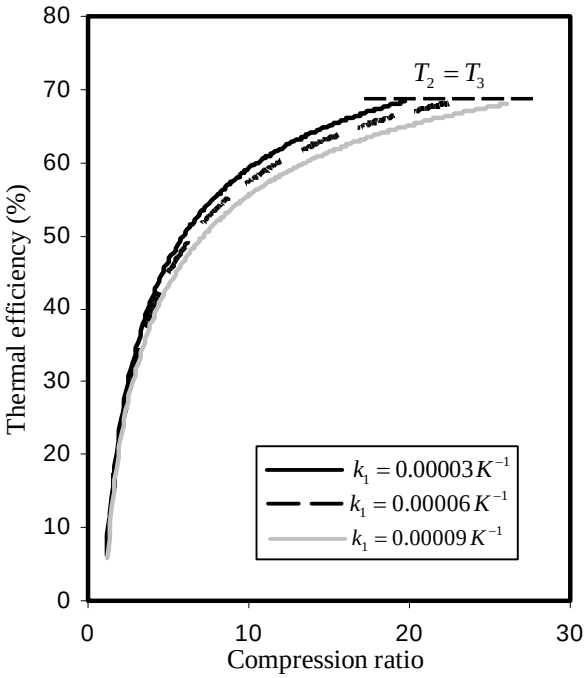

Figure 6. Effect of k_1 on the variation of the thermal efficiency with compression ratio $\left(\gamma_o = 1.41\right)$

Correspondence to:
Rahim Ebrahimi
Department of Agriculture Machine Mechanics
Shahrekord University, P.O. Box 115
Shahrekord, Iran
Tel/Fax: 0098-381-4424412
Email:Rahim.Ebrahimi@gmail.com

Reference

[1] Al-Sarkhi, A., Al-Hinti, I., Abu-Nada, E. and Akash, B., 2007. Performance evaluation of irreversible Miller engine under various specific heat models, International Communications in Heat and Mass Transfer. 34, 897–906.

[2] Aragon-Gonzalez, G., Ganales-Palma, A. and Leon-Galicia, A., 2000. Maximum irreversible work and efficiency in power cycles. Journal of Physics D: Applied Physics. 33(11), 1403–1409.

[3] Aragon-Gonzalez, G., Canales-Palma, A., Leon-Galicia, A. and Morales-Gomez, J.R., 2006. Optimization of an irreversible Carnot engine in finite time and finite size. Revista Mexicana de Fisica. 52 (4), 309–314

[4] Bejan, A., 1996. Entropy-generation minimization: the new thermodynamics of finite-size device and finite-time processes. Journal of Applied Physics. 79(3), 1191–218.

[5] Blank, D.A. and Wu, C., 1994. The effects of combustion on a power optimized endoreversible dual cycle. Energy Conversion and Management. 14(3), 98–103.

[6] Brunt, M.F.J., Rai, H. and Emtage, A. L., 1998. The calculation of heat release energy from engine cylinder pressure data. SAE Paper No. 981052.

[7] Ceviz, M.A. and Kaymaz, I., 2005. Temperature and air–fuel ratio dependent specific heat ratio functions for lean burned and unburned mixture. Energy Conversion and Management. 46, 2387–404.

[8] Chen, L. Ge, Y. and Sun, F., 2008. Unified thermodynamic description and optimization for a class of irreversible reciprocating heat engine cycles. Proceedings of the Institution of Mechanical Engineers, Part D: Journal of Automobile Engineering. 222, 1489-1500.

[9] Chen, L., Ge, Y., Sun, F. and Wu, C., 2006. Effects of heat transfer, friction and variable specific-heats of a working fluid on performance of an irreversible Dual cycle. Energy Conversion and Management. 47(18/19), 3224–3234.

[10] Chen, L., Sun, F. and Wu, C., 2004. Optimal performance of

an irreversible Dual cycle, Applied Energy. 79 (1), 3-14.

[11] Chen, L., Wu, C., Sun F. and Cao, S. 1998. Heat transfer effects on the net work output and efficiency characteristics for an airstandard Otto cycle. Energy Conversion and Management. 39, 643–648.

[12] Ebrahimi, R., 2006. Experimental study on the auto ignition in HCCI engine. Ph.D. Thesis, Valenciennes et du Hainaut-Cambrésis, France, (In French).

[13] Ebrahimi, R., 2009. Effects of cut-off ratio on performance of an irreversible Dual cycle. Journal of American Science, 5, (3), 83-90.

[14] Egnell, R., 1998. Combustion diagnostics by means of multizone heat release analysis and NO calculation. SAE Paper No. 981424.

[15] Klein, M., 2004. A Specific Heat Ratio Model and Compression Ratio Estimation. Department of Electrical Engineering, Ph.D. Thesis, Linköping University. Sweden.

[16] Klein, M. and Erikson, L., 2004. A specific heat ratio model for single-zone heat release models. SAE Paper No. 2004-01-1464.

[17] Lin, J., Chen, L., Wu, C. and Sun, F., 1999. Finite-time thermodynamic performance of Dual cycle. International Journal of Energy Research. 23 (9), 765-772.

[18] Gatowski, J.A., Balles, E.N., Chun, K.M., Nelson, F., Ekchian J.A. and Heywood, F.B., 1984. A heat release analysis of engine pressure data. SAE Paper No. 841359.

[19] Ge, Y., Chen, L. and Sun, F., 2008a. Finite time thermodynamic modeling and analysis of an irreversible Otto cycle. Applied Energy, 85(7), 618-624.

[20] Ge, Y., Chen, L. and Sun, F., 2008b. Finite time thermodynamic modeling and analysis for an irreversible Diesel cycle. Proceedings IMechE, Part D: Journal of Automobile Engineering. 222(D5), 887-894.

[21] Ge, Y., Chen, L. and Sun, F. 2009. Finite time thermodynamic modeling and analysis for an irreversible Dual cycle. Mathematical and Computer Modeling. 50(1/2), 101-108.

[22] Ge, Y., Chen, L., Sun, F. and Wu, C., 2007. Performance of Diesel cycle with heat transfer, friction and variable specific heats of working fluid. Journal of the Energy Institute. 80(4), 239–242.

[23] Ghatak, A. and Chakraborty, S., 2007. Effect of external irreversibilities and variable thermal properties of working fluid on thermal performance of a Dual internal combustion engine cycle. Strojnicky Casopis (Journal Mechanical Energy). 58, 1–12.

[24] Hou, S.S., 2004. Heat transfer effects on the performance of an air standard Dual cycle. Energy Conversion and Management. 45(18/19), 3003-3015.

[25] Parlak, A., 2005. Comparative performance analysis of irreversible dual and diesel cycles under maximum power conditions. Energy Conversion and Management. 46(3), 351–359.

[26] Parlak, A. and Sahin, B., 2006. Performance optimization of reciprocating heat engine cycles with internal irreversibility. Journal of the Energy Institute. 79(4), 241-245.

[27] Parlak, A. Sahin, B. and Yasar, H., 2004. Performance optimization of an irreversible Dual cycle with respect to pressure ratio and temperature ratio experimental results of a ceramic coated IDI Diesel engine, Energy Conversion and Management. 45(7/8), 1219-1232.

[28] Parlak, A., Yasar, H., Soyhan, H.S. and Deniz, C., 2008. Optimization of an irreversible Diesel cycle: experimental results of a ceramic coated indirect-injection supercharged Diesel engine. Energy & Fuels. 22, 1930–1935.

[29] Sahin, B., Kesgin, U., Kodal, A. and Vardar, N., 2002a. Performance optimization of a new combined power cycle based on power density analysis of the Dual cycle. Energy Conversion and Management. 43(15), 2019-2031.

[30] Sahin, B., Ozsoysal, O.A. and Sogut, O.S., 2002b. A comparative performance analysis of endoreversible Dual cycle under maximum ecological function and maximum power conditions. Journal of the Energy Institute. 27 (2), 173-185.

[31] Ust, Y., Sahin, B. and Sogut, O.S., 2005. Performance analysis and optimization of an irreversible Dual cycle based on an ecological coefficient of performance criterion. Applied Energy. 82 (1), 23-39.

[32] Wang, W. Chen, L. Sun, F. and Wu, C., 2002. The effects of friction on the performance of an air stand Dual cycle. . Journal of the Energy Institute. 2(4), 340-344.

[33] Zhao, Y. and Chen, J., 2006. Performance analysis and parametric optimum criteria of an irreversible Atkinson heat-engine. Applied Energy. 83, 789–800.

[34] Zhao, Y. and Chen, J., 2007. An irreversible heat engine model including three typical thermodynamic cycles and the optimum performance analysis. International Journal of Thermal Sciences. 46(6), 605–613.

Design and Prototyping of a Microcontroller Based Synchrocheck Relay for Improved Reliability

Ali Peiravi

Ferdowsi University of Mashhad,
Department of Electrical Engineering, School of Engineering, Mashhad IRAN
Telephone number: (0098) 511-881-5100
Ali_peiravi@yahoo.com

Abstract: Redesign of traditional relays with microcontroller-based relays can be used to achieve a higher level of reliability. In this study, the results of redesign and prototyping of a synchrocheck relay using an 8952 microcontroller with improved reliability is discussed. These relays are usually used for paralleling two load-generation islands, or for closing an open loop in an electric power system. The designed circuit measures voltage, frequency and phase angle difference between the voltage signal on the two sides of an open circuit breaker; evaluates the existence of necessary conditions for synchronism, and then decides whether or not a command should be issued to allow the circuit breaker to close. If these conditions do not exist when the circuit breaker closes, the power system equipment on the two sides of the circuit breaker may be damaged due to the inrush current at the instant of closing the circuit. The integration of three timer-counters, internal code and data memory plus the single-bit handling and 8-bit divide and multiply instructions of 8952 make it suitable for this application. No external RAM or EPROM are needed and the processor internally performs all the necessary computations. [Journal of American Science 2009;5(5):181-188]. (ISSN: 1545-1003).

Key words: Synchrocheck Relay, Power System, Protection, Microcontroller, Reliability Improvement

1. Introduction

As part of a manual control system, an operator makes adjustments to the generator voltage and frequency using a synchroscope or lamps, and then attempts to manually close the breaker. This manual synchrocheck protection will qualify that the two systems are closely matched before permitting the breaker to close. As part of an automatic synchronizing arrangement, a synchroceck relay can be used as an independent backup or checking device to ensure that the two systems are suitably matched before the breaker is closed.

Synchronism is referred to the conditions on both sides of an electric connection where the voltages on the two sides are equal to each other, are in phase with each other, and have the same frequency. This requires the measurement and/or determination of voltage, frequency and phase angle difference for the power signals on the two sides of the circuit breaker before closing. The rms value of the voltage is needed.

Conventional synchrocheck relays are of either induction or electronic types. In the induction type of synchrocheck relays, there are two electromagnets each consisting of two coils. In the first electromagnet which is the driver, the coils are connected to each other in such a manner that the two voltages applied are added together to produce the induced torque in the disc resulting in a closure of the relay's contacts. The failure rate of electromagnetic devices is much higher than that of electronic devices. One of the best approaches to the reliability improvement of protective relays in power systems is the substitution of classical relays with modern ones using integrated electronic circuits. The use of programmable chips that helps reduce hardware is another means of improving reliability. The present study reports the design and prototyping of synchrocheck relays using microcontroller implementation of the sync check relay function.

Synchrocheck relays are usually used to parallel two load-generation islands or closing an open loop of a section of the power system. The first responsibility of a synchrocheck relay is measuring voltage and frequency on both sides of the circuit breaker. Then the voltages and frequencies must be compared with each other to determine whether or not they are close enough to allow the circuit breaker to close. The relay electrically determines if the difference in voltage magnitude, frequency and phase that usually varies with the location on the power system angle fall within allowable limits. Synchrocheck relays usually do not

provide indication of the voltage magnitude, frequency or phase angle, but internally determine whether or not conditions for closing are satisfied. In this design, much of the signal processing and decision making is carried out by software in order to reduce hardware complexity and achieve a higher level of reliability.

Manual closing of circuit breakers is made possible by the use of synchroscopes in power plants. Synchrocheck relays can be used to automate the control of synchronism conditions and allow the closing of the circuit breaker to prevent improper closing. There are also automatic synchronizers in modern power plants that send pulses to the generator exciter and governor to change the voltage and frequency. Then the synchronizer will automatically close the circuit breaker when it is within allowable range. Nowadays, since most circuit breaker operations are done remotely, synchrocheck relays are usually used to supervise closing of breakers.

Voltage zero-crossing has been widely used to measure frequency in power systems. The sensitivity of this approach to noise, DC value and harmonics led to its being abandoned. Curve fitting and data smoothing were used by Begovic et al. [1] who presented zero-crossing, DFT and phase demodulation to measure the instantaneous value of power system frequency, phase and voltage magnitude. They reported that these techniques perform well in the presence of noise and harmonics. Phase angle has also been estimated or measured using transducers or electronic means.

Real time microprocessor-based phasor measurement and its application to obtaining synchronizing information for current differential protection was presented by Thorp et al. [2]. Their focus was on adaptive protection whereby the relay characteristics are modified in response to external signals. However, this is not the case in the problem under consideration in this paper with the goal of redesign of synchrocheck relays to assist in the semi-automatic paralleling of two AC power systems or two sides of a separated power system. The relay contacts should be allowed to change state when the voltage level, phase relationship and frequency are within allowable synchronizing limits. Connecting two power systems that are not closely matched can cause expensive damage to the electrical system. It may even lead to a severe disturbance of the power system. Using synchrocheck relays ensures that such undesirable events do not occur.

Certain equipment including power transformers (PT), lamps, voltmeters, a synchroscope, etc. are used in the process of manual synchronization. In practice, an operator has to check the proper conditions for synchronism before the circuit breaker is closed to connect the two sides together. For an automatic closure, synchrocheck relays are used to verify synchronized conditions on the two sides of the circuit breaker. Once the existence of these conditions is verified, synchrocheck relays automatically issue a signal permitting the circuit breaker to close. The actual act of closure is to be performed by operator, the synchronizer or the auto-recloser. Synchrocheck relays are also used for delayed reclosure after the occurrence of a contingency results in disconnection of a line.

Considering the lower failure rates and programmability of modern microprocessors and microcontrollers, the replacement of traditional relays with microcontroller-based relays can be used to improve reliability. Since much of the necessary signal processing is also possible through software, the reduction of hardware complexity can also help further improvement of reliability.

In this paper, the results of research carried out in the design and prototyping of a synchrocheck relay are presented. These relays are usually used for paralleling two generation and load zones, or for closing an open ring in a section of the power system. The main processor used in this system is an 8952 microcontroller. The integration of three timer-counters, internal code and data memory plus the single-bit handling and 8-bit divide and multiply instructions of this microcontroller make it very suitable for this application. There is no need for any external RAM or EPROM memory, and the processor can internally perform all the necessary computations at a very fast rate. The necessary signal processing functions are done through software, and the availability of proper conditions for synchronism is checked after measurements are made on both sides of the circuit breaker. The code developed senses voltage and frequency on both sides of the circuit breaker, determines the phase difference, and checks for the availability of proper preconditions for synchronization. Once the conditions for sysnchronism are established, a signal is issued to permit or enable the connection.

2. Hardware Design

The design of hardware for a microcontroller-based synchrocheck relay is shown in Fig. 1. In this design, an

8952 microcontroller is used with 8K EEPROM, 256 bytes of RAM, 4 eight bit I/O ports, 3 sixteen bit timer/counters, serial port interface with 64KB of external addressable memory for code, Boolean operations on bits, 210 bit-addressable locations and fast 8 bit divide and multiply operations. No external memory was used in the designed system.

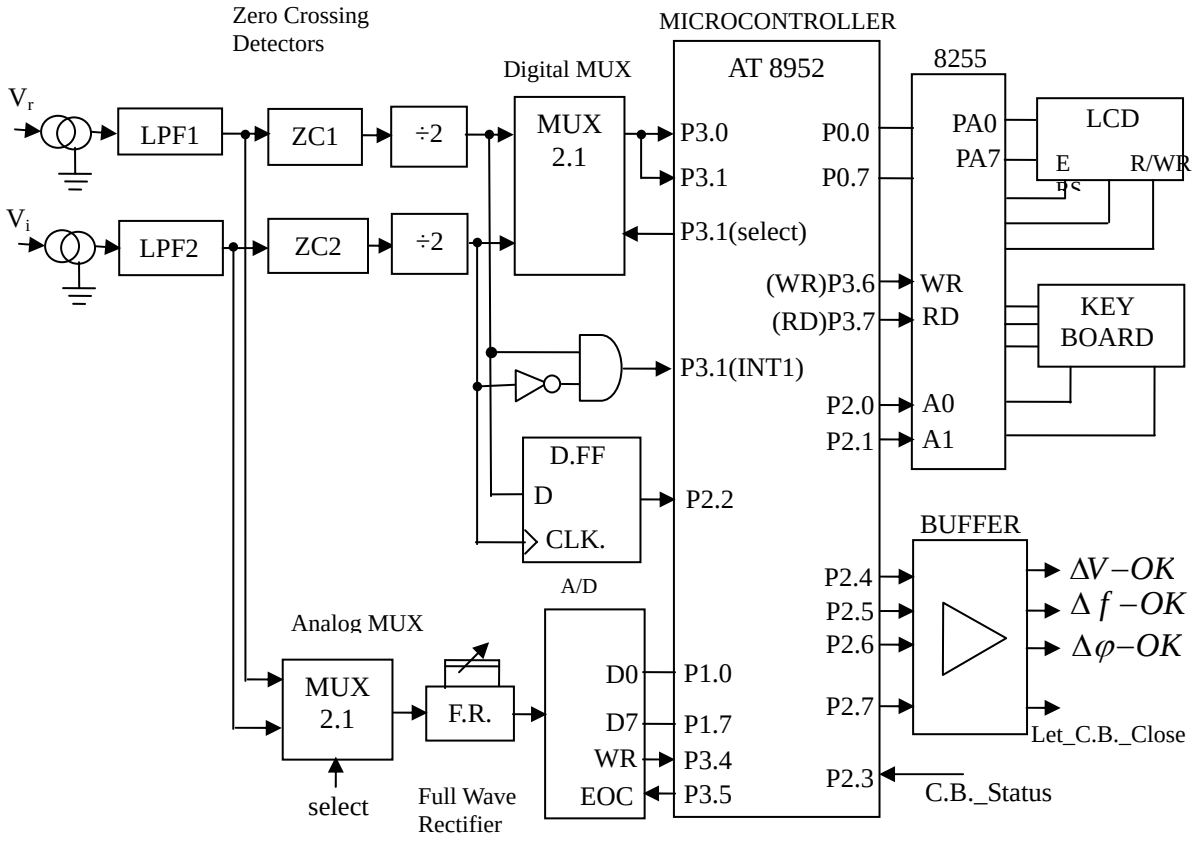

Figure 1. The hardware block diagram of the microcontroller-based synchrocheck relay

3 Voltage Measurement

In this study, the fact that voltage and frequency variations in power systems are slowly changing parameters due to the high inertia of the power system is used to compute these parameters using software. The effective value of the main component of the voltage signal is measured. The rectified voltage measured is first input to an 8 bit A/D converter. Sampling is done during a complete cycle and the effective value of the voltage is computed by the microcontroller based on the results obtained from the A/D conversion of the samples taken as shown in Figure 2.

The voltage on both sides of the circuit breaker is computed using recursive discrete Fourier Transform over the full cycle.

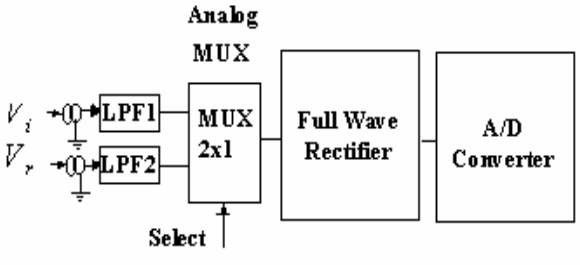

Figure 2 Voltage rectification and conversion to digital value

The real and imaginary parts of the main component of the voltage are computed from the following:

$$V_x = \frac{2}{N}\sum_{j=0}^{N-1} v_j .Cos\left(\frac{2\pi}{N}\right).j \quad (1)$$

$$V_y = \frac{2}{N}\sum_{j=0}^{N-1} v_j .Sin\left(\frac{2\pi}{N}\right).j \quad (2)$$

where N=40 representing the number of samples used in each cycle (f=50Hz). Then the rms value of the voltage is computed as follows:

$$V_{rms} = \frac{1}{\sqrt{2}}\sqrt{\left(V_x{}^2 + V_y{}^2\right)} \quad (3)$$

The sampling starts at the beginning of the cycle of a sinusoidal wave at its zero crossing. Therefore, at that instant, equation (3) above may be rewritten as:

$$\begin{cases} V_x = 0 \\ V_{rms} = \dfrac{1}{\sqrt{2}} \cdot V_y \end{cases} \quad (4)$$

In the system designed, the interrupt service routine for Timer 2 is programmed to compute the rms voltage as shown in Figure 3.

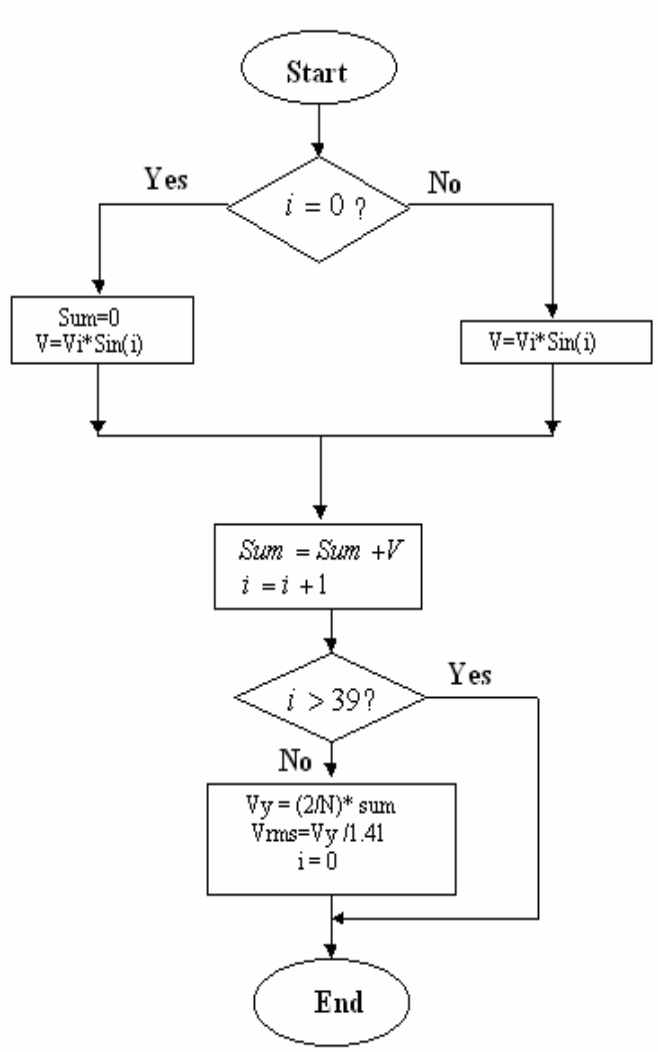

Figure 3 The flowchart of computing the effective value of the voltage

This value is recursively averaged as follows:

$$f_{s\_avg} = (f_{s\_old} + f_{s\_new})/2 \quad (6)$$

4 Frequency Measurement

Various different techniques have been proposed for measuring the frequency of a power system. Wang et al. [3] proposed a curve fitting approach using digitized samples of voltage at a relaying point. Petrovic et al. [4] proposed a digital method of power frequency measurement using rectifiers, a microcontroller, latch, RAM, EEPROM, a 16 bit A/D converter, etc. and a PC. Lee and Devaney [5] proposed a software-based technique for frequency measurement based on the estimation of zero crossings and measuring the time between an even number of estimated zero crossings with smoothing. Their approach is iterative in nature with an adjusted sample rate to be a multiple of the estimated frequency to allow a progressive refinement of frequency.

The approach adopted in this study to measure the power system frequency on either side of the circuit breaker is based on software to calculate the inverse of the average value of period of the voltage waveform over 40 consecutive cycles. Since the frequency difference between the two sides of the circuit breaker is important, it is computed as follows:

$$f_s = |f_2 - f_1| \quad (5)$$

5 Phase Angle Measurement

It is known that real power flow occurs based on

$$P = \frac{V_s \cdot V_r}{X_L} Sin\delta \quad (7)$$

where V_s is the voltage on one side of the circuit breaker, V_r is the voltage on the other side of the circuit breaker, X_L is the impedance and δ denotes the phase angle between the two sides of the

circuit breaker when closed. Should there be a large phase angle difference between the two sides of the circuit breaker at the time of closing a large power flow may result in damage to the equipment. Therefore, the phase angle should be measured on both sides, and the difference should be computed. One possible application of this measurement would be in real time security monitoring as proposed by Soonee et al. [6] for the Indian electric power system. They made phase angle measurements at various strategic locations in the integrated Indian power system to provide knowledge about the neighboring system for regional control centers in the absence of a national control center. One possible approach to phase angle determination proposed by them is the use of the formula below if the needed parameters are known.

$$\delta = Sin^{-1}\frac{P \cdot X_L}{V_S V_r} \tag{8}$$

A second approach is to use a voltage/angle transducer. A more sophisticated approach would be to use digital circuits or even benefit from the software/hardware capabilities of microprocessors/microcontrollers. Al-Ali et al. [7] presented an intelligent system to monitor the phase angle continuously and initialized corrective action if the phase angle deviated beyond allowable limits in order to continuously compensate for the difference by continuously changing a variable capacitor. They used an 8 bit microcontroller, an 8 bit D/A converter, zero crossing detectors and programmable capacitance to achieve this goal.

In this study, the voltage signal of each side of the circuit breaker is passed through anti-aliasing low pass filters. Then they are fed to a zero crossing detection circuit which provides a high digital output as soon as the input goes above zero and a low digital output as soon as the input goes slightly below zero, thereby changing the sinusoidal shape of the input to a square wave. This waveform is passed through a frequency divide by two as shown in Fig 4.

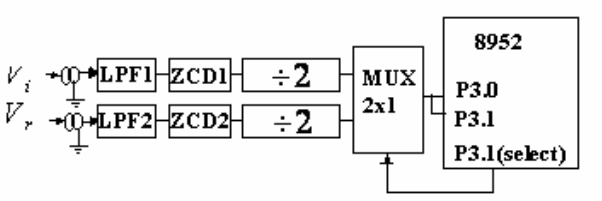

Figure 4 The low pass filter, zero-crossing detection and divide by two operations on voltages

The outputs from the two sides are fed to an AND gate which generates a pulse whose width is proportional with the voltage phase difference. Then this is input to the zero interrupt input of the microcontroller which computes the frequency with software. The waveforms are as shown in Figure 5.

6 Conditions of Synchronism

After the voltage, the frequency and the phase angle on the two sides of the circuit breaker are obtained, the conditions for synchronization must be evaluated. Equations (9) and (10) are used for this purpose.

$$\frac{|V_r - V_i|}{V_n} \times 100 \le \Delta V \tag{9}$$

$$|f_r - f_i| \le \Delta f \tag{10}$$

where Δf is the maximum allowable frequency difference between the two sides, ΔV is the maximum allowable percent voltage difference between the two sides, and V_n is the system's nominal voltage. The flowchart of the operation of the designed microcontroller-based synchrocheck relay indicating how a decision is made to close the circuit breaker is shown in Fig 6. The system continuously monitors the voltage difference and only goes on to compute the frequency and the frequency difference if this condition is met. It also only computes phase angle difference after the voltage difference and frequency difference conditions are met.

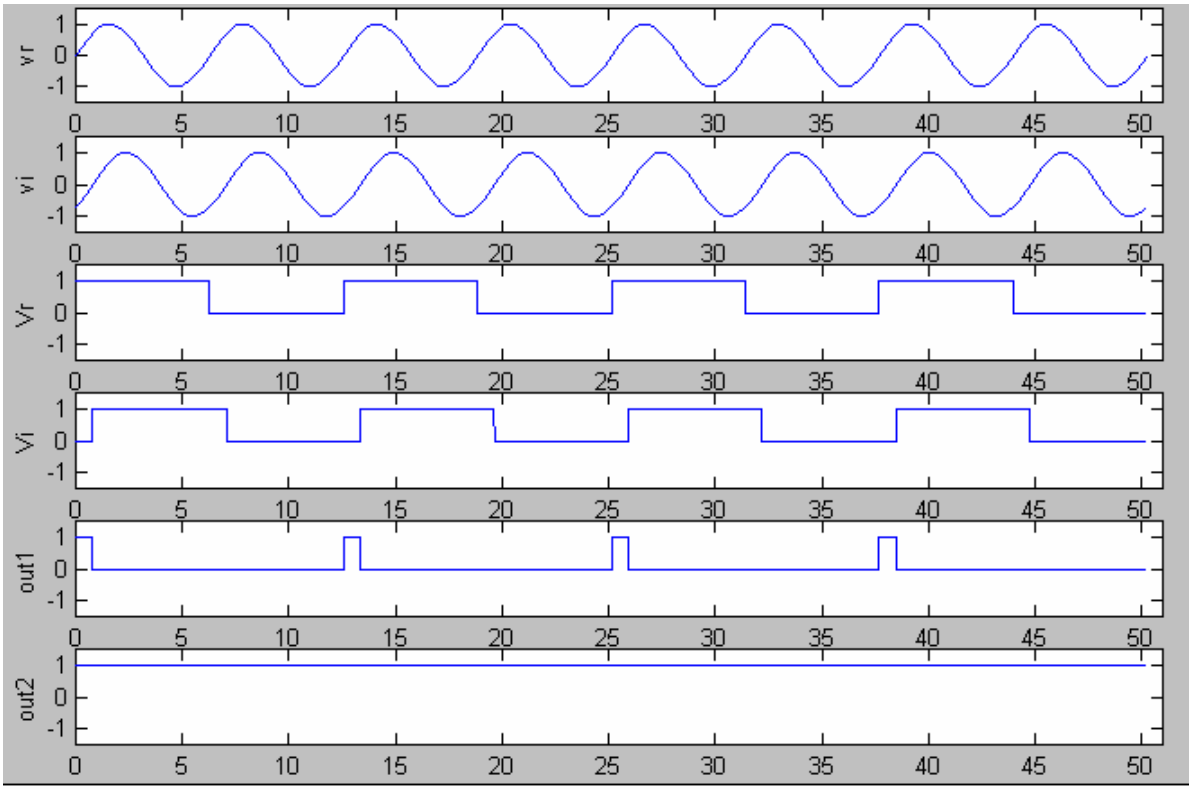

Figure 5 Action of zero crossing detectors for the voltages on the two sides of the circuit breaker. The width of Out1 indicates the time from the zero crossing of Vr to the zero crossing of Vi.

6 Conclusions

A prototype of this design was built using an 8 bit microcontroller, an 8 bit A/D converter, a digital multiplexer, an analog multiplexer, a parallel I/O port, an LCD, a keyboard plus several other gates. The proposed method of measuring frequency, voltage and phase angle used in the design of this microcontroller based synchrocheck relay all work well. The precision used is 0.01Hz for frequency, and 0.1 degrees for phase angle. Discrete Fast Fourier (DFT) transform was used for measuring voltage, and high frequency components were eliminated using hardware low pass anti-aliasing filters. The DFT itself acts as a natural filter for high frequency harmonics, too. The algorithm successfully measures the main characteristics of the voltage on both sides of the circuit breaker. The recursive nature of the algorithm eliminates the need for storing samples taken and by eliminating external RAM and simplifying the resulting circuit greatly improves its reliability. Another major design feature of this relay which also simplifies the circuit and improves reliability is the use of a precise full wave rectifier so that employing just an 8 bit D/A converter provides sufficient accuracy for the synchrocheck relay. An 8952 microcontroller which has 256 byte RAM, 8KByte EPROM, 128 bytes of bit addressable memory and three 16bit timer/counters is used. The integration of all needed circuits into a single microcontroller chip greatly improves the reliability of the synchrocheck relay. The ability of this chip to perform 8bit multiply/divide operations in only two microseconds plus its bit addressable I/O capability makes it a very suitable choice for a reliable sysnchrocheck relay design.

Acknowledgement

I would like to thank Mr. Ebrahim Sagvandi for carrying out the initial work and his help in the practical aspects of the circuit prototyping and testing. I also like to thank the Office of Vice Chancellor of Research and Technology of Ferdowsi University of Mashhad for the grant project that has assisted me in the preparation of this manuscript.

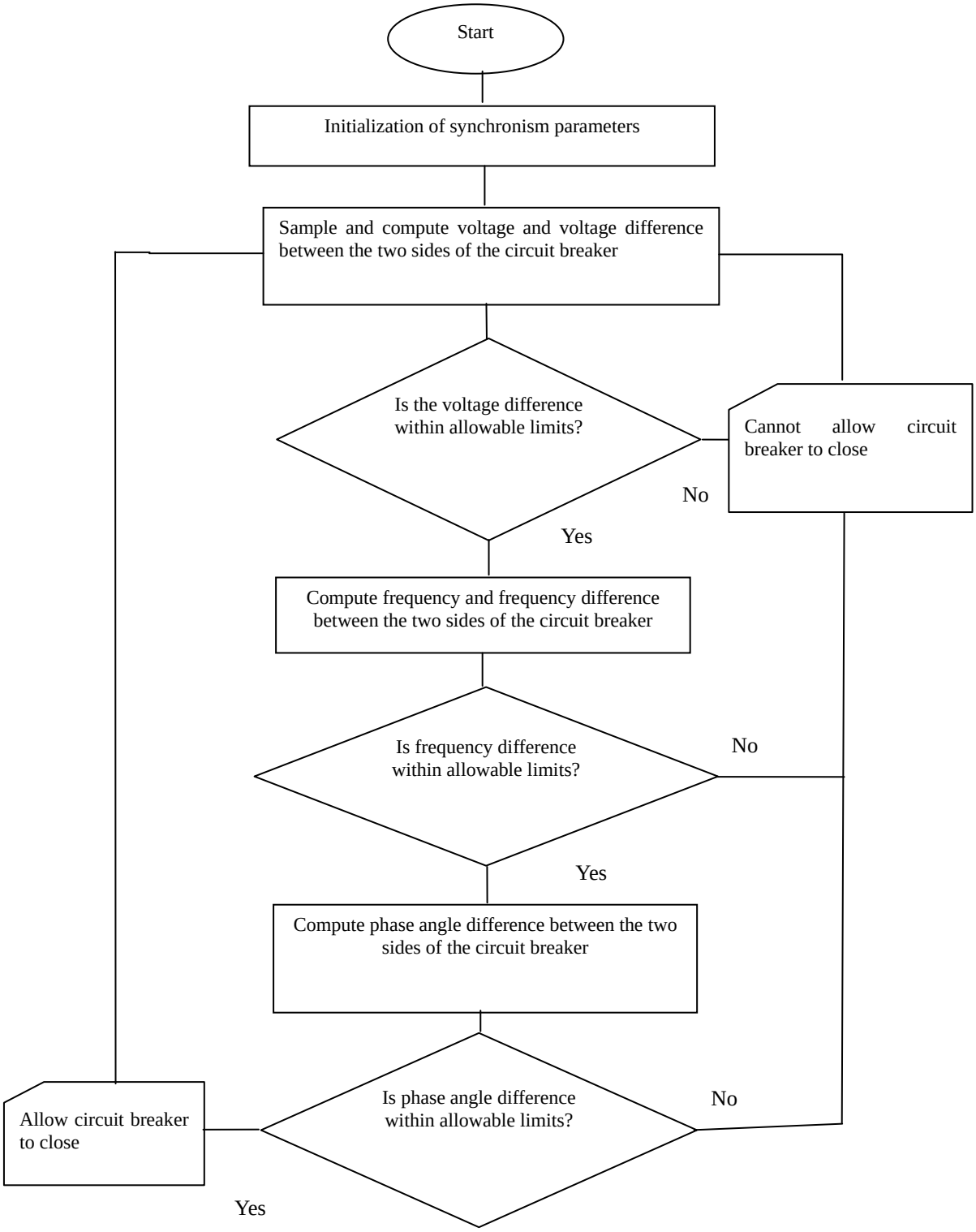

Figure 6 Flowchart of the decision making process of the designed synchrocheck relay

References

[1] M. M. Begovic, M. Djuric, G. Phadke, Frequency tracking in power networks in the presence of harmonics, IEEE Transactions on Power Delivery, Vol. 8, No. 2, (1993), pp.480-486.

[2] J. S. Thorp, A. G. Phadke, S. H. Horowitz, M. M. Begovic, Some applications of phasor measurements to adaptive protection, IEEE Transactions on Power Systems, Vol. 3, No. 2, (1988), pp.791-798.

[3] A. D. Wang, Y. Z. Ge, L. L. Lai, A. T. Johns, A new digital algorithm for power system frequency measurements, IEE 2nd International Conference on Advances in Power System Control, Operation and Management, Hong Kong, (1993), pp.729-733.

[4] P. Petrovic, S. Marjanovic, M. Stevanovic, Digital method for power system frequency measurement using synchronous sampling, IEE Proc. Electr. Power Appl., Vol. 146, No. 4, (1999), pp.383-390.

[5] J. H. Lee, M. J. Devaney, Accurate measurement of line frequency in the presence of noise using time domain data, Proceedings of the 10th Anniversary Instrumentation and Measurement Technology Conference IMTC'94, (1994), pp. 1016-1019.

[6] S. K. Soonee, S. R. Narasimhan, R. K. Porwal, S. Kumar, R. Kumar, V. Pandey, Application of phase angle measurement for real time security monitoring of Indian Electric Power System - An Experience, Water and Energy International, Vol. 65, No. 3, (2008).

[7] A. K. Al-Ali, M. T. Abuelma'atti, I. Hussain, Microcontroller-based phase-angle measurement and correction technique, International IEEE/IAS Conference on Industrial Automation and Control: Emerging Technologies, 22-27, (1995), pp.569-571.

Yacht Construction In Myanmar

Kay Thwe, Gao Gao

Naval Architecture and Ocean Engineering Dept, Wuhan University of Technology, 430063, China
thwe.kay@gmail.com, gaogao1949@yahoo.com.cn

Abstract: This paper reviews the construction of the yacht Sunshine that influences the Myanma Shipyards (MS). Historically, the wooden yachts have been built in Myanmar since 19th century. Myanma Shipyards has been building and repairing the various kinds of ships since 1970. Fortunately, the classic-yacht Moonbeam was repaired in 1998 and approved by the regional Lloyd's surveyor. Interestingly, the owner, Peter Wood, Corvette Shipping Ltd, France, of the yacht Sunshine was seduced by the place where Moonbeam rebuilt. In early 2000, the construction of the Sunshine was started. The hull design plans were supported by the owner. The steel frames and hull plates were cut with CNC machine and there was no human error. Everything on the yacht was made locally, nearly all the fittings are from local foundries and the carpenters made all the wood work. It was challenging and time-consuming for the construction of the latest Fife design in Myanma Shipyards. For future development and commercialization of yacht constructions, this paper will describe the specifications and functionality enhancement of Myanma Shipyards. [Journal of American Science 2009;5(5):189-196]. (ISSN: 1545-1003).

Key words: Yacht, CNC (Computer Numerical Control), NDT (Non Destructive Testing)

1. Introduction

This paper sets out to review some of the construction problems of the yacht faced by MS. The restoration of the yacht doesn't need the design process but construction of a new yacht requires the design process. The owner of the yacht Sunshine gave full-size lofted frame templates so that Detail Design stage was eliminated.

There are a large number of processes that are required for the construction of yacht. The design process is the major step to satisfy the customer's requirements because yacht construction is a design-oriented view. To improve the way of the construction of ship is to reduce costs, manhours, and administration and improve quality. For the type of classic-yacht, the cost is not the object. The goal or purpose of the yacht is to win the best 4 of 7 match races around a specific course made up of known angles and distances. So the biggest job is to determine the velocity potential of a design to the wind speed, sailing angle, and the dimensions of the hull and rig. For pleasure yacht, the owners specify a target cost, speed, cruising range, and some description of accommodations for the yacht. Actually, it is difficult to get an optimum design. There are many design phases to consider for the best design.

MS started constructing the first yacht in March 2000. Delivery was late, but quality on the first yacht was excellent. Since that time, MS has built in traditional measurement terms and it is a small shipyards. Now MS is a commercial-oriented shipyard, a second facility, floating dry-dock, and a growing work backlog from repeat and new customers.

2. Historical Perspectives

In Myanmar, the best hardwoods held out the promise of a slow but faithful restoration by repair. There is no doubt that a wooden deck, interior decoration and superstructure is a beautiful sight from both without and within. The owner of Moonbeam discovered the low labour rates, skilled craftsmen and access to supplies of the best hardwoods in Myanmar. The hull had been copper sheathed and this had protected the wood below the waterline. Moonbeam had only left a steel skeleton which retained its original shape and the keel and deadwood remained attached to stabilize the structure. Two-thirds of the original steel had been saved and the shape was unaltered. The hull shape was fairly straightforward but manhandling.

The whole of the interior was hand-built by local craftsmen with all of the paneling coming from a single tree of padauk on satinwood frames. She has beautiful accommodation for six guests staying on board. While there is space for many more during day racing. The rosewood-pannelled saloon is an absolute feast of traditional woodwork and a great credit to the craftsmen who painstakingly re-created it.

Although there are many survivors in the cutter category few classic schooners still exist today, so it was thought appropriate in building a replica, that should be borne in mind. Also the early 1900's was probably the time when sailing ships and yachts were at the height of their evolution, before steam and diesel engines, and racing rating rules, began to interfere with the purity of their original function and beauty. Looking into the future it is also likely that there will be a

reduction in the numbers of original vessels in existence, due to the high and ever increasing costs of maintaining these few remaining original vessels.[4]

The yacht Sunshine was built in Yangon, as the facility there at MS, is very suitable and the building and handcraft techniques can still be found in Myanmar, that are as close as one could find to the skills originally employed in the England of the early 20th century.

The yacht Sunshine is a two masted gaff rigged identical to the two earlier Fife Schooners. The hull and rig are exactly faithful to the original 1900 design. By early 2000, the boat was plated and ready to be turned over in the yard. Her keel is steel box section with lead poured in from the inside. [3]

Metal yacht construction has been around for a long time, long enough for its benefits and drawbacks to be common knowledge. However, with the acquisition of knowledge and technology, the methods of working with and treating materials change for the better, expanding the benefits and limiting the drawbacks.

Developments in hull shapes and plating techniques have also gone a long way in helping to reduce the prejudice against steel yachts. The secret of a good steel design is clean simplicity, in both the hull and the deck. The more cutting and welding that can be eliminated while maintaining good aesthetics, the more successful the design is likely to be.

Figure.1 Moonbeam

Figure.2 Schooner Sunshine

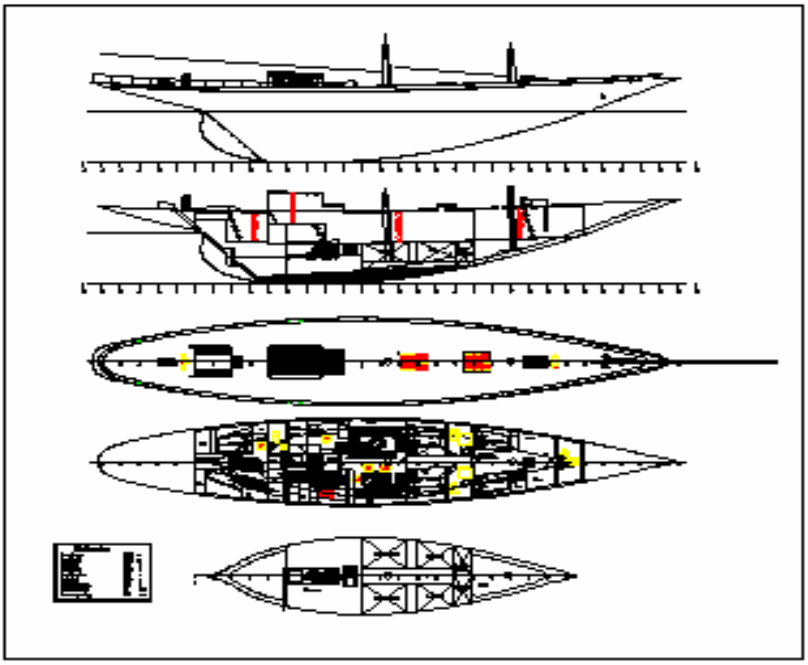

Figure.3 G.A Plan of Sunshine

3. Construction Activities

Construction activities include the followings:

- Material supply
- Fabrication
- Body assembly and shell plate erection
- Overturning
- NDT check
- Outfitting
- Piping and Machinery
- Launching
- Superstructure and Interior Decoration

The steel hull construction, outfitting and piping works were done by employees of MS. It was also performed to test NDT check and some design performance. Some skillful craftsmen from external contractor were hired to do superstructure and interior decorations works.

3.1 Material Supply

Hull materials, machineries, outfitting, anchoring and mooring equipments for construction of yacht and working drawings were approved by Lloyd's class and supported by owner. Some parts had been cut by CNC machine and other necessary parts were cut by CNC at MS.

3.2 Fabrication

For fabrication, the parts of frames were assembled and arranged by their numbers and tack-welded the frames together. To strengthen the frames, face plates of 50x6mm were used to become T-frames. After checking against the patterns, make the final welds. A good way to avoid distortion is to follow the same sequence for assembling each frame. To get the camber of main deck, hydraulic press machine was used for deck beams according to template of workshop floor.

3.3 Body assembly and shell plate erection

After fabrication, the frames, girders and bulkheads were arranged to their positions from aft to forward. Upside-down method was used because most of the important hull welding can be done in the down-hand position and made it easier to install the radius plating. Care must be taken to get the correct level, alignment and to fix exact frame situations. First, the deck stringers, deck girders and bulkheads were installed and then bottom centerline girder and tank top plate. When the frames were complete, shell plating was started. Because of the radius chine and bow curvature, the skillful welders had done with much care.

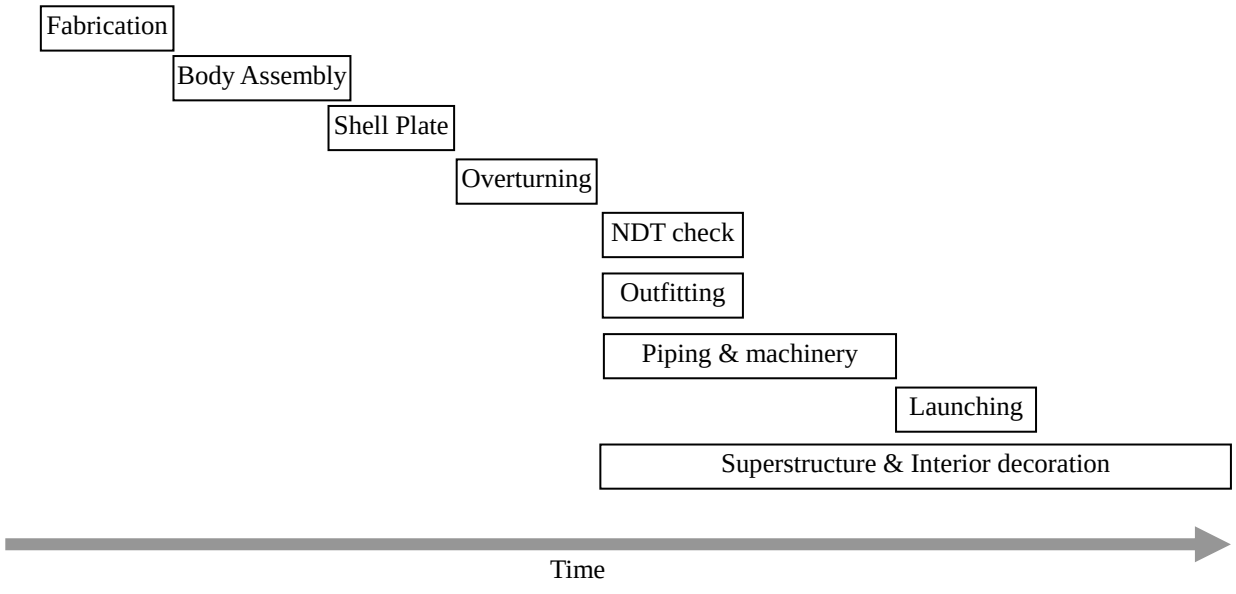

Figure.4 The Construction Time Plan

Table 1. The frames and plates used in this yacht

Material Specification		***measurements (mm)***
All Plating		Grade A
Profiles		Certificate from manufacturer according to grade A
Transverse Frames		
Hullframe spacing above tanktop		1000 mm
Hullframe spacing under tanktop		500 mm
Hull frames above tanktops		120x4 & flange 50x5
Hull frames below tanktops		120x5 & flange 50x5
Web frames above tanktops		L120x10+100x8
Web frames below tanktops		L120x8 & flange 60x8
Deck beams		Hp 80x5 and Hp 100x6
Longitudinal members		
Side Shell Stringers		60x6
Deck girders		100x6 and flange 60x8
Deck stringer		500x7 and 400x6 (ends)
Hull Plating		
Keel & side plate till 2000 mm		
Above base		8
Side plating from 2000 mm above base		6
Weather deck		45 mm wood
Tanktop		5
Bulwarks		6
Bulkheads		
Fr.0	Plating	4
	Stiff.	50x5 (Spacing 450)
Fr.5	Plating	4
	Stiff.	60x8 (Spacing 450)
Fr.15	Plating	4
	Stiff.	60x8 (Spacing 450)
Fr.21	Plating	4
	Stiff.	60x40x5 (Spacing 450)
Equipment Number According to LRSSC		
Rules for the Classification – Certification of Yachts		
Engine	62.96	
Anchor	2	
Weight	75/55 kg	
Chain	110 m each	12.5 mm

3.4 Overturning

The hull turning was a social event and it was done in 12/22/2000. Leveling, alignment and dimensions were checked again. After making some temporary staging, some overhead welding were finished. The hull was pulled out along with the carriage and then lifted with cranes.

Figure. 5 Overturning Process

3. 5 NDT check

Shell plate welding joints were checked with radiographic inspection method. Fuel tanks, grey water tank, black water tank and drinking water tank were tested with air pressure text.

3.6 Outfitting

After construction the main body, bulwark, hawse pipe, fairlead, fore-stay, bow sprit heel, echo sounder seating, watertight doors, dolphin striker, main and fore mast arrangement, daily service tank, eye piece, eye bolt, anchor davit socket & crane, manhole cover, side scuttles and zine anode fittings were fitted. Lead weight 3,466 kg per cubic meter combined with its low melting point of 327°C was used for superior ballast material. 25 ton of lead was melted and then poured into the steel box keel section.

3.7 Piping and machinery

Bilge system, fuel oil service system, fresh water service system, black and grey water system were designed by MS. For bilge piping system, one bilge pump was electrically powered unit situated in the lowest point of the bilge and two hand-operated bilge pumps were fitted on the main deck. Semi-rotary hand pump with Ø32 and one fuel oil transfer pump were used for fuel service system.

Cummins Marine Diesel Engine of Model 6CTA-83 MI, 300 BHP @ 2500 RPM for a good cruising speed and Onan Gen-set of 17.5 KVA were fitted in the engine room. Chockfast was used to fit stern tube and propeller shaft.

3.8 Launching

After fabricating the hull construction, it had to put on the cradle. Because of the high lightship draft, the cradle must be modified from 2 feet to 1 foot in high. After finishing of block assemblies, it was turned over and seated onto the modified cradles which were placed at the auxiliary side slipway. Before side shifting onto the small traverser, special side supports were provided because of having very steep in depth. Then it was released into the basin. Finally it was successfully launched on the day of 22-7-2002.

Figure. 6 Launching Processes

3.9 Superstructure and interior decoration

The interior design of the yacht was built almost entirely of teak wood. The interior which is hand crafted from teak and rosewood has been compromised from the original layout to allow for the required modern safety standards, such as the 4 watertight bulkheads. The deck is laid down in long thick lengths of solid teak planks over the steel frames, and caulked with cotton in the traditional way. The masts and spars are all of Sitka Spruce and the standing rigging is of galvanised steel.

Figure.7 Deck floor

Figure.8 Salon

Figure.9 Hatch, Mast and Boom

4. Improving yacht design and construction

It is often said that there is nothing new in yacht design, that whatever we come up with that is innovative has been done by someone else in the near or distant past. That applies to radius chine hulls as much as to anything else. Each designer or builder has developed his own version of it which works well for his own style of yacht design or construction. Most modern yachts tend to have little, if any, curvature to the topsides near to the bow. Radius chine construction gives straight sections in this area, with all the radius below waterline. This can give a wet boat if there is not good flare to the hull to prevent the bow wave from coming straight up on deck.

Naval architecture department of MS made some design performance of the yacht Sunshine[1], [2]. Designers always have some ideas on how to improve or optimize an existing design, especially if the previous boat has been built and the designer has had a chance to evaluate the result. For racing yacht, the design improvements and changes are smaller and there is a greater need for an objective analysis of the changes. This is where parametric analysis and design optimization can be used most effectively.

Computer can help the design process by providing an easy way to start with a complete hull shape. Many accurate calculations can be performed. Detailed weight information and the layout of the arrangements and determination of whether everything fits can also be supported by computer.

Designers involved with the computer use both hull design program and a general purpose CAD program. The hull design program is used to create, fair and perform calculations on a 3D mathematical model of the hull. The general purpose CAD program is used to receive either the 3D model of the hull to create a full 3D interior, or to receive several 2D views of the required plans.

In a competitive shipbuilding market, MS wants to improve the construction of ships including yacht. Because of product complexity, such as tank and cargo barges, tug boats, power barges, passenger vessels, offshore vessels and vessel repair, MS wants to improve return on past and future investment decisions.

Since yacht is not mass produced, the synergy of multiple brains and experiences will tend to challenge or reject bad information and concentrate on good information. Management information is critical to productivity. The process tends to build organizational learning, shared vision, team function, and while reducing fear and mistrust and misunderstanding. MS recorded of action assignments, performance measurements, recognized unknowns, and other useful management information of the yacht.

MS has skilled and experienced employees who are very astute concerning their role in acquiring knowledge. Employees can also learn beyond the experience curve. Productivity can increase by the accessible knowledge base, skill and related learning, work organization, communication and leadership, and attitudes, such as willingness to accept change under the tent of corporate culture. MS has facilitated self-directed or conscious learning by encouraging and rewarding employee suggestions and innovation

Technology supports productivity by leveraging human abilities through facilities; suite choices; arrangement of production, support equipment, and tools; communication and information systems; and maintenance and safety equipment. Designers and engineers had thought little about work specification that could be enhanced with computer-aided design or manufacturing technology.

MS business functions depend on external help. MS also hires contractors to perform those functions on new vessels and vessels under repair that are beyond in-house capability. Contractors also provide training and services, such as insurance, accounting, payroll, and so fourth.

The construction cost will depend mainly on the weight of the hull. MS quoted low price to the owner of Sunshine because he gave full-size lofted frame templates. The price will be noticeably lower since the 3D computer hull form model will eliminate all traditional lofting by hand. If MS has to be selected the detail design, the owner has to discuss the exact type of information. The longer the owner waits, the more he increases his chances of having to modify his design and drawings.

Since MS is commercial-oriented shipyard, it constructs and repairs various kinds of vessels and it is not specialized in yacht building. For racing yacht, it is also necessary to design rig. It includes sailplans, respective structural calculations, mast and boom section. All structural elements can be dimensioned to comply with the ABS classification rules for Offshore Racing Yacht or for more efficient structures, finite element analysis can be performed. To complete the detail design, it can take much time on design processes.

5. Conclusion

The shipyards in Myanmar construct and repair mainly the inland waterway transport vessels. MS has been constructed many kinds of classed ships up to 90 m in length. There are many customers from foreign countries. The good management factor, the skillful workers and the advanced technology satisfy the customers.

From the first construction of racing yacht, MS had learnt much knowledge about yacht design and construction from the experiences. Although MS doesn't have well-trained yacht designers, the owners can discuss their required information about yacht design. If a similar designed metal yacht wanted to build in MS, it would not be time-consuming and well-trained workers and carpenters can work better than the old one.

composting processes. Adjusting operation conditions through changing key factors, optimal operation condition could be determined through comparing the results of numerical simulation. In this study, the optimal way of air supply was designed with the help of numerical model. Real experimental results showed that it could reduce 79.61% of oxygen supply with the same compost efficiency. Therefore, developed numerical model is of great significance to instruct the operation of real composting processes and reduce the operation cost.

Acknowledgement:

The author's work is supported by Myanma Shipyards, Yangon, Myanmar.

Correspondence to:
Kay Thwe
Wuhan University of Technology
Wuhan 430063, China
Telephone: 86-27-63995353
Emails: thwe.kay@gmail.com

References

[1] International Measurement System. A Handicapping system for Crusing/Racing Yachts. ORC, World Leader in Rating Technology. 2001 Offshore Racing Council

[2] Guide for Building and Classing, Offshore Racing Yachts, 1994, American Bureau of Shipping

[3] http://www.boatcouncil.com/boat-details.asp/vessel/43626/boats-filter_frm_auto/1/mode/3/page/1/p//boat-categories/cruising-racing-sailboats.asp

[4] http://www.classicyacht.info/modules/yachts/Moonbeam+IV-TName-yachts_detail-464.html

[5] http://www.boatquest.com/Sail/Fife/Category/Length/13415/Feet/USD/1/boats_pictures.aspx

Desalinization of Saline Soils Aimed at Environmentally Sustainable Agriculture: A New Thought

Abul Hasnat Md. Shamim[1, 2] and Takeo Akae[1]

[1]Department of Environmental Management Engineering, Faculty of Environmental Science and Technology, Okayama University, Okayama 700-8530, Japan
[2]School of Agriculture and Rural Development, Bangladesh Open University, Gazipur-1705, Bangladesh
E-mail: abulhasnats@yahoo.com and akae@cc.okayama-u.ac.jp

Abstract: This article describes the desalinization of saline soils aimed at environmentally sustainable agriculture. [Journal of American Science 2009;5(5):197-198]. (ISSN: 1545-1003).

Salinity, defined as the concentration of dissolved mineral salts present in the soil or water, is one of the most severe environmental factors limiting the productivity of agricultural crops. Most of the crops are sensitive to salinity caused by high concentrations of salts in the soil. Salinization commonly occurs as an outcome of agricultural practices. Salinization associated with agriculture occurs when salts build up in the root zone, either because the soil is inherently saline or because the drainage of water from the sub-soil is not adequate to prevent saline waters rising into the root zone.

Increasing salinity is a major abiotic stress affecting approximately 7 % of the world's total land area (Munns, 2005) resulting in billion dollar losses in crop production around the globe (Norbors and Dykes, 1984). Without proper agricultural and ecological practices salt problems and/or salt accumulation can occur under virtually any climate regime. However, arid land climates and poorly draining soils are particularly susceptible to salinization due to evaporation that leaves the salt behind. World wide, approximately one third to one half of all the irrigated lands has salt problems; the majority of which is in less developed arid regions. And, every year, millions of acres of irrigated lands go out of production due to salt. Indeed, there is already twice as much salty land as the irrigated land. If this trend will continue, we will have finally reached the point where there are no new 'virgin' lands left to salinize.

In amelioration of saline-sodic soils, gypsum is used as agricultural lime but it is to some extent expensive. Moreover, the efficiency of gypsum application is reduced because it is precipitated by dissolved CO_3^{2-} and HCO_3^-, forming insoluble $CaCO_3$. However, this option applicable only when pH of soil > 8.5 (sodic soil), claimed by many scientists. In recent decades, phytoremediation has also proved to be as efficient, inexpensive and environmentally acceptable strategy to ameliorate saline-sodic soils (Qadir and Oster, 2002). But it reduces sodicity very slowly than chemical treatments. Moreover, it has very limited application under condition of high level of soil salinity and sodicity (ECe >20 dSm^{-1}, ESP >70). As a result, farmers often become reluctant to ameliorate saline soils. Unfortunately, fertilizers do not solve the salinity problems. Fertilizers are just plant nutrients and do not remove salt from the soil. However, organic fertilizers and mulching may help reduce soil salinity by improving soil structure and therefore increasing percolation. It may be tempting to remove the surface clay/silt layer as the quickest way to get rid of the salt. However, bear in mind that just one centimeter of sediment per hectare equals 100 cubic meters. One cubic meter is approximately 15 full wheel barrows, and a standard large truck load is eight to ten tons. This option can only be justified under exceptional circumstances, such as clearing for high value cash crops. In this case, the economic cost/benefit should be calculated first. Moreover, appropriate disposal of saline soil is also a great problem; coastal dumping may be effective from a salinity point of view, but carries other environmental risks.

One way to remove salt from soil is to leach it out. Here, a drain system is installed in the field. Large amounts of fresh water are added to the field and the salt dissolves in the water which is moved off the field by the drain system. The collected water can then be treated further to remove the dissolved salt. Moreover, the continuous irrigation over the years has resulted in a rise of the ground water table in turn resulted in development of salinity and water-logging and also leaching the nutrients of the soil. In another way, the soil can be dug up, then literally washed like in a washing machine and then put back into place. Obviously, the last alternative is not very realistic because of costs, however it could

be done.

In improving those saline soils to find out the effective (an efficient and low cost) method is required. Slaking is the process of soil aggregates collapse when they are rewetted after drying. Soil slaking has long been studied from the stand point of stability of aggregates. However, it has not been studied from that of salt removal. Drying followed by rewetting and slaking is commonly found in a natural soil processes. During the process, salt in the soil moves and accumulates to the inter and outer surface of soil blocks and released to outer solution. Recent study revealed that the maximum salt is released at the soil moisture of maximum slaking. In addition, the amount of salt released into equilibrium water after 24 hours slaking was proportional to the slaking rate[1]. The $EC_{1:5}$ of the equilibrium water surrounding the slaked soil blocks were measured, which is an exact measure of the amount of salt released[2] from the soil block. Here, we can find a chance to improve the saline soil by simply rewetting the soil at the proper soil moisture by land drying practice. Moreover, proper amount of water management can limit salinization. This is because the salt concentration and amounts of irrigated water content in soil is dependent each other. If saline soil is irrigated by too much water like ponding irrigation, salt concentration decreases abruptly to cause dispersion and swelling of soil particles and plugging percolation pores. It results in great drop in water movement. On the other hand, if soil is irrigated by small amount of water enough to slake and flush the salt under relatively dry condition, the salt will decrease smoothly because water can moves well without plugging pores by dispersion. It is also environmentally sound and economic as well as saving water resource.

In this respect, it is imperative to focus at soil dryness or soil moisture content at which slaking initiates and is mostly enhanced. Accordingly, the specific points are (1) to identify the optimum soil moisture content for slaking, (2) to evaluate salt released accompanied by slaking and (3) to discuss the effect and mechanism of drying on slaking, which deserve attention due to increasing global water shortage and awareness of the environmental impacts associated with irrigation.

[1]Slaking Rate of Soil
The slaking rate was calculated by using the following equation;

Slaking rate (%) = Weight of slaked soil/Weight of soils (slaked + unslaked) X 100

Where, slaked soil refers 'the soils which fell down through sieve with 4.75 mm openings' and unslaked soil refers 'the soils which was left on the sieve' after 24 hours wetting.

[2]Released Salt
The salt left in the soil blocks (after 24 hours immersion) was calculated using $EC_{1:5}$ of soil and EC of solution by the following equation;
Salt in slaked soil = k ($EC_{1:5}$ X 5 X Ws)/ρw… (1)
Salt in unslaked soil = k ($EC_{1:5}$ X 5 X Ws)/ρw… (2)
The total salt remains in the soil = (1) + (2)… (3)
Salt released into the water after 24 hours immersion = k (EC X Vw)… (4)
Proportion of salt remaining in soil (%) = (3)/ {(3) + (4)} X 100… (5)
Proportion of salt released in water (%) = (4)/ {(3) + (4)} X 100... (6)

Where, Ws represents the weight of soil; Vw refers to the volume of bulk water for slaking test; k indicates the co-efficient of proportionality between salt concentration and EC of solution, ρw means the density of water.

References

[1]. Munns R. Genes and salt tolerance: bringing them together. New Phytol. 2005; 167: 645-663
[2]. Norbors M and Dykes T. Obtaining cereal cultivars with increase tolerance to salt, drought and acid stressed soils through tissue culture, LARCS on Biotec. 23-27 April, Manila, p. 51-60; 1984
[3]. Qadir M and Oster JD. Vegetative bioremediation of calcareous sodic soils: history, mechanisms and evaluation. Irrigation Science 2002; 21: 91-101

Correspondence to:

Abul Hasnat Md. Shamim
Ph. D Student
Graduate School of Environmental Science,
Okayama University, Okayama 700-8530, Japan.
Telephone and fax number: 0081-086-251-8874
E-mail: abulhasnats@yahoo.com

Developing a Portable Reading Machine for the Blinds

Erwin Normanyo [1,*], Dzinyefa Kodzo Tsolenyanu [2], Isaac Adetunde [3]

1. University of Mines and Technology, Department of Electrical and Electronic Engineering, Tarkwa, Ghana
2. Process and Plant Automation, P. O. Box SR 95, Accra, Ghana
3. University of Mines and Technology, Department of Mathematics, Tarkwa, Ghana

E-mail address: enormanyo@umat.edu.gh

Abstract: Prevalence of the causes of blindness, especially cataract, is alarming and most sighted people may get it in their old age. Most blind do not have access to readily transliterated documents such as instructions on food packaging, medication and newspapers. Hitherto existing touch-based methods of Moon and Braille for text cognition by the blind and visually impaired are no longer acceptable technologically. In this work, a reading machine for the blind and visually impaired has been developed enabling them to read novels, newspapers, books and letters. In the development, scanner, optical character recognition, and text-to-speech technologies were employed. The Fourier Transform was involved in signal and image processing. Software implementation made use of XML-based speech synthesis markup language. Orientation of the document/paper does not matter during the scanning process. The SSML (Natural reader software) can still identify the right position of words and read them in a natural sounding voice. Li-Ion batteries used give high energy density and higher voltage ensuring reliability. With the implementation of the reading machine developed, information should be carried indiscriminately to the blind and visually impaired [The Journal of American Science. 2009; 5(5):199-212]. (ISSN: 1545-1003).

Key words: the blind; portable reading machine; natural reader software; Fourier transformation; visually impaired.

1. Introduction

Blindness is particularly devastating in the developing world where it has a profound impact on the quality of life for the blind person and his or her community. Life expectancy of the blind is usually less than half that of someone with eyesight the same age. The desperateness of this situation is augmented by the fact that a blind person is unable to contribute to the family income. Not only does blindness mean a father is unable to work, or a mother cannot collect water or go to market, but someone with eyesight must care for him or her. Effectively two income producing individuals are lost. This creates a devastating economic impact on the family and the community. Restored eyesight allows the individual to return to a normal life of work and a traditional role in the family.

In Ghana, about 4.4% of the population is blind and people above the age of 50 years experience low vision. Pitifully enough, many novels, newspapers, books and letters are not readily transliterated into Braille to convey the information to the blind. Means of communication between the sighted and the blind is chiefly vocal. Therefore, the need for a reading machine is paramount. Out of the 20 million people living in Ghana, it is estimated that 200,000 are blind and over 600,000 more people are visually impaired. Thus, blindness is affecting about 4.4 % of the Ghanaian population and people beyond the age of 50 years experience low vision (Dogbe, 2004). A cross-sectional drawing of the eye is given in Figure 1.

Blindness is the total or partial inability to see due to disease or disorder of the eye, optic nerve, or brain (Microsoft Encarta, 2007). The term blindness typically refers to vision loss that is not correctable with eyeglasses or contact lenses (Microsoft Encarta, 2007). Blindness may not mean a total absence of sight, because, some people who are considered blind may be able to perceive slowly moving lights or colors. The term low vision is used for moderately impaired vision. People with low vision may have a visual impairment that affects only central vision (the area directly in front of the eyes) or peripheral vision (the area to either side of and slightly behind the eyes). Some people with low vision are able to function with their remaining sight while others need help to learn to use their sight more efficiently with training and special tools

Color blindness, for example, does not reduce visual acuity and should more accurately be called color-perception deficiency. Color blindness occurs almost exclusively in males, and the most common form is the inability to differentiate between certain shades of red and green. Night blindness, the inability to see in low levels of light, is commonly associated with a lack of vitamin A in the diet or with inherited diseases such as retinitis pigmentosa, a condition involving progressive degeneration of the eye's retina and abnormal deposits of pigment. In Ghana about a million people are blind (Dogbe, 2004).

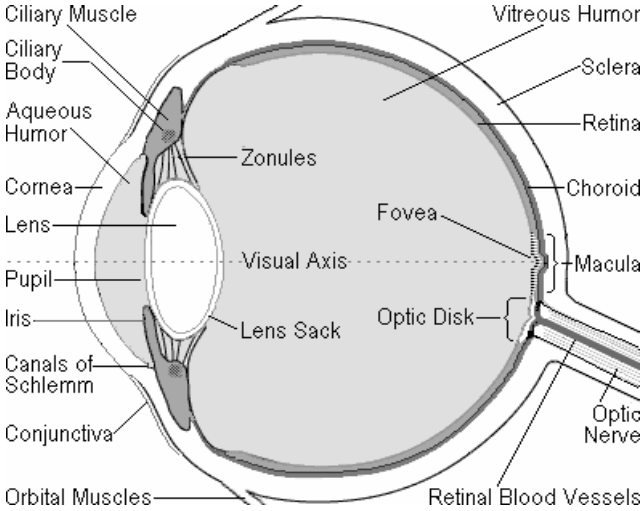

Figure 1. Cross sectional drawing of the eye (side view)

In spite of the progress made in surgical techniques in many countries during the last ten years, cataract (47.9 %) remains the leading cause of visual impairment in all areas of the world, except for developed countries (WHO, 2009a). With the exception of age-related macular degeneration (AMD), the rest are the causes of avoidable visual impairment worldwide. However, in developed countries, AMD is the leading cause of blindness, due to the high life expectancy of over 70 years of age. In the least-developed countries, and in particular Sub-Saharan Africa, the causes of avoidable blindness are primarily, cataract (50 %), glaucoma (15 %), corneal opacities (10 %), trachoma (6.8 %), childhood blindness (5.3 %) and onchocerciasis (4 %) (WHO, 2009a). In Table 1 is given the global estimate of visual impairment.

1.1 Causes of Blindness and Visual Impairment

1.1.1 Cataracts of the Eye

Cataracts are formed in the lens of the eye which is behind the black dot (pupil) in the middle of the eye. It is a clouding of the lens, which prevents a clear, sharp image being produced. A cataract forms because the lens is sealed in a capsule (pupil as shown in Fig. 1) and as old cells die they get trapped in the capsule, with time this causes a clouding over of the lens (Fig. 2.). This clouding results in blurred images. This is when the lenses become opaque meaning that no light goes through.

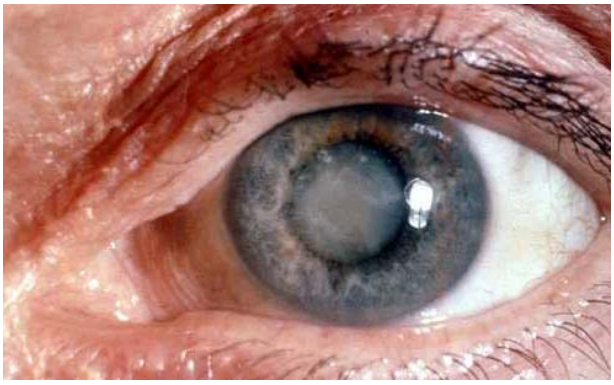

Figure 2. An eye with cataract
(Source: Microsoft Encarta reference library, 2007)

1.1.2 Glaucoma of the Eye

Another disease is called glaucoma (Figure 3). The most common type of this disease occurs in people who are 40 years or older and the other type occurs in babies when they are born. The eye produces a clear fluid (aqueous humor) from the lacrimal gland that fills the space between the cornea and the iris as shown in 3. This fluid produces tears to clean, moisten and lubricate the eyes and then drains the excess fluid into the nose through a complex drainage system. It is the balance

between the production and drainage of this fluid that determines the eyes intraocular pressure (IOP).

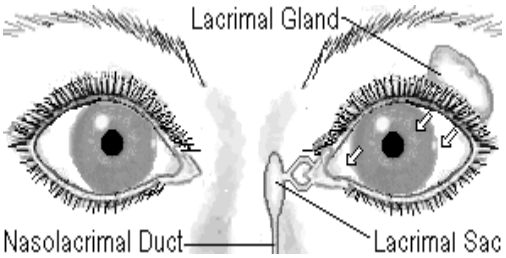

Figure 3. Glaucoma of the eye

1.1.3 Trachoma of the Eye

Trachoma popularly known in Ghana as "Apollo" is one of the oldest infectious diseases known to mankind. It is caused by Chlamydia trachomatis – a micro organism which spreads through contact with eye discharge from the infected person (on towels, handkerchiefs, fingers, etc.) and through transmission by eye-seeking flies. After years of repeated infection, the inside of the eyelid may be scarred so severely that the eyelid turns inward and the lashes rub on the eyeball, scarring the cornea (the front of the eye). If untreated, this condition leads to the formation of irreversible corneal opacities and blindness.

1.1.4 Age-Related Macular Degeneration

Macular degeneration makes people not see things at the center of their field of vision. This is a degenerative condition of the macula (the central retina). It is caused by the hardening of the arteries that nourish the retina. This deprives the retinal tissue of the nutrients and oxygen that it needs to function and causes deterioration in central vision. This disease cuts off the circulation of blood in the center of the retina. It can be treated with a laser. This loss of sight often occurs as people's age increases.

1.1.5 Diabetic Retinopathy

Diabetic retinopathy happens to people who have diabetes mellitus for a few years. Diabetes changes the blood vessel of the retina. The retina is the part of the eye that absorbs light rays. Sometimes the blood vessels will burst and cause bleeding in the eye. Sometimes the retina is detached from the back of the eye. Another case is when fluid leaks from capillaries in the retina. If your retina is detached or you have bleeding in the eye the clear fluid fills the center of the eye that can cause blindness.

1.2 Distribution of Visual Impairment

Visual impairment distribution is done according to age, gender, and geographical location factors.

1.2.1 Age

Visual impairment is unequally distributed across age groups. More than 82 % of all people who are blind are 50 years of age and older, although they represent only 19% of the world's population. Due to the expected number of years lived in blindness (blind years), childhood blindness remains a significant problem, with an estimated 1.4 million blind children below age 15 (WHO, 2009b).

1.2.2 Gender

Available studies consistently indicate that in every region of the world, and at all ages, females have a significantly higher risk of being visually impaired than males (WHO, 2009b).

1.2.3 Geographical Location

Visual impairment is not distributed uniformly throughout the world. More than 90% of the worlds visually impaired live in developing countries (WHO, 2009b).

1.3 Reading Techniques

Reading is an activity characterized by the translation of symbols, or letters, into words and sentences that have meaning to the individual. The ultimate goal of reading is to be able to understand written material, to evaluate it, and to use it for one's needs. Reading exposes people to the accumulated wisdom of human civilization. Mature readers bring to the text their experiences, abilities, and interests; the text, in turn, allows them to expand those experiences and abilities and to find new interests. In order to read, one must follow a sequence of characters arranged in a particular spatial order. For example, English flows from left to right, Hebrew from right to left, and Chinese from top to bottom. The reader must know the pattern and use it consistently.

Ordinarily, the reader sees the symbols on a page, transmit the image from the eye to the brain and pronounce them in the mind or aloud through the vocal cavity. However, reading techniques for the blind namely the Moon and the Braille are quite different from the sighted person. The technique employed by a blind is shown in Figure 4.

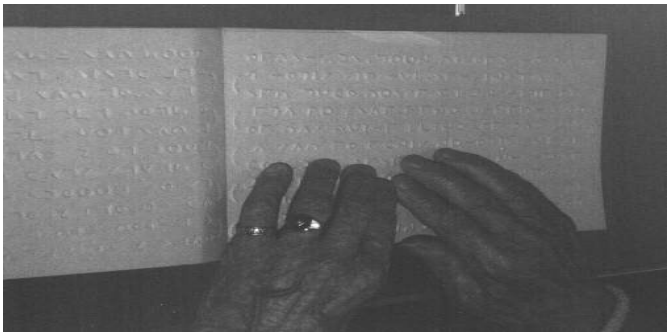

Figure 4. A person reading moon or braille.
(Source: Microsoft Encarta library, 2007)

Table 1. Global estimate of visual impairment

	African Region	Region of the Americas	Eastern Mediterranean Region	European Region	South-East Asia Region	Western Pacific Region	Total
Population	672.2	852.6	502.8	877.9	1,590.80	1,717.50	6,213.90
Number of blind people	6.8	2.4	4	2.7	11.6	9.3	36.9
Percentage of total blind	18 %	7 %	11 %	7 %	32 %	25 %	100 %
Number with low vision	20	13.1	12.4	12.8	33.5	32.5	124.3
Number with visual impairment	26.8	15.5	16.5	15.5	45.1	41.8	161.2

(Source: WHO, 2009b)

1.3.1 Braille

Braille is a writing system which enables blind and partially sighted people to read and write through touch. It was revised by Louis Braille (1809-1852), a French teacher of the blind. It consists of patterns of raised dots arranged in cells of up to six (6) dots in a 3 x 2 configuration as shown in Figure 5. Braille has been adapted to writing many different languages including even Chinese, and is also used for musical and mathematical notations. Each cell represents a letter, numeral or punctuation mark. Some frequently used words and letter combinations also have their own single cell patterns.

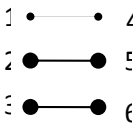

Figure 5. Six dots in 3 × 2 configuration

Braille can be categorized into the grades 1, 2, and 3. Grade 1 consists of the 26 standard letters of the alphabet and punctuation. It is only used by people who are first starting to read Braille. Secondly**,** grade 2

consists of the 26 standard letters of the alphabet, punctuation and contractions.

The contractions are employed to save space because a Braille page cannot fit as much text as a standard printed page. Books, signs in public places, menus, and most other Braille materials are written in Grade 2 Braille. Last but not least grade 3 which is used only in personal letters, diaries, and notes. It is a kind of shorthand, with entire words shortened to a few letters.

(1) Formation of Letters of the Alphabet in Brail

The formation of letters of the alphabet is best organized as: letters from A – J which are the first ten (10) upper dots followed by the letters from K – T which are letters formed by adding dot three (3) to each of the first ten letters, letters of from U – Z are formed by adding dot six (6). Table 2 gives the summary of table representation of basic letters and abbreviations of some words. Braille representation of words and abbreviations is presented in Table 3.

Table 2. Summarized table representation of basic letters

a	b	c	d	e	f	g	h	i	j	k	l	m

(Source: Anon, 1999a)

Table 3. Braille representation of words and abbreviations

a	but	can	do	every	from	go	have	just	knowledge	like	more	not
people	quite	rather	so	that	us	very	will	it	you	as	and	for
of	the	with	child/ch	gh	shall/sh	this/th	which/wh	ed	er	out/ou	ow	bb
cc	dd	en	gg; were	in	st	ing	ar					

(Source: Anon, 1999a)

(2) Sample Texts in Braille

The Braille text below in Figure 6 is transliterated to mean, “Be kind to others”

Figure 6. Braille representation of "Be Kind to Others"

Braille text in Figure 7 below is the article 1 of the universal declaration of human rights.

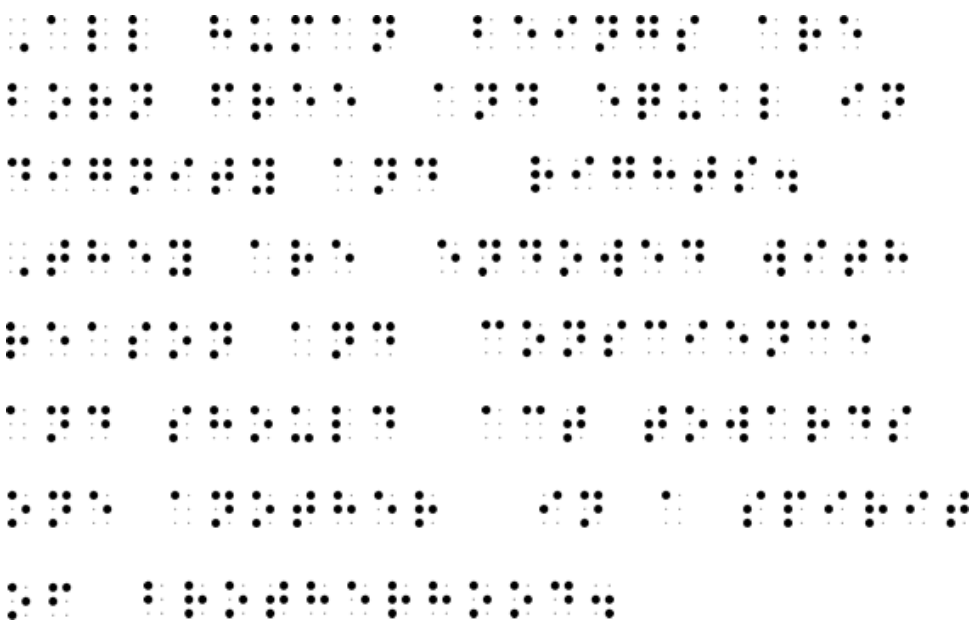

Figure 7. Article 1 of the universal declaration of human rights in braille
(Source: Anon, 1999a)

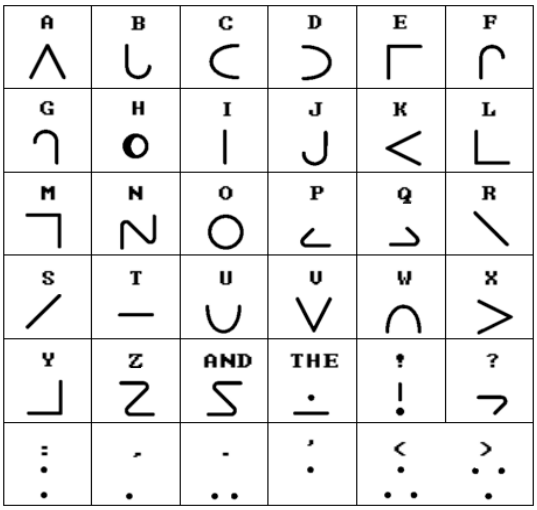

Figure 8. The moon alphabets (Source: Anon, 1999b)

The text in Figure 7 is transliterated as "All human beings are born free and equal in dignity and rights. They are endowed with reason and conscience and should act towards one another in a spirit of brotherhood."

1.3.2 The Moon Alphabets

The Moon system of embossed reading was invented in 1845 by Dr William Moon of East Sussex. The Moon is a simple method of reading based upon the standard alphabet. The Moon alphabet is made up of 14 characters used at various angles, each with a clear bold outline. For many elderly blind people especially, Moon is easier than the more complex Braille system, although many people gain confidence from learning Moon to move onto Braille. The Moon alphabets are presented in Figure 8.

2. Materials and Methods

2.1 Signal Processing and Reading Machine Technologies

Signal processing is the extraction of information bearing attributes from measured data, and any subsequent transformation of those attributes for the purposes of detection, estimation, classification, or waveform synthesis. It is observed that the signals typically used in signal processing are functions of time, such as temperature measurements, velocity measurements, voltages, blood pressures, earth motion, and speech signals. Most of these signals are initially continuous signals (also called analogue signals) which are measured by sensors that convert energy to electricity. Some of the common types of sensors used for collecting data are microphones, which measure acoustic or sound data; seismometers, which measure earth motion; photocells, which measure light intensity; optical scanners, which measure printed character representation; thermistors, which measure temperature; and oscilloscopes, which measure voltage.

When continuous electrical signals are collected from sensors, the continuous signal is converted to a digital signal (a sequence of values) with a piece of hardware called an analogue-to-digital (A/D) converter. Once digital signals are collected, computer could be applied to digital signal processing (DSP). These DSP techniques are designed to perform a number of operations such as: removing noise that is distorting the signal, extracting information from the signal, separating components of the signal, encoding the information in a more efficient way for transmission, detecting information in a signal just to mention a few of signal processing techniques. For some applications, an analog or continuous output signal is needed, and thus a digital-to-analogue (D/A) converter is used to convert the modified digital signal to a continuous signal. Another device called a transducer can be used to convert the continuous electrical signal to another form; for example, a speaker converts a continuous electrical signal to an acoustical signal.

In this section the three basic signals processing techniques for a reading machine are presented first from a theoretical point of view, secondly from an implementation point of view, and lastly from an applications point of view. The theoretical point of view includes the development of mathematical models and the development of software algorithms and computer simulations to evaluate and analyze the models both with simulated data and with real data. Real-time implementation can use VLSI (very large scale integration) techniques, with commercial DSP chips, or it can involve custom design of chips, MCMs (multichip modules), or ASICs (application-specific integrated circuits).

2.2 Mathematical Model: Fourier Transform

The Fourier transform is a mathematical tool that is used to expand signals into a spectrum of sinusoidal components to facilitate signal analysis and system performance. The Fourier transform is also used for spectral analysis, or for spectrum shaping that adjusts the relative contributions of different frequency components in the filtered result. In other applications the Fourier transform is important for its ability to decompose the input signal into uncorrelated components, so that signal processing can be more effectively implemented on the individual spectral components. Decorrelating properties of the Fourier transform are important in frequency domain adaptive filtering, sub band coding, image compression, and transform coding.

Classical Fourier methods such as the Fourier series and the Fourier integral are used for continuous-time (CT) signals and systems, i.e., systems in which the signals are defined at all values of t on the continuum $-\infty < t < \infty$. A more recently developed set of discrete Fourier methods, including the discrete-time (DT) Fourier transform and the discrete Fourier transform (DFT), are extensions of basic Fourier concepts for DT signals and systems. A DT signal is defined only for integer values of n in the range $-\infty < t < \infty$. Fourier methods are particularly useful as a basis for digital signal processing (DSP) because it extends the theory of classical Fourier analysis to DT signals and leads to many effective algorithms that can be directly implemented on general computers or special-purpose DSP devices.

2.2.1 Classical Fourier Transform for CT Signals

The CT Fourier transform is useful in the analysis and design of CT systems, i.e., systems that process CT signals. Fourier analysis is particularly applicable to the design of CT filters which are characterized by Fourier magnitude and phase spectra, i.e., by $|H(j\omega)|$ and arg. $H(j\omega)$, where $H(j\omega)$ is commonly called the frequency response of the filter.

A CT signal $s(t)$ and its Fourier transform $S(j\omega)$ form a transform pair that are related by the equation (1) for any $s(t)$ for which the integral (1a) converges (Madisetti and Williams, 1999):

$$s(j\omega) = \int_{-\infty}^{\infty} s(t)\, e^{-j\omega t}\, dt \qquad (1a)$$

$$s(t) = \frac{1}{2\pi} \int_{-\infty}^{\infty} s(j\omega)\, e^{j\omega t}\, dt \qquad (1b)$$

Equation (1a) is simply called the Fourier transform, whereas Eq. (1b) is called the Fourier integral. The relationship $S(j\omega) = F\{s(t)\}$ denotes the Fourier transformation of s(t), where F{} is a symbolic notation

for the integral operator and where ω is the continuous frequency variable expressed in radians per second. A transform pair s(t) ↔ S(jω) represents a one-to-one invertible mapping as long as s(t) satisfies that condition which guarantee that the Fourier integral converges.

The operation of uniformly sampling a continuous time signal s(t) at every T sec is characterized by Eq. 2 presented below:

$$s_a(t) = \sum_{n=-\infty}^{\infty} s_a(t)\,\delta(t-nT) = \sum_{n=-\infty}^{\infty} s_a(nT)\,\delta(t-nT) \quad (2)$$

Where, $\delta(t)$ is a symbol used to denote a CT impulse function that is defined to be zero for all $t \neq 0$, undefined for $t = 0$, and has unit area when integrated over the range: $-\infty < t < \infty$. Since $s_a(t)$ is in fact a CT signal, it is appropriate to apply the CT Fourier transform to obtain an expression for the spectrum of the sampled signal:

$$F\{s_a(t)\} = F\{\sum_{n=-\infty}^{\infty} s_a(nT)\,\delta(t-nT)\} = \sum_{n=-\infty}^{\infty} s_a(nT)[e^{j\omega T}]^{-n} \quad (3)$$

Since the expression on the right-hand side of Eq. (3) is a function of $e^{j\omega T}$ it is customary to express the transform as F ($e^{j\omega T}$) = F {s_a (t)}. If ω is replaced with a normalized frequency, $\omega' = \omega / T$, so that $-\pi < \omega' < \pi$, then the right side of Eq. 3 becomes identical to the discrete time Fourier transform that is defined directly for the sequence s[n] = s_a(nT) (Madisetti and Williams, 1999).

2.2.2 DT Fourier Transform

The DT Fourier transfom (DTFT) is obtained directly in terms of the sequence samples s(n) by taking the relationship obtained in Eq. (3) to be the definition of the DTFT. By letting T = 1 so that the sampling period is removed from the equation and the frequency variable is replaced with a normalized $\omega' = \omega$T, the DTFT pair is defined by Eq. (4). In order to simplify notation it is not customary to distinguish between ω and ω', but rather to rely on the context of the discussion to determine whether ω refers to the normalized (T = 1) or to the unnormalized (T ≠ 1) frequency variable.

$$S(e^{j\omega'}) = \sum_{n=-\infty}^{\infty} s[n]\,e^{-j\omega' n} \quad (4a)$$

$$s[n] = \frac{1}{2\pi}\int_{-\pi}^{\pi} s(e^{j\omega'})\,e^{jn\omega'}\,d\omega' \quad (4b)$$

The spectrum S ($e^{j\omega'}$) is periodic in ω' with period 2π the fundamental period in the range $-\pi < \omega' < \pi$ sometimes referred to as the baseband, is the useful frequency range of the DT system because frequency components in this range can be represented unambiguously in sample form (without aliasing error). In much of the signal-processing literature the explicit primed notation is omitted from the frequency variable. However, when so many related Fourier concepts are discussed within the same framework.

By comparing (Madisetti and Williams, 1999) Eqs. (3) and (4a), and noting that $\omega' = \omega$T we see that:

$$F\{s_a(t)\} = DTFT\{s[n]\} \quad (5)$$

Where,

$$s[n] = s(t)\big|_{t=nT}$$

This demonstrates that the spectrum of s_a (t) as calculated by the CT Fourier transform is identical to the spectrum of s[n] as calculated by the DTFT. Therefore, although s_a (t) and s[n] are quite different sampling models, they are equivalent in the sense that they have the same Fourier domain representation.

A reading machine relies on three basic technologies as follows:

- Scanner technology to scan an image into computer memory
- Digital image processing or optical character recognition (OCR) technology to convert the image to text
- Text-to-speech (TTS) technology to convert the text into intelligible speech.

3. Results

The reading machine, is the combination of three ubiquitous technologies, namely the scanner technology, the optical character recognition technology, and the text-to-speech technology.

3.1 Composite Parts of Reading Machine

3.1.1 Scanner

The scanner technology comprising the lamp, mirror, lens, CCD, and ADC converts the printed text to a bitmapped signal that is easily interpreted by the processor. The IRIS-Pen handheld scanner is the most fit for this work. It works just like a highlighter. Simply slide it over printed information from books, newspapers, magazines, faxes, letters, spreadsheets etc. and instantly it converts words and numbers into the reading processor application.

3.1.2 Processor

The processor, which engulfs the digital image processing technology and the text-to-speech technology, is the brain behind the entire operation. The output signal from the digital image processing is fed into the front-end compartment of the TTS. This first part has to process the signal through: text analysis, phonetic analysis, and prosodic analysis. A phoneme is the sound associated with each letter. These signals in turn drive the speech synthesizer circuits in the back-end block compartment. Fig. 9 gives the block diagram representation of the reading machine.

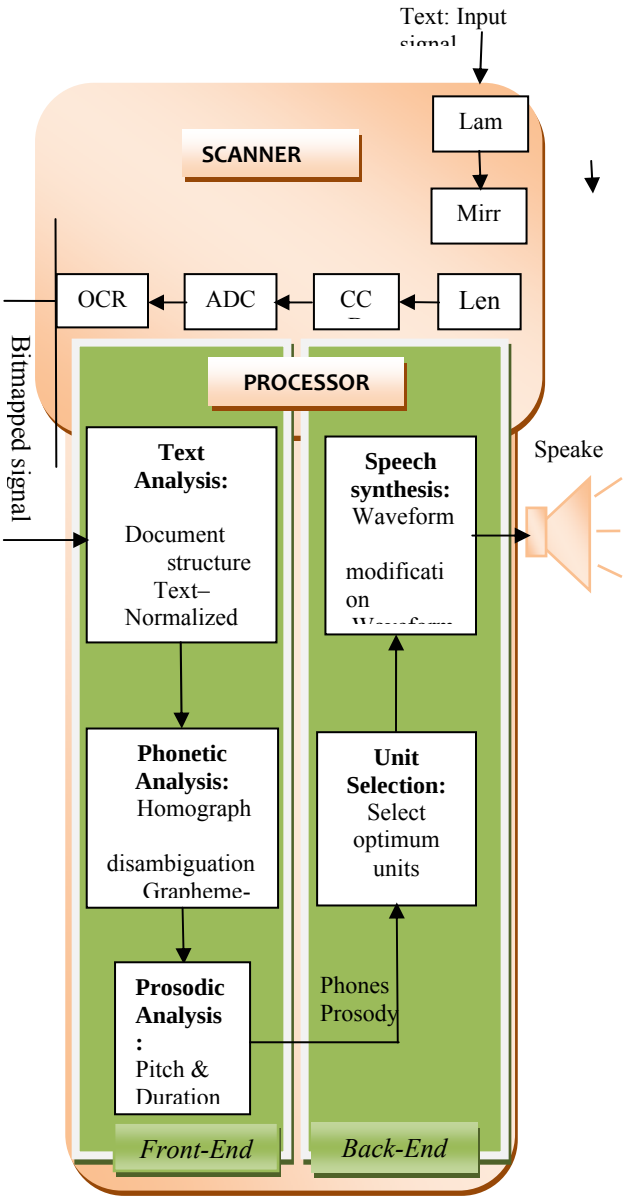

Figure 9. Block diagram of reading

4. Discussion

4.1 Operation of Reading Machine

The sequence of operation of the reading machine begins when the scanner using an integrated scanning array scans the letters in each word and feeds the data directly into the processor. The Euraka handheld scanner and Iris-Pen express 6 handheld scanner are capable of doing this work perfectly. The Iris-Pen hand held scanner has these technical specifications: an universal serial bus (USB) interface, a personal computer platform, 16-bit (64 k colors) maximum color depth and dimensions; width 1.41 inch, depth 0.94 inch, height 5 inch and weight 0.24 lb. Figure 10 shows samples.

Figure 10. Sample of Iris-Pen handheld Scanners (Source: Anon, 2000)

A shape analysis program identifies the words and convert them into bitmap text code. If necessary, other programs using contextual and other clues assist in the identification. The TTS processes are made up of two giant blocks namely the front-end and back-end blocks.

4.1.1 Front-End Processing

The front-end section accepts text as input and produces a sequence of phones and associated prosody at its output. The front-end section can be subdivided into three distinct blocks: text analysis, phonetic analysis, and prosodic analysis.

The text analysis block performs a preprocessing step to analyze the document structure and organize the input sentences into manageable lists of words. In particular, punctuation must be correctly handled. For example, the text analysis block must understand that the colon in '23:45' indicates a time, and to disambiguate between an end of sentence period and decimal point such as in the sentence 'It is 3.14 miles to the city.' Text normalization deals with transforming abbreviations, acronyms, numbers, dates, and times into full text. This requires careful processing. For example, '20/08/1976' must be transformed into 'twentieth of August nineteen seventy six' and not erroneously as 'twenty forward slash zero eight forward slash one thousand nine hundred and seventy six'. It should be clear from these examples that the performance of the document structure and text normalization tasks is critical for ensuring accuracy of the TTS system. The text analysis block also performs some linguistic analysis. The part of speech category (e.g. noun, verb, adjective, etc.) for each word is determined based on its spelling.

The phonetic analysis block is concerned with grapheme-to-phoneme conversion (also called letter-to-sound conversion). Pronunciation dictionaries are employed at word level to provide the phonetic transcriptions. In order to keep the size of the dictionary manageable, words are generally restricted to morphemes. A set of morphophonemic rules is applied to determine how the phonetic transcription of a target word's morphemic constituents is modified when they are combined to form that word. Automatic grapheme-to-phoneme conversion based on rules is used for words not found in the dictionary as a fallback, though this approach is often error prone. The phonetic analysis block must also provide homographic disambiguation. For example 'how much produce do they produce?' Contextual information can aid in selecting the right pronunciation. A popular approach is to use a trained decision tree called a Classification and Regression Tree (CART) that captures the probabilities of specific conversions given the context.

The prosodic analysis block deals with determining how a sentence should be spoken in terms of melody, phrasing, rhythm, and accent locations – factors critical to ensure both intelligibility and naturalness of the resultant speech. From the perspective of the speech signal, prosody manifests as dynamic pitch changes, amplitude and duration of phones, and the presence of pauses.

4.1.2 Back-End Processing

The back-end stage of a concatenative TTS synthesizer consists of storing, selecting, and smoothly concatenating prerecorded segments of speech (units) in addition to modifying prosodic attributes such as pitch and duration of the segments i.e. subject to the target prosody supplied by the front-end. This section takes into account some of the key design questions such as: what unit of speech to use in the database, how the optimum speech units are chosen given phonetic and prosodic targets, how the speech signal segments are represented or encoded, and how prosodic modifications can be made to the speech units.

Different types of speech unit may be stored in the database of a concatenative TTS system. Obviously, whole words may be stored. However, whole word units are impractical for general TTS due to the prohibitively

large number of words that would need to be recorded for sufficient coverage of a given language. Also, the lack of coarticulation at word boundaries results in unnatural sounding speech.

Modern speech synthesizers have evolved away from using databases with a single, 'ideal' diphone for a given context to databases containing thousands of examples of a specific diphone. By selecting the most suitable diphone example at runtime, and in many cases avoiding making quality-affecting prosodic adjustments to the segment, significant improvements in the naturalness of the speech can be obtained.

4.2 Software Implementation

Speech synthesis markup language (SSML) is a standard, extensible markup language (XML-based), markup annotation for instructing speech synthesizers how to convert written language input into spoken language output employed by NaturalReader software. SSML is primarily intended to help application by controlling aspects of the speech output such as pronunciation, volume, pitch and rate. SSML can also express playback of prerecorded audio.

4.2.1 Document Structure

SSML documents are identified by the media type application/ssml+xml. Table 4 summarizes the elements and attributes defined in SSML. The basic structure of an SSML document is illustrated in Figure 11:

```
<?xml version="1.0" encoding="UTF-8"?>
<speak version="1.0"
       xmlns="http://www.w3.org/2001/10/synthesis"
       xmlns:xsi="http://www.w3.org/2001/XMLSchema-instance"
       xsi:schemaLocation="http://www.w3.org/2001/10/synthesis
                  http://www.w3.org/TR/speech-synthesis/synthesis.xsd"
       xml:lang="en-GB">
Hello world!
</speak>
```

Figure 11. Sample structure of SSML document (Burke, 2007)

All SSML documents include the root element <speak>. The version attribute indicates the version of SSML and is fixed at 1.0. The default namespace for the SSML <speak> element and its children is indicated by the xmlns attribute and is defined as http://www.w3.org/2001/10/synthesis. The xmlns:xsi attribute associates the namespace prefix of xsi to the namespace name http://www.w3.org/2001/XMLSchema-instance. The namespace prefix is defined since it is needed for the attribut, xsi:schemaLocation.

The xsi:schemaLocation attribute indicates the location of the schema to validate the SSML document against. The xml:lang attribute indicates the language for the document and optionally also indicates a country or other variation. The format for the xml:lang value follows the language tag syntax. Table 4 illustrates examples of language identifiers.

The <p> element and <s> element can be used explicitly to demarcate paragraphs and sentences.

Table 4 Elements and Attributes Defined in SSML

Elements	Attributes	Description
<Speak>	Version Xmlns Xml:lang xmlns:xsi xsi:schemaLocation xml:base	Root element for SSML documents.
<lexicon>	uri type	References an external pronunciation lexicon document
<p>	xml:lang	Explicitly demarcates a paragraph
<s>	xml:lang	Explicitly demarcates a sentence
<audio>	src	Inserts a recorded audio file.
<phoneme>	ph alphabet	Provides a phonemic/phonetic pronunciation for the contained text.
<sub>	alias	Provides acronym / abbreviation expansions.
<say-as>	interpret-as format	Used to indicate information on the type of text construct contained within the element.

	detail	
<break>	time strength	Controls the pausing or other prosodic boundaries between words.
<emphasis>	level	Requests that the contained text be spoken with emphasis.
<voice>	xml:lang gender age variant name	Requests a change to the speaking voice
<prosody>	pitch contour range rate duration volume	Provides control of the pitch, speaking rate and volume of the speech output.
<mark>	name	Places a marker into the text/tag sequence.
<meta>	name http-equiv content	Contains metadata for the document
<metadata>	—	Contains metadata for the document

(Burke, 2007)

4.2.2 Interpreting Text

The <say-as> element is used to indicate information about the type of text construct contained within the element and to help specify the level of detail for rendering the contained text. Interpreting the contained text in different ways will typically result in a different pronunciation of the content (although a speech synthesizer is still required to pronounce the contained text in a manner consistent with how such content is normally produced for the language).

The <say-as> element has three attributes: interpret-as, format and detail. The format, and detail attributes are optional. The <interpret-as> attribute indicates the content type of the contained text construct, e.g. date to indicate a date, or telephone to indicate a telephone number. The optional format attribute provides further hints on the precise formatting of the contained text, e.g. a value of dmy could be used to indicate that a date should be spoken in the format of date, then month, then year. The optional detail attribute indicates the level of detail to be spoken although it is not defined for many interpret-as types.

In Figure 12 below are some common examples of <say-as>:

```
<say-as interpret-as="date" format="mdy">2/3/2006</say-as>
<!-- Interpreted as 3rd of February 2006 -->
<say-as interpret-as="time" format="hms24">01:59:59</say-as>
<!-- Interpreted as 1 second before 2 o'clock in the morning -->
```

Figure 12. Sample structure of prosodic interpretation. (Burke, 2007)

4.3 Power Management

Li-Ion batteries are leading edge battery technology and are an ideal selection for use on portable computers and cellular phones due to their high energy density and high voltage. A typical Li-Ion cell is rated at 3.6V and this is three times more than the typical NiCd or NiMH cell voltage (1.2V).

4.3.1 Features of Lithium Ion Batteries

These features are as follows:

- High energy density that reaches 400 Wh/L (volumetric energy density) or 160 Wh/Kg (mass energy density).
- High voltage. Nominal voltage of 3.6 V or even 3.7 V on newer Li-Ion batteries.
- No memory effect. Can be charged any time, but they are not as durable as NiMH and NiCd batteries.
- High charge currents (0.5-1A) that lead to small charging times (around 2-4 hours).
- Flat discharge voltage allowing the device to stable power throughout the discharge period.
- Typical charging Voltage 4.2 ± 0.05V.
- Charging method: constant current - constant voltage (CV-CC).
- Typical operation voltage 2.8 V to 4.2 V
- Recommended temperature range 0-4 ^{0}C

4.3.2 Safety Circuits inside the Li-Ion Battery Pack

Inside a Li-Ion battery pack there is always a safety circuit that consists of four main sections: the controller IC, control switches, temperature fuses, and the thermistor (Figure 13). The controller IC monitors each cell (or parallel cells) voltage and prevents the cells to overcharge or over discharge controlling accordingly the cutoff switches. Also the voltage across the switches is monitored in order to prevent over current. The control switches usually comprise FET structures that cutoff the charge or discharge depending on the control signals of the controller IC. The temperature fuses cutoff the current if the control switches experience abnormal heating. This fuse is not recoverable. The thermistor, usually called PTC measures the battery temperature inside the pack. Its terminals are connected to the charger so it can sense the temperature of the pack and control the charge current until the battery is fully charged.

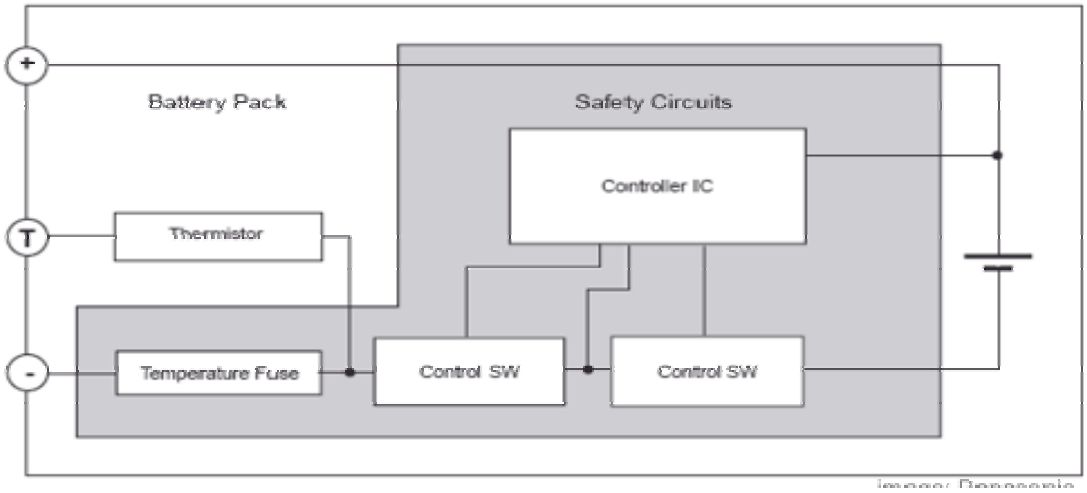

Figure 13. A typical block diagram of Li-Ion battery pack
(Source: Anon, 2004)

5. Conclusions

The architecture of a reading machine designed to achieve a high rate of correct interpretation of text by the blind and visually impaired has been presented. Three ubiquitous technologies were invoked: the scanner, the optical character recognition, and text-to-speech technologies. Multiple algorithms in a Fourier transform domain were used in signal and image processing. With the implementation of the reading machine developed, the feasibility of reading unconstrained printed materials will be achieved and information should be carried indiscriminately to the blind and visually impaired.

Acknowledgments

The authors wish to sincerely thank the anonymous reviewers whose comments were invaluable in the final submission of this article.

Correspondence to:
Normanyo Erwin
University of Mines and Technology
P. O. Box 237
Tarkwa 0362,
Western Region
Ghana
Telephone number: +233 (0)24 221 4103
Facsimile number: +233 362 20306
E-mail address: enormanyo@umat.edu.gh

References

[1] Anon, 1999a. Braille, retrieved on 6th February, 2008 from http://www.omniglot.com/writing/braille.htm.
[2] Anon, 1999b. Moon, retrieved on 6th February, 2008 from http://www.omniglot.com/writing/moon.htm.
[3] Anon, 2000. Scanners. Retrieved on 14th February, 2008 from http://www.irislink.com
[4] Anon, 2004. Li Ion construction, retrieved on 15th December, 2007, from

http://www.electronicslab.com/articles/Li_Ion_reconstruct

[5] Burke, D., 2007. Speech Processing for IP Networks, John Wiley & Sons Ltd, The Atrium, Southern Gate, pp 79 – 88

[6] Dogbe, L., 2004. The Consequence of Being Blind in Ghana, retrieved on 6th January, 2008, from http://www.ghanaeyefoundation.org/index.htm

[7] Madisetti, V, Williams, D. B., 1999. (ed.) Digital Signal Processing Handbook. CRC Press, ghghghgh, 1st Edition, 1776 pp. ISBN: 084 9385725

[8] Microsoft Encarta Reference Library DVD, 2007

[9] WHO (World Health Organization), 2009a. Causes of Blindness and Visual Impairment. Retrieved on July 5, 2009 from **http://www.who.int/blindness/causes/en/**

[10] WHO (World Health Organization), 2009b. Magnitude of Blindness and Visual Impairment. Retrieved on July 5, 2009 from http://www.who.int/blindness/causes/magnitude/en/index.html

Renal Stem Cell

Hongbao Ma *, ***, Shen Cherng **, Yan Yang ***

* Bioengineering Department, Zhengzhou University, Zhengzhou, Henan 450001, China, mahongbao@zzu.edu.cn, 01186-137-331-67674

** Department of Electrical Engineering, Chengshiu University, Niaosong, Taiwan 833, China, cherngs@csu.edu.tw; 011886-7731-0606 ext 3423

*** Brookdale University Hospital and Medical Center, Brooklyn, NY 11212, USA, youngjenny2008@yahoo.com

Abstract: The renal disease is a common problem in human society. End-stage renal disease is a big heath problem in the United States and in all places of the world. Embryonic stem cells, pluripotent derivatives of the inner cell mass of the blastocyst, are the most primitive cell type likely to find application in cell therapy. Their potential to generate any cell type of the embryo makes them to be the most attractive stem cell therapy. It is possible to introduce stem cells into a damaged adult kidney to aid in repair and regeneration. Transdifferentiation offers the possibility of avoiding complications from immunogenicity of introduced cells by obtaining the more easily accessible stem cells of another tissue type from the patient undergoing treatment, expanding them in vitro, and reintroducing them as a therapeutic agent. Adult stem cells may possess a considerable degree of plasticity in the differentiation. Immunoisolation of heterologous cells by encapsulation creates opportunities for their safe use as a component of implanted or ex vivo devices. [Journal of American Science. 2009;5(5):213-222]. (ISSN 1545-4570).

Keywords: stem cell; renal; kidney; disease; treatment

1. Introduction

Normally to say, stem cells could grow to all kinds of cells. In animal tissues stem cells serve as an internal repair system to replace other cells as long as the life is still alive. When a stem cell divides, it could remain a stem cell or become another type of adult cell, such as a muscle, nerve, red blood or a sperm cell. Stem cell is the origin of an orgnism's life (Ma, 2005).

End-stage renal disease (ESRD) is a big heath problem in the United States and it costs more than US$30 billion each year on ESRD therapy in USA (Arnold, 2000; Mai et al., 2006; Ross et al., 2006). It is estimated that there are over 2 million patients in USA who suffer from ESRD. Chronic kidney disease is increasing at the rate of 6-8% per year in the Unite States. The acute renal failure (ARF) is even worse. The cause of death by ARF is generally the development of systemic inflammatory syndrome. It is important to know the kidney's role in reclamation of metabolic substrates and there is considerable drive to develop improved therapies for renal failure (Mehta et al., 2007). About 60,000 patients in the United States are waiting for a kidney transplant, and some patients have waited for several years before an appropriate donor can be found. The shortage of donor organs limits treatment for the ESRD patients and requires many patients to make dialysis to extend the life time. At present, dialysis and transplantation are the common treatment options. However, it is possible to use stem cells and regenerative medicine for kidney disease treatment (Hopkins et al. 2009). The alternate methods stem cell therapy is offering new hope for the renal disfunction patients (Berzoff et al., 2008; Sirmon, 1990).

The kidney dialysis and transplantation techniques have been proved successful, but are marred by inflammation and limited organ availability and graft survival due to immune rejection. Recently, hope has been placed in the development of stem cell therapies. Possible sources for these cells include differentiated embryonic stem (ES) cells and adult renal stem cells. Using the patient's own stem cells to repair kidney damage could circumvent the problems of immune rejection and organ availability.

Embryonic stem cells are the stem cell that can be grown in large numbers in the laboratory and retain the ability to grow into any type of cells including renal, nerve, heart muscle, bone and insulin-producing cells. Adult stem cells, such as skin, nerve and bone marrow stem cells, normally grow into a limited number of cell types (Snykers et al. 2008). The role of embryonic or adult stem cells, in particular bone marrow-derived stem cells, in regenerating the kidney after injury has been the subject of intensive investigation. Bone marrow-derived stem cells have been shown to give rise to small numbers of most renal cell types, including tubular cells, mesangial cells, podocytes, vascular cells and interstitial cells. Injections of bone marrow-derived cells do improve renal function in many animal models of renal disease. Many stages of nephrogenesis can be studied using cultured embryonic kidneys. ES cells

have unlimited developmental potential and can be manipulated at the molecular genetic level by a variety of methods. ES cell technology may obtain a versatile cell culture system in which molecular interventions can be used in vitro on the normal kidney development program in vivo can be studied (Steenhard et al. 2005).

Stem cells and progenitor cells are necessary for repair and regeneration of injured renal tissue. Many factors influence the stem cell growth in damaged kidney. For example, low levels of erythropoietin induce mobilization and differentiation of endothelial progenitor cells and erythropoietin ameliorates tissue injury. Full regeneration of renal tissue demands the existence of stem cells and an adequate local milieu, a so-called stem cell niche. Stem cell may eventually contribute to novel therapies of the kidney disease (Perin et al. 2008).

Recently researchers used a rat model of chronic renal failure in which one kidney is excised so as to increase the load of the remaining kidney, thus causing a chronic deterioration that resembles the clinical situation of renal failure (Alexandre et al. 2008). In Alexandre's project, **t**he rats were divided into 4 groups: Group 1 were sham operated and both kidneys left in place; Group 2 had a kidney removed but were not administered cells; Group 3 were administered $2x10^6$ lineage negative bone marrow cells on day 15 after one of the kidneys was removed; Group 4 were administered $2x10^6$ lineage negative bone marrow cells on days 15, 30, and 45 after one of the kidneys was removed. They found: (1) Expression of inflammatory cytokines was reduced on day 16 in the kidneys of rats receiving stem cells as compared to rats that were nephrectomized but did not receive cells. (2) On day 60 rats receiving stem cells had decreased proteinuria, glomerulosclerosis, anemia, renal infiltration of immune cells and protein expression of monocyte chemoattractant protein-1, as well as decreased interstitial area. (3) Injured rats had higher numbers of proliferating cells in the kidney, whereas rats receiving stem cells had less. (4) Protein expression of the cyclin-dependent kinase inhibitor p21 and of vascular endothelial growth factor increased after nephrectomy and decreased after stem cell treatment. (5) On day 120, renal function (inulin clearance) was improved in the rats which were administered bone marrow cells compared to controls. This study supports the possibility of using bone marrow cells for various aspects of kidney failure. Other studies have demonstrated that administered stem cells promote kidney repair by secretion of insulin growth factor-1 (Cornelissen et al. 2008).

Bone marrow stromal cells, also known as mesenchymal stem cells or fibroblastic colony-forming units, are multipotent non-hematopoietic stem cells adhering to culture plates (Abdallah and Kassem 2009). Mesenchymal stem cells of the bone marrow have the ability to renew and differentiate themselves into multiple lineages of conjunctive tissues, including bone, cartilage, adipose tissue, tendon, muscle, and bone marrow stroma. Those cells have been first described by Friedenstein et al., who found that mesenchymal stem cells adhere to culture plates, look like in vitro fibroblasts, and build up colonies (Friedenstein et al. 1987).

Bone marrow is the site of hematopoiesis and bone marrow transplant has been successfully used for decades as a means of treating various hematological malignancies in which the recipient hematopoietic compartment is replaced by donor-derived stem cells. Progenitor cells in bone marrow are capable to differentiate into other tissues, such as cardiac tissue. Clinical trials have been conducted demonstrating beneficial effects of bone marrow infusion in cardiac patients. It is believed that injured tissue, whether neural tissue after a stroke, or injured cardiac tissue, has the ability to selectively attract bone marrow stem cells, perhaps to induce regeneration. Bone marrow has therapeutic effect in conditions ranging from liver failure, to peripheral artery disease, and the possibility of using bone marrow stem cells in kidney failure has been relatively understudied (Ma et al. 2009).

Mesenchymal stem cells have been brought to the attention of many researchers, because these cells are of great interest for treating various human diseases. Many studies have isolated mesenchymal stem cells and controlled, in vitro, its differentiation into cartilaginous tissue and bone using specific growth factors, with the objective of using this technology for repairing injured tissues of mesenchymal origin (Xian and Foster 2006; Kurdi and Booz 2007).

The origins for renal parenchymal cells could be: (1) re-entry into cell cycle of differentiated cells; (2) direct transdifferentiation of one cell type into another; (3) differentiation from stem cells of the kidney.

2. Native Renal Stem Cells and Renal Regeneration

In embryo, most types of renal parenchymal cells are derived from metanephric mesenchymal cells. In animal models, embryonic metanephroi transplanted into the abdominal cavity of adult animals are colonized by host vasculature, undergo nephrogenesis and produce urine, even if the operation is carried out across species barriers, and with a surprising lack of rejection (Little 2006). Human and porcine embryonic kidney progenitor cells have been isolated and, when injected into mice, can lead to the formation of miniature kidneys producing urine (Dekel et al. 2003), or protect against acute renal failure (Lazzeri et al. 2007). However, there are ethical issues to deal with human ES

cells. It is important to identify the stem cells. In adult mammals, many methods have been used to identify potential multipotent precursor cells, such as label retention in slow cycling cells, identification of a side population, and expression of stem cell markers (e.g. CD133), etc. This has led to the identification of several candidate renal stem cells which are located amongst the tubular cell population (Dekel et al. 2006; Gupta et al. 2006), in the Bowman's capsule, papillary region or cortical interstitium (Bussolati et al. 2005; Sagrinati et al. 2006; Rad et al. 2008). Of note, other studies have not confirmed the presence of a large pool of precursor cells amongst the tubular population and instead argue that regeneration occurs through proliferation of differentiated tubular cells (Vogetseder et al. 2008; Witzgall 2008). Some of the candidate renal stem cells have been shown to enhance recovery after tubular injury, possibly by integration in the tubular epithelium (Rad et al. 2008).

3. Bone Marrow-Derived Stem Cells and Renal Regeneration

Bone marrow stem cells would be an ideal source of multipotent cells: they are an unlimited source of expandable autologous cells, plasticity and easy to harvest. The plasticity has been observed both for the haematopoietic stem cell and for the bone marrow mesenchymal stem cells. There are important discrepancies in the literature addressing the role of bone marrow cells in renal regeneration. The bone marrow transplantation is the most common technique to study bone marrow cell plasticity. The host bone marrow is replaced by donor bone marrow, and after bone marrow chimerism is established, donor cells are tracked down in the kidney. The donor bone marrow cells are distinguished from host cells by virtue of their chromosome content, the expression of a reporter molecule (β-galactosidase, luciferase, enhanced green fluorescent protein), or the performance of a function (re-establishment of a function in a knockout mouse model). The type of host cell that the bone marrow-derived cell has given rise to (tubular, mesangial, etc.) is ascertained most often using immunohistochemistry.

Discrepancies between studies are attributable to several factors: (1) observations in different species (mouse, rat, human); (2) use of different models of renal damage (ischaemia/reperfusion, toxic, immunological); (3) different protocols for bone marrow transplantation (irradiation doses, quantity of cells injected); (4) injection of different subgroups of bone marrow cells (whole bone marrow, haematopoietic stem cell, mesenchymal stem cell); (5) sensitivity and specificity of the detection method for bone marrow cell origin (in situ hybridization for the Y chromosome, detection of reporter molecules, functional assays), and (6) sensitivity and specificity of the detection method of the renal cell type (immunohistochemistry for specific cell types such as tubular cell, mesangial cells, etc.). Renal failure can be the result of an initial insult directed against the tubular epithelium, the glomerular cells or the vascular compartment. In the search for remedies for these varied renal diseases, studies have therefore addressed potential bone marrow origin for various renal cell types. It is useful to bear in mind these technical variations when analysing results reported in the literature (Roufosse and Cook 2008).

4. Tubular Epithelium

Only a small proportion of tubular cells are bone marrow-derived, and there is disagreement over whether mesenchymal stem cells, haematopoietic stem cells or both are contributing (Humphreys and Bonventre 2008). The predominant source of tubular regeneration is through the proliferation of differentiated tubular cells (Lin et al. 2005). A few authors have not found any bone marrow cells engrafted in tubules, and propose that positive observations of bone marrow-derived tubular cells are the result of artifact (Bussolati et al. 2009). Firstly, under certain circumstances, bone marrow engraftment in tubules can be dramatically increased. Held et al. made use of a transgenic fumarylacetoacetate (FAH)-/- mouse, in which discontinuation of the rescue drug NTBC leads to acute tubular necrosis (Held et al. 2006). After transplanting bone marrow from wild-type mice into FAH-/- mice, a few bone marrow-derived tubular cells are noted. In a subset of the FAH-/- mice, there is, in addition, loss of heterozygosity (LOH) in the liver for homogentistic acid hydrogenase, which induces a more severe, ongoing form of acute tubular necrosis. In FAH-/- animals with additional hepatic LOH, up to 50% of tubular cells are bone marrow-derived cells. Engraftment of these wild-type bone marrow-derived cells leads to morphological resolution of ATN and to disappearance of the aminoaciduria present in control mice. In this model, the bone marrow cells have a strong survival advantage over native tubular cells, due to their ability to metabolise toxic products. It is possible that this strong positive selective pressure is necessary for regeneration to occur through wild-type bone marrow cells. Interestingly, most of the bone marrow-derived tubular cells are derived from cell fusion between bone marrow cells and tubular cells. This is supported by a study by Li et al. in which fusion of bone marrow cells to tubular cells account for part of bone marrow-derived tubular cells after ischaemia/reperfusion (I/R) injury, but not all. In this model without selective pressure, the percentage of bone marrow-derived tubular cells is low (1.8%) (Li et al. 2007b). Secondly, although there is disagreement

concerning the underlying mechanism, injection of bone marrow cells, particularly mesenchymal stem cells, has repeatedly been shown to improve renal function in ATN, whether induced by toxins (cisplatin and glycerol) or I/R (Imai and Iwatani 2007). With the role of actual engraftment of bone marrow cells as tubular cells thought to be minimal or absent, mesenchymal stem cells may exert their beneficial effects through their antiapoptotic, mitogenic, immunomodulatory and angiogenic properties, or through the contribution of the bone marrow cells to endothelial cell replacement in the peritubular capillaries. It is important to know the nature of the mediators involved in these properties, and the mechanisms governing the homing of mesenchymal stem cells to the kidney (Imai and Iwatani 2007). Imberti et al. confirmed the importance of paracrine mechanisms using co-culture of mesenchymal stem cells with tubular cells in a Transwell® culture excluding contact between the two cell types, which led to less cisplatin-induced tubular cell death. mesenchymal stem cells have been shown to produce vascular endothelial growth factor, basic fibroblast growth factor, monocyte chemoattractant protein-1, hepatocyte growth factor, and insulin-like growth factor, as well as immunomodulators TGF-β and PGE_2 (Imai and Iwatani 2007; Imberti et al. 2007). In a recent study, administration of conditioned medium from cultured stromal cells provided the same renoprotective effects as injection of mesenchymal stem cells, suggesting that systemic administration of the beneficial mediators may be just as good as mesenchymal stem cell injection, and safer (Imberti et al. 2007). It is a concern that there have been a few observations of adipogenesis associated with fibrosis and osteogenesis after injection of mesenchymal stem cells (Imai and Iwatani 2007).

Mesenchymal stem cell homing to the kidney has been linked to interactions between molecules upregulated in the injured kidney (SDF-1, hyaluronic acid and PDGF) and ligands expressed on mesenchymal stem cells (respectively, CXCR4, CD44 and PDGF-R) (Imai and Iwatani 2007). Similar beneficial effects on renal function may be induced by mobilizing bone marrow cells from the patient's own bone marrow by administration of growth factors (GF) such as granulocyte colony-forming factor, granulocyte/monocyte colony-forming factor, monocyte colony-forming factor, and stem cell factor. Possible explanations for improved renal function include increased numbers of bone marrow-derived tubular cells, a decrease in neutrophilic infiltrate, or increased cell proliferation and decreased apoptosis in kidneys of GF-treated mice (Roufosse and Cook 2008).

The role the bone marrow-derived tubular cells play in improved renal function is probably insignificant, with intrinsic renal cells, either stem cells or differentiated, more likely to play the predominant role in regeneration. Administration of bone marrow cells or mobilization of bone marrow cells using GF may be used to protect against renal injury. There may be a therapeutic role for bone marrow-derived cells engineered to replace a defective gene, due to a local strong positive selective pressure. mesenchymal stem cells have emerged as the most promising candidate for stem cell therapy, and appear safe, such that phase I clinical trials of mesenchymal stem cell injection for the treatment of acute kidney injury are scheduled to begin shortly (Imai and Iwatani 2007).

5. Isolation of Kidney Stem Cells

It is difficult to find a definitive marker for kidney stem cells that makes it difficult to isolate and define kidney stem cells. However, kidney stem cells have been isolated from other organs using 4 different ways. For the first method, when the DNA of the cells is labeled with a marker such as bromodeoxyuridine, the cells retain the label for a long period of time. This label retention is used to identify and isolate stem cells. The second method references the side-population (SP) cells that extrude Hoechst dye through the activity of multidrug resistance proteins, which are part of the ATP-binding cassette transporter superfamily. The third method isolates kidney stem cells referencing specific cell surface markers that have been used to identify stem cells in other organs or the metanephric kidney. The markers used to isolate kidney stem cells include Oct-4, Nanog, CD24, CD133 and stem cell antigen-1 (Sca-1). The fourth method uses culture conditions that select stem cells in other organ systems (http://content.karger.com/produktedb/produkte.asp?typ=fulltext&file=000117311#SA4).

As Zheng et al described in 2008, any unique characteristic can be used to isolate a pure population of stem cell is still lacking. There is few specific biomarker found for epidermal stem cells alone, but epidermal stem cells and transient-amplifying cells share some biomarkers (Bickenbach, 2003) (Zheng, et al, 2008).

6. Culture of Renal Stem Cell

Shimony et al characterized a new model of renal, stromal and mesenchymal stem cell (MSC) matrix deprivation, based on slow rotation cell culture conditions (ROCK). This model induces anoikis using a low shear stress, laminar flow. The mechanism of cell death was determined via FACS (fluorescence-activated cell sorting) analysis for annexin V and propidium iodide uptake and via DNA laddering. Their results showed while only renal epithelial cells progressively died in STCK, the ROCK model could induce apoptosis in stromal and transformed cells; cell survival decreased in ROCK versus STCK to 40%, 52%, 62%

and 7% in human fibroblast, rat MSC, renal cell carcinoma (RCC) and human melanoma cell lines, respectively. Furthermore, while ROCK induced primarily apoptosis in renal epithelial cells, necrosis was more prevalent in transformed and cancer cells [necrosis/apoptosis ratio of 72.7% in CaKi-1 RCC cells versus 4.3% in MDCK (Madin-Darby canine kidney) cells. The ROCK-mediated shift to necrosis in RCC cells was further accentuated 3.4-fold by H(2)O(2)-mediated oxidative stress while in adherent HK-2 renal epithelial cells, oxidative stress enhanced apoptosis. ROCK conditions could also unveil a similar pattern in the LZ100 rat MSC line where in ROCK 44% less apoptosis was observed versus STCK and 45% less apoptosis versus monolayer conditions. Apoptosis in response to oxidative stress was also attenuated in the rat MSC line in ROCK, thereby highlighting rat MSC transformation. They concluded that the ROCK matrix-deficiency cell culture model may provide a valuable insight into the mechanism of renal and MSC cell death in response to matrix deprivation (Shimony et al., 2008)

(1) Morphology and proliferation: Mixed population of cells with approximately 70% attached cells and the other 30% in suspension; need to change cell culture media every day after 48 hours of initial cell culture or when the media starts changing color to slight yellow for pink. Fast growing cell culture. Change media with Celprogen's Human Kidney Stem Cell Complete Growth Media with the appropriate Human Stem Cell Extracellular matrix and tissue culture media for differentiation, expansion or maintaining stem cells in their un-differentiated stage. Temperature 37^0C in 5% CO_2 humidified incubator. Positive markers could be CD34, Nestin & CD133.

(2) Subculturing

A. Thaw the vial with gentle agitation in a 370C water bath or a dry 370C shaking incubator. For water bath thawing
B. Keep the O-ring out of the water, thawing time 2-3 minutes.
C. Remove the thawed vial and wipe with 70% ethanol. Then transfer to the tissue culture hood.
D. Transfer the vial contents to a 15 ml sterile centrifuge tube, and gently add 7 ml of pre-warmed Human Kidney Stem Cell Complete Media to the centrifuge tube. Use an additional 0.5 ml of Human Kidney Stem Cell complete media to rinse the vial and transfer the liquid to the centrifuge tube repeat this once more to ensure you have all the cells transferred to the 15 ml centrifuge tube. Add 1 ml of Human Kidney Stem Complete Media to bring the final volume to 10 ml in the 15 ml centrifuge tube.
E. Centrifuge the cells at 100 g for 5 minutes. Remove the supernatant and resuspend the cell pellet in 500 ul of Human Kidney Stem Cell Complete Growth Media.
F. Add the 500 ul of cells to T75 flask pre-coated with Human Kidney Stem Cell Extracellular matrix with 15 ml of Human Stem Cell Complete Growth Medium.
G. Incubate the cells in the T75 flask in a 37^0C in 5% CO_2 humidified incubator. Perform 100% Media Change every 24 to 48 hours.
H. Medium renewal every day, and recommended sub-culturing ratio: 1:3.

(3) Freezing Medium: Human Stem Cell Complete growth Medium supplemented with 90% Fetal Bovine Serum with 10% DMSO.

(4) Storage temperature: liquid nitrogen vapor phase (San Pedro, CA 90731, USA, http://www.celprogen.com; http://ftp.celprogen.com/Technical_Resources/36100-27%20Human%20Kidney%20Stem%20cell%20data%20sheet.pdf.

7. Application of Kidney Stem Cells

Stem cell has powerful potential application purpose in science, medicine and industry, but it is also potentially danger for its enexpected plasticity. The evidence for bone marrow-derived stem cell contributions to renal repair has been challenged. The research and application for adult renal stem cells are also debated. The use of embryonic tissue in research continues to provide valuable insights but will be the subject of intense societal scrutiny and debate before it reaches the stage of clinical application. Embryonic stem cells, with their ability to generate all of kind of cell in living body, are great chance for our human civilization but have ethical and political hurdles for human use (Brodie and Humes, 2005). Stem cell research has attracted great attention because it could be used for the regeneration of damaged organs that are untreatable by conventional medical techniques, and stem cells (such as endothelial stem cells and neural stem cells) have been discovered to be practical useful in clinical applications. The potential for stem cell gene therapy has increased and many therapeutic applications have already been done. Chronic renal failure is a candidate for stem cell gene therapy. In the application of renal stem cell in medical treatment, mesenchymal stem cells could be transplanted, and in contrast, hematopoietic stem cells may be used for gene delivery for diseases, which need foreign cytokines and

growth factors, such as glomerulonephritis. The stem cell gene therapy for chronic renal failure and the potential of the novel strategy and the major practical challenges of its clinical application are big targets for the stem cell researches (Yokoo et al., 2003). Ectopic expression of the human telomerase reverse transcriptase gene in human mesenchymal stem cells can reconstitute their telomerase activity and extend their replicative life-spans (Li, et al, 2007).

8. Discussion

Kidney is derived from the ureteric bud and metanephrogenic mesenchyme, and these two progenitor cells differentiate into more than 26 different cell types in adult kidney. The ureteric bud contains the precursor of the epithelial cells of the collecting duct and the renal mesenchyme contains precursors of all the epithelia of the rest of the nephron, endothelial cell precursors and stroma cells, but the relatedness among these cells is unclear. A single metanephric mesenchymal cell can generate all the epithelial cells of the nephron, indicating that the kidney contains epithelial stem cells. These stem cells also are present in the adult kidney. Embryonic renal epithelial stem cells can generate other cell types (Al-Awqati and Oliver, 2002). The key important target in kidney stem cell research and application is to get kidney stem cells from other types of the cells, and it is also important to find the better way to change kidney stem cells to other cell types. As the nature will, to live eternally is an extracting dream in all the human history. Stem cell is the original of life and all cells come from stem cells. Germline stem cell (GSC) is the cell in the earliest of the cell stage. It is possible to inject the GSC into adult human body to get the eternal life. This article is to try to describe the stem cell and to explore the possibility of the eternal life with the stem cell strategy The production of functional male gametes is dependent on the continuous activity of germline stem cells. The availability of a transplantation assay system to unequivocally identify male germline stem cells has allowed their in vitro culture, cryopreservation, and genetic modification. Moreover, the system has enabled the identification of conditions and factors involved in stem cell self-renewal, the foundation of spermatogenesis, and the production of spermatozoa. The increased knowledge about these cells is also of great potential practical value, for example, for the possible cryopreservation of stem cells from boys undergoing treatment for cancer to safeguard their germ line (Ma, et al, 2007).

It is possible to introduce stem cells into a damaged adult kidney to aid in repair and regeneration. Transdifferentiation offers the possibility of avoiding complications from immunogenicity of introduced cells by obtaining the more easily accessible stem cells of another tissue type from the patient undergoing treatment, expanding them in vitro, and reintroducing them as a therapeutic agent. Adult stem cells may possess a considerable degree of plasticity in the differentiation. However, the differentiation of stem cells is normally unresolved. Pluripotent cells can be derived from fibroblasts by ectopic expression of defined transcription factors. A fundamental unresolved question is whether terminally differentiated cells can be reprogrammed to pluripotency (Hanna et al., 2008).

Developing nephrons are derived from renal stem cells and transplantation of fetal kidneys may be thought of as a therapeutic stem cell application. There are two bioengineering programs with the aim of producing a device providing full renal replacement therapy in the short to medium term. Both employ biomaterial scaffold structures to overcome the as yet insurmountable difficulties inherent in marshalling cells into organized three-dimensional structures capable of coordinated filtration, resorption / meta- / catabolism / secretion, collection, and disposal of waste. Initial experiments involved adult rabbit renal cortex harvested and fractionated into glomeruli, distal, and proximal tubules, expanded separately in vitro, and seeded onto biodegradable polyglycolic acid sheets for subcutaneous implantation into syngenic hosts. The potential impact of advances in stem cell technology on all the prospective cell-based therapeutic approaches for the treatment of renal failure discussed above is enormous. The kidney has a dramatic capacity to regenerate after injury. Whether stem cells are the source of the epithelial progenitors replacing injured and dying tubular epithelium is an area of intense investigation. Many surviving renal epithelial cells after injury become dedifferentiated and take on mesenchymal characteristics. These cells proliferate to restore the integrity of the denuded basement membrane, and subsequently redifferentiate into a functional epithelium. An alternative possibility is that a minority of surviving intratubular cells possess stem cell properties and selectively proliferate after damage to neighboring cells. Some evidence exists to support this hypothesis but it has not yet been rigorously evaluated (Vigneau et al., 2007).

In recent years, it has been shown that functional stem cells exist in the adult bone marrow, and they can contribute to renal remodelling or reconstitution of injured renal glomeruli, especially mesangial cells, and hMSC found in renal glomeruli differentiated into mesangial cells in vivo after glomerular injury occurred (Wong et al., 2008). In mice with cisplatin-induced acute kidney injury, administration of bone marrow-derived mesenchymal stem cells (MSC) restores renal tubular structure and improves renal function (Imberti et al., 2007).

Correspondence to:
Hongbao Ma
Bioengineering Department
Zhengzhou University
Zhengzhou, Henan 450001, China
Email: mahongbao@zzu.edu.cn
Telephone: 01186-137-331-67674

References

1. Abdallah BM, Kassem M. The use of mesenchymal (skeletal) stem cells for treatment of degenerative diseases: current status and future perspectives. J Cell Physiol 2009;218(1):9-12.
2. Al-Awqati Q, Oliver JA. 2002. Stem cells in the kidney. Kidney Int 61(2):387-395.
3. Alexandre CS, Volpini RA, Shimizu MH, Sanches TR, Semedo P, VL DIJ, Saraiva NO, Seguro AC, Andrade L. Lineage-Negative Bone Marrow Cells Protect against Chronic Renal Failure. Stem Cells 2008.
4. Alison MR, Choong C, Lim S. Application of liver stem cells for cell therapy. Semin Cell Dev Biol 2007;18(6):819-826.
5. Alison MR. Stem cells in pathobiology and regenerative medicine. J Pathol 2009;217(2):141-143.
6. Arnold WP. 2000. Improvement in hemodialysis vascular access outcomes in a dedicated access center. Semin Dial 13(6):359-363.
7. Berzoff J, Swantkowski J, Cohen LM. 2008. Developing a renal supportive care team from the voices of patients, families, and palliative care staff. Palliat Support Care 6(2):133-139.
8. Bickenbach JK. 2003. The continuing saga of epidermal stem cells. J Invest Dermatol 121(5):xv-xvi.
9. Bohle A. Strutz F MG. On the pathogenesis of chronic renal failure in primary glomerulopathies: a vicw from the interstitium.
10. Brodie JC, Humes HD. 2005. Stem cell approaches for the treatment of renal failure. Pharmacol Rev 57(3):299-313.
11. Broekema M, Harmsen MC, van Luyn MJ, Koerts JA, Petersen AH, van Kooten TG, van Goor H, Navis G, Popa ER. Bone marrow-derived myofibroblasts contribute to the renal interstitial myofibroblast population and produce procollagen I after ischemia/reperfusion in rats. J Am Soc Nephrol 2007;18(1):165-175.
12. Bruce SJ, Rea RW, Steptoe AL, Busslinger M, Bertram JF, Perkins AC. In vitro differentiation of murine embryonic stem cells toward a renal lineage. Differentiation 2007;75(5):337-349.
13. Bussolati B, Bruno S, Grange C, Buttiglieri S, Deregibus MC, Cantino D, Camussi G. Isolation of renal progenitor cells from adult human kidney. Am J Pathol 2005;166(2):545-555.
14. Bussolati B, Hauser PV, Carvalhosa R, Camussi G. Contribution of stem cells to kidney repair. Curr Stem Cell Res Ther 2009;4(1):2-8.
15. Chen J, Park HC, Addabbo F, Ni J, Pelger E, Li H, Plotkin M, Goligorsky MS. Kidney-derived mesenchymal stem cells contribute to vasculogenesis, angiogenesis and endothelial repair. Kidney Int 2008;74(7):879-889.
16. Chou SY, Cai H, Pai D, Mansour M, Huynh P. Regional expression of cyclooxygenase isoforms in the rat kidney in complete unilateral ureteral obstruction. J Urol 2003;170(4 Pt 1):1403-1408.
17. Cornelissen B, McLarty K, Kersemans V, Reilly RM. The level of insulin growth factor-1 receptor expression is directly correlated with the tumor uptake of (111)In-IGF-1(E3R) in vivo and the clonogenic survival of breast cancer cells exposed in vitro to trastuzumab (Herceptin). Nucl Med Biol 2008;35(6):645-653.
18. Dekel B, Burakova T, Arditti FD, Reich-Zeliger S, Milstein O, Aviel-Ronen S, Rechavi G, Friedman N, Kaminski N, Passwell JH, Reisner Y. Human and porcine early kidney precursors as a new source for transplantation. Nat Med 2003;9(1):53-60.
19. Dekel B, Zangi L, Shezen E, Reich-Zeliger S, Eventov-Friedman S, Katchman H, Jacob-Hirsch J, Amariglio N, Rechavi G, Margalit R, Reisner Y. Isolation and characterization of nontubular sca-1+lin- multipotent stem/progenitor cells from adult mouse kidney. J Am Soc Nephrol 2006;17(12):3300-3314.
20. Friedenstein AJ, Chailakhyan RK, Gerasimov UV. Bone marrow osteogenic stem cells: in vitro cultivation and transplantation in diffusion chambers. Cell Tissue Kinet 1987;20(3):263-272.
21. Gupta S, Verfaillie C, Chmielewski D, Kren S, Eidman K, Connaire J, Heremans Y, Lund T, Blackstad M, Jiang Y, Luttun A, Rosenberg ME. Isolation and characterization of kidney-derived stem cells. J Am Soc Nephrol 2006;17(11):3028-3040.
22. Hanna J, Markoulaki S, Schorderet P, Carey BW, Beard C, Wernig M, Creyghton MP, Steine EJ, Cassady JP, Foreman R, Lengner CJ, Dausman JA, Jaenisch R. 2008. Direct reprogramming of terminally differentiated mature B lymphocytes to pluripotency. Cell 133(2):250-264.
23. Held PK, Al-Dhalimy M, Willenbring H, Akkari Y, Jiang S, Torimaru Y, Olson S, Fleming WH, Finegold M, Grompe M. In vivo genetic selection of renal proximal tubules. Mol Ther 2006;13(1):49-58.
24. Hishikawa K, Fujita T. [Kidney regeneration update]. Nippon Rinsho 2008;66(5):941-947.

25. Hopkins C, Li J, Rae F, Little MH. Stem cell options for kidney disease. J Pathol 2009;217(2):265-281.
26. Humphreys BD, Bonventre JV. Mesenchymal stem cells in acute kidney injury. Annu Rev Med 2008;59:311-325.
27. Imai E, Iwatani H. The continuing story of renal repair with stem cells. J Am Soc Nephrol 2007;18(9):2423-2424.
28. Imberti B, Morigi M, Tomasoni S, Rota C, Corna D, Longaretti L, Rottoli D, Valsecchi F, Benigni A, Wang J, Abbate M, Zoja C, Remuzzi G. 2007. Insulin-like growth factor-1 sustains stem cell mediated renal repair. J Am Soc Nephrol 18(11):2921-2928.
29. Imberti B, Morigi M, Tomasoni S, Rota C, Corna D, Longaretti L, Rottoli D, Valsecchi F, Benigni A, Wang J, Abbate M, Zoja C, Remuzzi G. Insulin-like growth factor-1 sustains stem cell mediated renal repair. J Am Soc Nephrol 2007;18(11):2921-2928.
30. Jiang T, Liebman SE, Lucia MS, Li J, Levi M. Role of altered renal lipid metabolism and the sterol regulatory element binding proteins in the pathogenesis of age-related renal disease. Kidney Int 2005a;68(6):2608-2620.
31. Jiang T, Wang Z, Proctor G, Moskowitz S, Liebman SE, Rogers T, Lucia MS, Li J, Levi M. Diet-induced obesity in C57BL/6J mice causes increased renal lipid accumulation and glomerulosclerosis via a sterol regulatory element-binding protein-1c-dependent pathway. J Biol Chem 2005b;280(37):32317-32325.
32. Jiang Y, Jahagirdar BN, Reinhardt RL, Schwartz RE, Keene CD, Ortiz-Gonzalez XR, Reyes M, Lenvik T, Lund T, Blackstad M, Du J, Aldrich S, Lisberg A, Low WC, Largaespada DA, Verfaillie CM. Pluripotency of mesenchymal stem cells derived from adult marrow. Nature 2002;418(6893):41-49.
33. Kim D, Dressler GR. Nephrogenic factors promote differentiation of mouse embryonic stem cells into renal epithelia. J Am Soc Nephrol 2005;16(12):3527-3534.
34. Kobayashi T, Tanaka H, Kuwana H, Inoshita S, Teraoka H, Sasaki S, Terada Y. Wnt4-transformed mouse embryonic stem cells differentiate into renal tubular cells. Biochem Biophys Res Commun 2005;336(2):585-595.
35. Kunter U, Rong S, Djuric Z, Boor P, Muller-Newen G, Yu D, Floege J. Transplanted mesenchymal stem cells accelerate glomerular healing in experimental glomerulonephritis. J Am Soc Nephrol 2006;17(8):2202-2212.
36. Kurdi M, Booz GW. G-CSF-based stem cell therapy for the heart--unresolved issues part B: Stem cells, engraftment, transdifferentiation, and bioengineering. Congest Heart Fail 2007;13(6):347-351.
37. Lazzeri E, Crescioli C, Ronconi E, Mazzinghi B, Sagrinati C, Netti GS, Angelotti ML, Parente E, Ballerini L, Cosmi L, Maggi L, Gesualdo L, Rotondi M, Annunziato F, Maggi E, Lasagni L, Serio M, Romagnani S, Vannelli GB, Romagnani P. Regenerative potential of embryonic renal multipotent progenitors in acute renal failure. J Am Soc Nephrol 2007;18(12):3128-3138.
38. Li J, Deane JA, Campanale NV, Bertram JF, Ricardo SD. The contribution of bone marrow-derived cells to the development of renal interstitial fibrosis. Stem Cells 2007a;25(3):697-706.
39. Li K, Zhu H, Han X, Xing Y. Ectopic hTERT gene expression in human bone marrow mesenchymal stem cell. Life Science Journal. 2007;4(4):21–24.
40. Li L, Truong P, Igarashi P, Lin F. Renal and bone marrow cells fuse after renal ischemic injury. J Am Soc Nephrol 2007b;18(12):3067-3077.
41. Lin CS, Lim SK, D'Agati V, Costantini F. 1996. Differential effects of an erythropoietin receptor gene disruption on primitive and definitive erythropoiesis. Genes Dev 10(2):154-164.
42. Lin F, Moran A, Igarashi P. Intrarenal cells, not bone marrow-derived cells, are the major source for regeneration in postischemic kidney. J Clin Invest 2005;115(7):1756-1764.
43. Little MH. Regrow or repair: potential regenerative therapies for the kidney. J Am Soc Nephrol 2006;17(9):2390-2401.
44. Ma AC, Chung MI, Liang R, Leung AY. The role of survivin2 in primitive hematopoiesis during zebrafish development. Leukemia 2009.
45. Ma H, Chen G. Stem cell. The Journal of American Science 2005;1(2):90-92.
46. Ma H, Cherng S. Eternal Life and Stem Cell. Nature and Science. 2007;5(1):81-96.
47. Ma H, Stephen Lee S, Nair S, Chou SY. Reduction of renal interstitial fibrosis and protection of renal function by pentoxifylline in chronic partial ureteral obstruction. FASEB Journal. 2008;22:917.4.
48. Mai ML, Ahsan N, Gonwa T. 2006. The long-term management of pancreas transplantation. Transplantation 82(8): 991- 1003.
49. Mehta RL, Kellum JA, Shah SV, Molitoris BA, Ronco C, Warnock DG, Levin A. 2007. Acute Kidney Injury Network: report of an initiative to improve outcomes in acute kidney injury. Crit Care 11(2):R31.
50. Miyajima A, Chen J, Lawrence C, Ledbetter S, Soslow RA, Stern J, Jha S, Pigato J, Lemer ML, Poppas DP, Vaughan ED, Felsen D. Antibody to

transforming growth factor-beta ameliorates tubular apoptosis in unilateral ureteral obstruction. Kidney Int 2000;58(6):2301-2313.
51. Nair S, Maini A, Ma H, Chou SY. Pentoxifylline Ameliorates Tubulointerstitial Fibrosis and Protects Renal Function in Chronic Partial Ureteral Obstruction. J Am Soc Nephrol 2007;18:400A-401A.
52. Nichols J, Ying QL. Derivation and propagation of embryonic stem cells in serum- and feeder-free culture. Methods Mol Biol 2006;329:91-98.
53. Oliver JA. 2004. Adult renal stem cells and renal repair. Curr Opin Nephrol Hypertens 13(1):17-22.
54. Perin L, Giuliani S, Sedrakyan S, S DAS, De Filippo RE. Stem cell and regenerative science applications in the development of bioengineering of renal tissue. Pediatr Res 2008;63(5):467-471.
55. Rad FH, Ulusakarya A, Gad S, Sibony M, Juin F, Richard S, Machover D, Uzan G. Novel somatic mutations of the VHL gene in an erythropoietin-producing renal carcinoma associated with secondary polycythemia and elevated circulating endothelial progenitor cells. Am J Hematol 2008;83(2):155-158.
56. Raval M, Ma H, Chung E, Suwangomolkul A, Chou SY. Hemodialysis Decreases Expression of the Platelet P2Y12 Adenosine Diphosphate Receptor. 28th Annual Dialysis Conference. Hemodialysis International. 2008;12(1):139.
57. Remuzzi G, Zoja C, Gagliardini E, Corna D, Abbate M, Benigni A. Combining an antiproteinuric approach with mycophenolate mofetil fully suppresses progressive nephropathy of experimental animals. J Am Soc Nephrol 1999;10(7):1542-1549.
58. Ross EA, Alza RE, Jadeja NN. 2006. Hospital resource utilization that occurs with, rather than because of, kidney failure in patients with end-stage renal disease. Clin J Am Soc Nephrol 1(6):1234-1240.
59. Roufosse C, Cook HT. Stem cells and renal regeneration. Nephron Exp Nephrol 2008;109(2):e39-45.
60. Sagrinati C, Netti GS, Mazzinghi B, Lazzeri E, Liotta F, Frosali F, Ronconi E, Meini C, Gacci M, Squecco R, Carini M, Gesualdo L, Francini F, Maggi E, Annunziato F, Lasagni L, Serio M, Romagnani S, Romagnani P. Isolation and characterization of multipotent progenitor cells from the Bowman's capsule of adult human kidneys. J Am Soc Nephrol 2006;17(9):2443-2456.
61. Saito S, Ugai H, Sawai K, Yamamoto Y, Minamihashi A, Kurosaka K, Kobayashi Y, Murata T, Obata Y, Yokoyama K. Isolation of embryonic stem-like cells from equine blastocysts and their differentiation in vitro. FEBS Lett 2002;531(3):389-396.
62. Schuldiner M, Yanuka O, Itskovitz-Eldor J, Melton DA, Benvenisty N. Effects of eight growth factors on the differentiation of cells derived from human embryonic stem cells. Proc Natl Acad Sci U S A 2000;97(21):11307-11312.
63. Shimizukawa R, Sakata A, Hirose M, Takahashi A, Iseki H, Liu Y, Kunita S, Sugiyama F, Yagami K. Establishment of a new embryonic stem cell line derived from C57BL/6 mouse expressing EGFP ubiquitously. Genesis 2005;42(1):47-52.
64. Shimony N, Avrahami I, Gorodetsky R, Elkin G, Tzukert K, Zangi L, Levdansky L, Krasny L, Haviv YS. 2008. A 3D rotary renal and mesenchymal stem cell culture model unveils cell death mechanisms induced by matrix deficiency and low shear stress. Nephrol Dial Transplant 23(6):2071-2080.
65. Sirmon MD. 1990. Renal disease in noninsulin-dependent diabetes mellitus. Am J Med Sci 300(6):388-395.
66. Snykers S, De Kock J, Rogiers V, Vanhaecke T. In vitro differentiation of embryonic and adult stem cells into hepatocytes: state of the art. Stem Cells 2008.
67. Steenhard BM, Isom KS, Cazcarro P, Dunmore JH, Godwin AR, St John PL, Abrahamson DR. Integration of embryonic stem cells in metanephric kidney organ culture. J Am Soc Nephrol 2005;16(6):1623-1631.
68. Sugimoto H, Mundel TM, Sund M, Xie L, Cosgrove D, Kalluri R. Bone-marrow-derived stem cells repair basement membrane collagen defects and reverse genetic kidney disease. Proc Natl Acad Sci U S A 2006;103(19):7321-7326.
69. Sun L, Halaihel N, Zhang W, Rogers T, Levi M. Role of sterol regulatory element-binding protein 1 in regulation of renal lipid metabolism and glomerulosclerosis in diabetes mellitus. J Biol Chem 2002;277(21):18919-18927.
70. Suzuki A, Iwatani H, Ito T, Imai E, Okabe M, Nakamura H, Isaka Y, Yamato M, Hori M. Platelet-derived growth factor plays a critical role to convert bone marrow cells into glomerular mesangial-like cells. Kidney Int 2004;65(1):15-24.
71. Taupin P. 2006. The therapeutic potential of adult neural stem cells. Curr Opin Mol Ther 8(3):225-231.
72. Vigneau C, Polgar K, Striker G, Elliott J, Hyink D, Weber O, Fehling HJ, Keller G, Burrow C, Wilson P. 2007. Mouse embryonic stem cell-derived embryoid bodies generate progenitors that integrate long term into renal proximal tubules in vivo. J Am Soc Nephrol 18(6):1709-1720.
73. Vigneau C, Polgar K, Striker G, Elliott J, Hyink D,

Weber O, Fehling HJ, Keller G, Burrow C, Wilson P. Mouse embryonic stem cell-derived embryoid bodies generate progenitors that integrate long term into renal proximal tubules in vivo. J Am Soc Nephrol 2007;18(6):1709-1720.
74. Vogetseder A, Picard N, Gaspert A, Walch M, Kaissling B, Le Hir M. Proliferation capacity of the renal proximal tubule involves the bulk of differentiated epithelial cells. Am J Physiol Cell Physiol 2008;294(1):C22-28.
75. Winkler J. 2003. Adult neural stem cells: therapeutic potential in neurology. Med Klin (Munich) 98 Suppl 2:27-31.
76. Winkler ME, Mauritz C, Groos S, Kispert A, Menke S, Hoffmann A, Gruh I, Schwanke K, Haverich A, Martin U. Serum-free differentiation of murine embryonic stem cells into alveolar type II epithelial cells. Cloning Stem Cells 2008;10(1):49-64.
77. Witzgall R. Are renal proximal tubular epithelial cells constantly prepared for an emergency? Focus on "the proliferation capacity of the renal proximal tubule involves the bulk of differentiated epithelial cells". Am J Physiol Cell Physiol 2008;294(1):C1-3.
78. Wong CY, Cheong SK, Mok PL, Leong CF. 2008. Differentiation of human mesenchymal stem cells into mesangial cells in post-glomerular injury murine model. Pathology 40(1):52-57.
79. Wong CY, Cheong SK, Mok PL, Leong CF. Differentiation of human mesenchymal stem cells into mesangial cells in post-glomerular injury murine model. Pathology 2008;40(1):52-57.
80. Wu DP, He DL, Li X, Liu ZH. Differentiations of transplanted mouse spermatogonial stem cells in the adult mouse renal parenchyma in vivo. Acta Pharmacol Sin 2008;29(9):1029-1034.
81. Xian CJ, Foster BK. Repair of injured articular and growth plate cartilage using mesenchymal stem cells and chondrogenic gene therapy. Curr Stem Cell Res Ther 2006;1(2):213-229.
82. Yamamoto M, Cui L, Johkura K, Asanuma K, Okouchi Y, Ogiwara N, Sasaki K. Branching ducts similar to mesonephric ducts or ureteric buds in teratomas originating from mouse embryonic stem cells. Am J Physiol Renal Physiol 2006;290(1):F52-60.
83. Yokoo T, Sakurai K, Ohashi T, Kawamura T. 2003. Stem cell gene therapy for chronic renal failure. Curr Gene Ther 3(5):387-394.
84. Zheng N, Wang L, Wu J, Li H, Wang Y, Zhang Q. Rapid enrichment of stem cell population by filter screening and biomarker-immunoassay from human epidermis. Life Science Journal. 2008; 5(4):33–37.

7/1/2009

The Journal of American Science

ISSN: 1545-1003

The international academic journal, "***The Journal of American Science*"** (ISSN: 1545-1003)**,** is registered in the United States, and invites you to publish your papers.

Any valuable papers that describe natural phenomena and existence or any reports that convey scientific research and pursuit are welcome, including both natural and social sciences. Papers submitted could be reviews, objective descriptions, research reports, opinions/debates, news, letters, and other types of writings that are nature and science related. All the manuscripts will be processed in a professional peer review. After the peer review, the journal will make the best efforts to publish all the valuable works as soon as possible.

This journal will be no charge for the manuscript contributors. If the author needs hard copy of the journal, it will be charged for US$100/issue to cover the printing and mailing fee. Here is a new avenue to publish your outstanding reports and ideas. Please also help spread this to your colleagues and friends and invite them to contribute papers to the journal. Let's work together to disseminate our research results and our opinions.

Papers in all fields are welcome, including articles of natural science and social science.

Please send your manuscript to editor@americanscience.org;
sciencepub@gmail.com;
americansciencej@gmail.com

For more information, please visit http://www.americanscience.org;
http://www.sciencepub.net; http://www.sciencepub.org

Marsland Press
2158 Butternut Drive
Okemos, MI 48864
The United States
Telephone: 347-321-7172; 718-404-5362; 517-349-2362
Email: editor@americanscience.org;
sciencepub@gmail.com;
americansciencej@gmail.com
Website: http://www.americanscience.org
http://www.sciencepub.net; http://www.sciencepub.org

The Journal of American Science

ISSN 1545-1003

Marsland Press

2158 Butternut Drive
Okemos, Michigan 48864
The United States
Telephone: (517) 349-2362

Emails: editor@americanscience.org;
americansciencej@gmail.com

Websites: http://www.americanscience.org;
http://www.sciencepub.net

ISSN 1545-1003

9 771545 100210